Winter 2008

Subcellular Localization of Human T-cell Leukemia Virus Type 1 Tax Oncoprotein

Kimberly Anne Fryrear
Old Dominion University

SUBCELLULAR LOCALIZATION OF HUMAN T-CELL LEUKEMIA VIRUS TYPE 1 TAX ONCOPROTEIN

by

Kimberly Anne Fryrear
B.S. December 1997, Old Dominion University
M.S. May 2008, Eastern Virginia Medical School

A Dissertation Submitted to the Faculty of
Eastern Virginia Medical School and
Old Dominion University in Partial Fulfillment of
the Requirement for the Degree of

DOCTOR OF PHILOSOPHY

BIOMEDICAL SCIENCE

EASTERN VIRGINIA MEDICAL SCHOOL AND
OLD DOMINION UNIVERSITY
December 2008

Approved by:

_____
G. John Semmes (Director)

_____
Ann Campbell (Member)

_____
Richard Drake (Member)

_____
Julie Kerry (Member)

ABSTRACT

SUBCELLULAR LOCALIZATION OF HUMAN T-CELL LEUKEMIA VIRUS TYPE 1 TAX ONCOPROTEIN

Kimberly Anne Fryrear
Old Dominion University and Eastern Virginia Medical School, 2008
Director: Dr. O. John Semmes

Human T-cell Leukemia Virus Type 1 (HTLV-1) is a transforming retrovirus that gives rise to Adult T-cell Leukemia (ATL) and a variety of other subneoplastic conditions such as HTLV- Associated Myelopathy/ Tropical Spastic Paraperesis (HAM/TSP). In ATL, the transformation and immortalization of T-lymphocytes has been attributed to the expression and activity of a single HTLV-1 viral protein, namely the *trans*-activating protein Tax. Although the exact mechanism of Tax-mediated transformation is uncertain, current studies support a model in which Tax induces genomic instability in the host cell through interference with DNA repair mechanisms, dysregulation of cell cycle progression, transcriptional activation of cellular genes, and protein-protein interactions with cellular partners leading to perturbation of their functions. Tax has both nuclear and cytoplasmic activities and shuttles between the two compartments via defined nuclear localization and nuclear export signals (NLS and NES, respectively), but the mechanisms regulating nucleocytoplasmic shuttling and targeting of Tax to distinct subcellular regions have yet to be determined. In this study we identified regions in Tax that regulate nucleocytoplasmic shuttling and dictate subnuclear targeting.

We identified the region in Tax containing the sequence that targets the protein into discrete nuclear foci named Tax Speckled Structures (TSS). These TSS are protein complexes that partially overlap with the cellular marker of splicing SC35 and contain other cellular proteins such as DNA-PKcs and Chk2. Targeting Tax to TSS places Tax in

a centralized location to affect transcription, DNA damage recognition and other processes, and targeting to these foci is therefore crucial to Tax-mediated transformation. We identified the Tax speckle targeting signal (TSTS) as the Tax region containing amino acids 50-75. This sequence lies downstream from the Tax NLS and is completely separable from the NLS. We demonstrated that a mutant missing the NLS and a mutant missing the TSTS can interact with each other and rescue proper localization through complementation of the deleted domains.

We also determined that dimerization of Tax is required for nuclear localization. The previously defined Tax dimerization domain spans 150 amino acids which represent nearly one-half of the protein. Within this larger domain are three subdomains that were identified as regions required for Tax dimerization. We created Tax mutants deleted in individual dimerization subdomains and assayed their ability to dimerize and their subsequent subcellular localization. Tax mutants deleted in one of the three dimerization subdomains were unable to efficiently homodimerize and were retained in the cytoplasm. They were able to weakly dimerize with wildtype Tax which resulted in partial rescue of nuclear localization. A mutant deleted in two dimerization subdomains was unable to dimerize with itself or with wildtype Tax and remained in the cytoplasm. A Tax mutant that was induced to become a dimer was subsequently able to translocate into the nucleus.

Our studies further identified that cellular proteins including the ubiquitin ligase RNF4 affect the subcellular localization of Tax. Previous studies suggested that ubiquitylation of Tax is associated with its cytoplasmic localization, but the specific ubiquitin ligase involved had not been identified. We demonstrated that RNF4 was able

to ubiquitylate Tax *in vitro*. This study is the first to identify a substrate protein for the ubiquitylation activity of RNF4. Overexpression of RNF4 led to an egress of Tax from the TSS and the nucleus. We co-purified Tax and RNF4 from transfected cell lystates and demonstrated that they are both present in a protein complex. Increasing RNF4 expression increased the cytoplasmic activity of Tax and decreased the nuclear activity of Tax in a dose-dependent manner, suggesting that RNF4's ubiquitylation of Tax affects its subcellular localization and subsequently affects Tax function.

Overall, in this study we have identified novel domains and interactions that contribute to the regulation of the subcellular localization of Tax. The knowledge gained through this work will provide a better understanding of Tax function and its role in cellular transformation.

This dissertation is dedicated to my husband, Jim, my mother, Linda, and my children, Noah, Rebekah, and Jonah, whose encouragement and patience have given me the inspiration to begin my studies and the strength to complete them.

ACKNOWLEDGMENTS

I would like to take this opportunity to thank the members of my dissertation committee, Dr. Ann Campbell, Dr. Richard Drake, Dr. Julie Kerry, and especially my mentor, Dr. O. John Semmes, for their patience, instruction, and guidance in conducting my research. I would also like to thank my coworkers, Mehdi Belgnaoui, Dr. Sarah Durkin, Dr. Cindy Guo, Dr. Sandy Gupta, and Jessica Tiedebohl, who provided technical assistance in many of the experiments presented in this dissertation. In addition, their advice, support, and friendship were invaluable to me in the completion of this work.

TABLE OF CONTENTS

Page

LIST OF FIGURES

SECTION 1

INTRODUCTION

Human T-Cell Leukemia Virus Type 1

Human T-cell Leukemia Virus-1 (HTLV-1) is an oncogenic retrovirus that is etiologically linked to both an aggressive malignancy of CD4+ lymphocytes, namely adult T-cell leukemia (ATL), and a neurodegenerative disease known as HTLV-Associated Myelopathy/Tropical Spastic Paraperesis (HAM/TSP) as well as several other subneoplastic conditions (1-4). HTLV-1 was the first discovered human retrovirus and was the first retrovirus to be linked to a human cancer (1). Retroviruses in general consist of a two-stranded positive sense RNA viral genome that is embedded in a nucleocapsid and packaged into enveloped virions. Retroviruses are subdivided into two classes: simple and complex. Simple retroviruses have only *gag, pro, pol,* and *env* genes while complex retroviruses also contain nonstructural regulatory genes.

HTLV-1 is a member of the *Deltaretrovirus* genera of the Orthoretrovirinae family (5). The genome for HTLV-1 is 9 kilobases in length and contains *gag, pol, pro,* and *env* genes along with 5' and 3' long terminal repeats (LTRs). The *gag* gene encodes for the capsid, nucleocapsid, and matrix proteins. The *pol* gene encodes the reverse transcriptase needed to reverse transcribe the RNA viral genome into DNA to be integrated into the host genome (6). The *pro* gene encodes for the viral protease that cleaves the products of the *gag* gene during maturation of the virion. The *env* gene encodes for the surface glycoprotein (SU) and the transmembrane protein (TM) that make

---

This dissertation follows the format of *The Journal of Biological Chemistry.*

up the viral envelope proteins (7). The long terminal repeats contain signals that regulate the transcription and expression of the viral genes.

In addition to the *gag, pol, pro* and *env* genes and the long terminal repeats (LTRs) that are common to most retroviruses, HTLV-1 contains a region at its 3' terminus designated as pX (8-10). At the time of the discovery of HTLV-1, this pX region gave the HTLV-1 viral genome a unique structure from other known animal retroviruses. This led to the establishment of a new retroviral group which now includes HTLV-2, HTLV-3, HTLV-4, Bovine Leukemia Virus (BLV), Primate T-Lymphotropic Virus (PTLV), and Simian T-cell Leukemia Virus (STLV) (11). Unlike other retroviruses that rely on cellular proteins for regulation, HTLV-1 can regulate itself through proteins encoded within the pX region. This pX region contains multiple overlapping ORFs which are responsible for encoding nonstructural accessory and regulatory genes such as *tax, rex, $p27^{I}$, $p12^{I}$, $p30^{II}$, $p13^{II}$,* and *HBZ* genes (9,12). The Tax and Rex proteins are two essential positive regulators of viral transcription required for viral replication. Rex is a 27 kDa RNA-binding protein that aids in the export of unspliced (gag/pro/pol) and singly spliced (env) mRNAs over doubly spliced mRNAs from the nucleus (13). A primary function of Tax is to potently activate viral transcription by recruiting cellular transcription factors to the viral LTR (9). Tax has, however, many other functions within the host cell which promote cellular transformation and will be later discussed in detail. The accessory proteins are not required for replication, but may be necessary for persistent infection and immune response evasion (12).

Replication of HTLV-1 follows that of all retroviruses (6). The retroviral life cycle begins with infection of the host cell. The enveloped retroviral virion binds to a

receptor on the surface of the host cell and enters the host cell by fusion of the viral envelope and plasma membrane (14). After the viral core has entered the host cell, the two-stranded positive sense RNA viral genome is reverse transcribed into double-stranded RNA/DNA hybrids by the viral enzyme reverse transcriptase. The RNA template is then degraded and the reverse transcriptase copies the single-stranded DNA into double stranded DNA during multiple steps. This provirus and additional viral proteins are transported into the nucleus, and the provirus is integrated into the host cell genome by the viral integrase at random sites (15). Viral genes are transcribed by host cell transcription machinery, and multiply spliced viral mRNAs, such as that of the regulatory proteins Tax and Rex, are transported to the cytoplasm. The expression of these regulatory proteins allows for the export of the singly and unspliced viral mRNAs. The differentially spliced mRNAs are translated into virion structural proteins and enzymes while the unspliced mRNAs become the viral RNA genomes for the newly developing virions. The virion proteins and viral genome are assembled in the cytoplasm, and the new virions are released by budding from the host cell. Capsid proteins are proteolytically processed within the new virions to become mature, infectious virus (6).

In the case of HTLV-1 infection, the production of virions can only be seen when infected cells or tissues are cultured *in vitro* (14,16). HTLV-1 can infect $CD4^+$ and $CD8^+$ T-cells, B cells, and synovial cells, but only $CD4^+$ T-cells are transformed and undergo clonal expansion to become ATL (17,18). The virus binds to the T-cells via the GLUT-1 glucose transporter, a cellular receptor present on nearly all mammalian cells (7,19,20). Binding between the viral Env and GLUT-1 allows for fusion of the cell and virus followed by viral entry. Transmission and persistence of HTLV-1 *in vivo* is

believed to occur via the exchange of infected T-cells and cell-to-cell contact infection rather than through production and transmission of infectious virions due to the low infectivity of HTLV-1 virions (14,16). Unlike HIV which relies on virions for infection of host cells, HTLV-1-infected T-cells can form syncytia with uninfected cells or may simply pass the viral genome and viral Gag protein from cell-to-cell via a reorganization of the cytoskeleton to form a "virological synapse" (21). The use of cell-to-cell transmission and clonal expansion of infected T-cells may allow HTLV-1 to spread without detection by the immune system.

Epidemiology of HTLV-1

It is estimated that globally there are currently 20-30 million people infected with HTLV-1 (22-24). The geographic distribution of HTLV-1 includes high prevalence in South America, Africa, southwestern Japan, and the Caribbean Islands with isolated pockets of infection occurring in Iran and Melanesia (9,25-30). In the Caribbean, it is estimated that 3-4% of the population is seropositive for HTLV-1 (31). In Japan, more than 1.2 million people are believed to be infected (9,32). In the United States, HTLV-1 infection seems to prevalent only in specific high risk groups including immigrants from endemic areas and their spouses, intravenous drug users and those involved in prostitution (22,31). Studies of the international prevalence of HTLV-1 infection, however, may be somewhat skewed due to the limited composition of the studied populations, the early use of enzyme-linked immunoassays (EIAs) with reduced-

specificity, and serologic assays that did not discriminate between HTLV-1 and HTLV-2 (22).

There are five different published subtypes of HTLV-1 including subtype A, also known as the cosmopolitan subtype, subtype B, subtype C, subtype D, and subtype E. These subtypes are based on differences in the proviral DNA sequence of the *env* gene and/or long terminal repeat region (33). Subtype A is the most studied and most widely distributed subtype and includes the sequence originally identified for HTLV-1 in Japan (34). Subtypes B, D, and F are found in Central Africa, and subtype E is found in South and Central Africa (33). Subtype C seems to have its origins and highest prevalence in Melanesia (35). Although the subtypes of HTLV-1 seem to be linked geographically, there has been no link observed between infection with a specific HTLV-1 subtype and development of either ATL or HAM/TSP (36,37).

Transmission of the virus occurs through sexual intercourse, sharing of needles and syringes during intravenous drug use, transfusion of infected blood products, and vertical transmission from mother to child during breastfeeding (28,31). Anti-HTLV-1 antibodies and proviral DNA sequences have both been detected in saliva suggesting that the virus could possibly be spread through contact with saliva, but there have been no reported cases of transmission by this route (38). HTLV-1 is believed to spread between hosts through the transmission of infected T-lymphocytes. Both breast milk and seminal fluid are rich stores of T-lymphocytes, and there is some evidence that seminal fluid enhances HTLV-1 replication through TGFβ-mediated upregulation of viral transcription (39). Transmission may occur during cell-to-cell contact on mucosal surfaces of the mouth during breastfeeding and the vagina or penis during intercourse, and transmission

rates may be enhanced by any sort of lesions or ulcerations of the mucosa (16). Blood transfusions or sharing of infected needles by intravenous drug users would allow direct transfer of infected T cells into the bloodstream of the new host. For this reason, the Food and Drug Administration (FDA) began recommending screening of all blood donations in the United States for HTLV-1 in 1988, and since then similar screening protocols have been established in Europe, Canada, Japan, and Brazil (22).

Following the initial HTLV-1 infection, infected T-cells may travel by means of the bloodstream or lymphatic vessels throughout the body to establish reservoirs of infection in areas like the skin, thymus, liver, spleen, lymphoid tissues, and perivascular regions in the central nervous system (16). The specific location of these reservoirs of infection may contribute to the development of specific HTLV-1 associated diseases and conditions.

Diseases of HTLV-1 Infection

Infection with HTLV-1 can lead to adult T-cell leukemia (ATL), HTLV-1 associated myelopathy/tropical spastic paraparesis (HAM/TSP), uveitis, mycosis fungoides, and infective dermatitis. In addition, there are a number of other conditions that appear to be related to HTLV-1 infection including arthritis, pneumonitis, urinary tract disorders, and susceptibility to other infections, but additional studies must be completed to confirm these associations with HTLV-1 (22).

HTLV-1 infected individuals possess a 5% lifetime risk of developing either Adult T-cell Leukemia or HAM/TSP. These two conditions are most often mutually exclusive, although there have been a few reported cases of presentation of both

HAM/TSP and ATL in the same patients (40-43). The criteria for determining which infected individuals will develop each condition remain unknown. Infection by vertical transmission through breastfeeding during childhood may increase the likelihood of developing ATL, while ATL cases following infection post-transfusion are very rare (44-47). This may be due in part to establishment of a reservoir of infection in the thymus early in life, and the subsequent infection of mature and immature thymocytes leading to development of ATL in later decades (16). Development of HAM/TSP seems to be linked to infection later in life through blood transfusion, intravenous drug use or sexual intercourse (22), but there are still no definitive answers as to why only a small percentage of infected individuals develop either of these two diseases.

Adult T-cell Leukemia/Lymphoma

Adult T-cell leukemia was the first cancer causally linked to a human retrovirus. In 1977 in Japan, Uchiyama *et al* described a leukemia with a unique morphology consisting of lobulated nuclei that they termed Adult T-cell leukemia (ATL) (48). In the United States in 1980, Poiesz *et al* described the isolation of a new retrovirus from a cell line derived from a patient with cutaneous T-cell lymphoma which they named Human T-cell Leukemia Virus (HTLV) (1). During continued research in Japan, two groups detected unique serum antibodies in ATL patients and eventually isolated a retrovirus that was named Adult T-cell Leukemia Virus (ATLV) (49,50). Subsequent studies led to the realization that the virus identified in the US and the virus identified in Japan were actually the same virus, and the decision was made to refer to the virus as Human T-cell Leukemia Virus Type 1 (HTLV-1) and the disease caused by the virus as Adult T-cell leukemia (ATL) (51).

Adult T-cell Leukemia is a lymphoproliferative T-cell malignancy that occurs in 1-5% of infected individuals after a long latent period of 20-30 years (22,52,53). Several different patterns of symptoms characterize the disorder, and therefore ATL is categorized into four forms: acute, chronic, smoldering, and lymphoma-type (6). Some patients develop a pre-ATL syndrome characterized by an elevated number of circulating white blood cells prior to the onset of symptoms. These individuals have abnormal lymphocytes that arise from a few HTLV-infected cells (54,55). The chronic or smoldering forms of ATL are characterized by low levels of circulating lymphoid cells and skin lesions caused by infiltration of leukemic cells (56,57). Some patients with chronic or smoldering ATL and some with pre-ATL progress to acute ATL.

Acute ATL is characterized by greatly elevated numbers of circulating $CD4^+$ malignant T- cells that arise from clonal expansion of cells that contain small numbers of integrated HTLV proviruses (2,10,49,58,59). These cells have a distinct morphology with multilobulated, convoluted nuclei and are also referred to as "flower cells" (48,56,60,61). Acute ATL patients often display skin lesions and have enlarged lymph nodes, liver, and spleen, and may exhibit hypercalcemia due to lysis of bone tissue (56,59,62-64). Lymphoma-type patients develop clonal T-cell lymphomas that contain integrated HTLV provirus (2,57,65). Between 50-75% of ATL cases are classified as acute or lymphoma-type, and about 25% are either chronic or smoldering (22,66). With no treatment, acute ATL is invariably and rapidly fatal, and current conventional chemotherapies are ineffective against acute ATL (22). Current studies of novel treatments such as interferon-α plus zidovudine, HDAC inhibitors, monoclonal antibodies, and allosteric stem cell transplantation have had limited successes, but none have been shown to

provide substantial improvement over chemotherapy (64). Patients with HTLV-1-associated lymphomas have a life expectancy of approximately 10 months; those with acute ATL have an average life expectancy of only 6 months with the usual causes of death being pulmonary complications, opportunistic infections, and sepsis (65,67,68).

HTLV-1 Associated Myelopathy/Tropical Spastic Paraparesis

HTLV-1 Associated Myelopathy/Tropical Spastic Paraparesis (HAM/TSP) is a progressive neurodegenerative disorder characterized by slow-onset spastic paraparesis accompanied by sphincter, proprioceptive, and sensory dysfunction (22). The disease develops from severe white matter degeneration and fibrosis resulting from the immunological response to HTLV-1 infection and parenchymal infiltration of mononuclear cells into the gray and white matter of the thoracic spinal cord (69). The disease is most often diagnosed in adults, and develops more frequently in women than in men (70). Evidence suggests that adult exposure to HTLV-1 through blood transfusion or sexual transmission of HTLV-1 predominantly leads to HAM/TSP rather than ATL (71,72). Current therapies for HAM/TSP include corticosteroids, immunosuppressive drugs, anti-spasmodics, and physical therapy, but for HAM/TSP patients, current treatments offer unsatisfactory results with huge costs both financially and in quality of life (22).

Uveitis and Other HTLV-1 Associated Conditions

There have been several other conditions with a suggested link to HTLV-1 infection. Rheumatologic conditions including polymyositis, brachioalveolar pneumonitis, uveitis, auto-immune thyroiditis and arthritis have all been associated with

viral genome or viral proteins detected in affected tissues, but only uveitis, mycosis fungoides, and infective dermatitis have enough epidemiologic evidence to support a causative role for HTLV-1 (16). In studies of HTLV-assiciated uveitis, researchers found a higher number of HTLV-1 infected T-lymphocytes within the vitreous fluid when compared to the peripheral blood compartment (73). Higher rates of arthritis were associated with HTLV-seropositive patients than seronegative ones in an epidemiologic study by Murphy *et al* (74), and high proviral load in peripheral blood and synovial compartments has been associated with rheumatoid arthritis in HTLV-1-infected patients (75), but more studies are needed to strengthen the link between these conditions and HTLV-1 infection.

Prevention

There have been several attempts to develop a vaccine against HTLV-1 infection. In a study by Shida *et al,* the *env* gene from HTLV-1 was cloned into the vaccinia virus with the hemagglutin (HA) gene to form a live recombinant virus. This virus induced antibody production in rabbits with some protection against HTLV-1 infection (76). Kataoka *et al* were able to demonstrate passive immunization with HTLV-1 immune serum in rabbits (77). More recently, a multivalent peptide CTL vaccine with three HTLV-1 Tax protein peptides was developed by Sundaram *et al* that elicited cellular responses in transgenic mice and mice infected with an HTLV-1 Tax recombinant vaccinia virus (78,79). This same group tested the immunogenicity of antibodies against the gp21 and gp46 subunits of the envelope glycoprotein of HTLV-1 that were able to prevent virus-induced syncytia formation (80). Despite these successes however, there are currently no HTLV-1 vaccines being tested in clinical trials.

Due to the lack of an effective vaccine against HTLV-1 infection, currently the best means of prevention of infection is education. At risk groups such as sex workers, intravenous drug users, and women in endemic areas need to be educated in the importance of safe sex practices, eliminating needle-sharing, and avoidance of breastfeeding by infected mothers. Health organizations need to implement these programs in addition to regular screening of all blood donations in order to prevent transmission of the virus through transfusions.

HTLV-1 OncoproteinTax

In ATL, the transformation of $CD4^+$ lymphocytes is mediated through the expression of the HTLV-1 *trans*-activating protein, Tax. The link between Tax expression and transformation has been well established through both *in vivo* and *in vitro* experiments. Introduction of *tax* into NIH 3T3 and Rat-1 cells resulted in transformation, and those cells became tumorigenic when injected into nude mice (81). Transfection of a Tax-expressing vector was shown to immortalize human T-lymphocytes, and *tax* transgenic mice exhibited neurofibromas, mesenchymal tumors and lymphomas (81-84).

Tax is a 353 amino acid protein primarily encoded by a region near the 3' LTR of the viral genome designated as the *pX* region. Tax is predominantly nuclear but has pleiotropic functions requiring that it shuttle between the nuclear and cytoplasmic compartments (85). Tax is phosphorylated on several serine and threonine residues, and our laboratory and others have found that this phosphorylation differentiates the "active" and "inactive" forms of Tax (86-88). Others laboratories have shown that Tax can be

both ubiquitinated and sumoylated, and these modifications contribute to the regulation of Tax subcellular localization (89,90).

The pleiotropic activities of Tax require it to interact with many different cellular proteins, and, as such, Tax has many previously identified functional domains. These include a nuclear localization signal (91,92), a nuclear export signal (85,93), a cyclic-AMP response element binding (CREB) interaction domain, p300/CBP binding domain, NF-κB binding domain (94-98), a zinc-finger domain (99), a dimerization domain (100-102), a PDZ-binding domain (103,104), a KIX-interacting domain (95,105), a leucine zipper-like domain (97), and an activation specific region (106). Additional motifs in Tax that may be involved in protein-protein interactions include an SH3 domain, a LIM domain, and a coiled-coil structure that would all expand the possible cellular binding partners of Tax (107). The exact mechanism of Tax-mediated transformation is unknown, but studies indicate that transformation is related to the ability of Tax to deregulate transcription of genes and signaling pathways involved in cellular proliferation, cell cycle control, DNA repair, and apoptosis.

Transcriptional Trans-activation by Tax

A primary function of Tax is to potently enhance transcription of viral genes. Tax has limited direct contact with DNA through a region in amino acids 89-110, but activates transcription through recruitment of cellular transcription factors to the viral LTR (108,109). The HTLV-1 LTR contains three highly conserved 21-bp repeat elements commonly referred to as the Tax-responsive elements (TRE) which are critical to Tax-mediated transcriptional activation (108). Each TRE has three regions, A, B, C,

and the center B region of the TRE has a conserved 8-nucleotide core sequence TGACGG(T/A)(C/G)(T/A) that closely resembles a consensus cAMP responsive element (CRE) (110). Tax recruits the cyclic-AMP responsive element binding protein (CREB) to the viral LTR and stabilizes the complex on the viral promoter via a domain in the N-terminus of Tax (111,112). The recruitment of CREB by Tax to the LTR provides a high-affinity binding site for transcriptional coactivators such as CREB binding protein (CBP), p300, and p300/CBP-associated factor (P/CAF) (111,113-116). These coactivators induce histone acetylation and chromatin remodeling to allow for an even more stable transcription complex at the promoter (107,115). Studies have shown that Tax can also recruit the coactivator CBP in the absence of CREB phosphorylation resulting in viral transcription (117,118).

Just as Tax activates transcription of the viral genes by recruiting cellular transcription factors to the viral LTR, Tax also *trans*-activates and *trans*-represses transcription of cellular genes through interactions with cellular transcription factors including CREB/ATF, AP-1, SRF, NF-κB and NFAT (119,120). Cellular genes with cAMP responsive elements can be *trans*-activated by Tax in the same manner as the viral LTR (113). Tax can also recruit other CREB/activating transcription factor (CREB/ATF) family members to CRE promoters to activate transcription (114).

Tax activates the NF-κB pathway through interactions with proteins in both the nucleus and the cytoplasm. The NF-κB family members are usually sequestered in an inactive form in the cytoplasm by inhibitory proteins such as IκBα and IκBβ (121,122). Tax activates transcription via the canonical NF-κB pathway by directly binding to IκB kinase γ/NF-κB essential modulator (IKKγ /NEMO), leading to phosphorylation and

degradation of IκB and release of NF-κB to translocate into the nucleus to activate transcription (96,123-125). Tax can also activate the noncanonical NF-κB pathway by interacting with IKKγ and p100, the precursor for p52 resulting in the processing of p100 into p52 and its release to the nucleus to activate transcription (124). In the nucleus, Tax can physically bind to p50, p65, c-Rel, and NF-κB-2 to stabilize these factors on NF-κB-responsive promoters (124). The result of Tax expression is the constitutive activation of the NF-κB pathway in HTLV-1-infected cells leading to upregulation of expression of genes involved with processes such as proliferation and evasion of apoptosis.

Tax is also able to interact directly with the serum response factor (SRF) and its cofactor, ternary complex factor (TCF) to activate or repress transcription at promoters with serum response elements (SREs) (119,126,127). This pathway is responsible for transcription of proto-oncogenes c-Fos, c-Jun, JunB, JunD, and Fra-1 which regulate expression of AP-1 responsive genes involved in evasion of apoptosis and cellular proliferation (8).

Through the interactions with these pathways Tax can cause major changes in the expression of hundreds of genes (119,128). In addition, Tax can physically interact with many cellular proteins and thereby activate or repress their functions (129-143). The downstream effects of Tax transcriptional activation of cellular genes and direct protein-protein interactions is manipulation of the cell cycle, accumulation of mutations due to interference with DNA repair, and evasion of apoptosis.

Tax-mediated Dysregulation of Cell Cycle

The cell cycle involves defined stages during which the cell doubles its number of organelles and volume of cytoplasm, duplicates DNA, segregates the DNA to opposite ends of the cell and then separates into two daughter cells (6). Theses stages are named the gap, or G phases (G1, G2, G0), the synthesis phase (S), and the mitotic phase (M). During G1 phase, the cell prepares for DNA replication by producing synthetic enzymes. G1 phase is followed by S phase during which chromosomes are duplicated. This is followed by G2 phase when the cell prepares for division which occurs during the M phase. The cell will then either return to the G1 phase or enter a quiescent state known as G0 phase (6). The progression of the cell cycle from one phase to the next is regulated by the phosphorylation state of proteins called cyclins that are phosphoryalated by cyclin dependent kinases (cdks) (144). Specific cyclin/cdk complexes regulate each phase of the cell cycle. Progress through the cell cycle is also governed by molecular checkpoints involving cdk inhibitors that can prevent the continuation of the cell cycle at specific phases (145).

Tax interacts with several cell cycle regulatory proteins resulting in accelerated progression past crucial checkpoints. In the G1 phase of the cell cycle, Tax transcriptionally upregulates the expression of several cyclins and cyclin-dependent kinases (cdks) including cyclin D2, cdk4, cdk2, and cyclin E (135,146), and Tax binds to cyclin D3, cyclin D2, and cdk4 and functions to stabilize cyclin D/cdk4 complexes (133). When the concentration of cyclin D/cdk complexes increases, the cell reaches what is known as the restriction point and is committed to completing the G1 phase of the cell cycle (144). Tax transcriptionally represses and/or physically represses cell cycle

inhibitors that would prevent passage throught the restriction point (132,145). Tax also activates transcription of E2F and alters the Rb-bound and Rb-unbound ratio of E2F (144). Together these events result in an abundance of activated cyclin D/cdk complexes and accelerated Rb phosphorylation and subsequent E2F release accelerating the cell through the G1 phase towards the G1/S checkpoint.

Tax expression abrogates the p53-mediated G_1/S checkpoint and dysregulates S phase. During the transition from G1 to S phase, the cell must pause to repair DNA damage before DNA replication to prevent fixing the errors in daughter cells (144). This G1/S checkpoint is regulated by p53. Tax stabilizes p53 and in doing so functionally inactivates p53 (147). Using an additional p53-independent transcriptional upregulation of $p21^{waf1}$ and repression of cyclin A, Tax represses the checkpoint cyclin A/cdk2 complex and promotes cyclin D/cdk2 complex formation and progression through the G1/S checkpoint (130,148-152). Tax repression of cyclin A prevents cyclin A/cdk2-mediated phosphorylation of pre-replication complexes and may also allow for redundant DNA replication during S phase (151). The decreased expression of cyclin A due to Tax-mediated repression may cause an acceleration of mitosis and contribute to the failure of mitotic checkpoint activation (151,153).

The G2/M checkpoint is the last chance for the cell to repair damaged DNA prior to mitosis. DNA damage is recognized by the recognition machinery regulated by ATM/ATR signaling pathways and activates the G2/M checkpoint through Chk1 and Chk2 (144). Tax interacts with both Chk1 and Chk2 and dysregulates the G2/M checkpoint (138). Our lab observed that Tax binds to Chk2 resulting in its activation and an accumulation of cells in G2/M that was relieved by caffeine, indicating that the

accumulation was due to G2 checkpoint activation rather than M checkpoint activation since caffeine inhibits ATM/ATR kinases (129,134). Conversely, Park *et al* have found that Tax physically interacts with Chk1 and impairs phosphorylation of p53 by Chk1. They also found that Tax was able to block degradation of cdc25A and attenuate G2 arrest caused by activation of Chk1 following γ-radiation (IR) (142). Additionally, Tax impairs mitosis by directly binding to the mitotic spindle proteins, mitotic arrest defective protein 1 and 2 (MADs), affecting their stability, localization, and functions and preventing checkpoint activation (136),(154). Tax interacts with APC^{cdc20} prematurely degrading securin and resulting in defective cytokinesis and improper chromatid separation leading to aneuploidy (139).

Overall the effects of Tax on the cell cycle lead to accelerated progression through G1 and S with inactivation of G1/S checkpoint and subsequent loss of DNA damage repair. Tax causes improper replication of DNA during S phase which may result in duplicated chromosomes. Tax abrogates S and G2 checkpoints which increases the likelihood of DNA damage becoming fixed in daughter cells.Tax-induced loss of mitotic checkpoints and premature degradation of regulatory proteins result in mistakes in chromosome separation during mitosis. The end result is genomic instability and eventual cellular transformation.

Tax-mediated Dysregulation of DNA Repair

Tax-expressing cells display a variety of chromosomal abnormalities including deletions, translocations, rearrangements, duplications, micronuclei formation and aneuploidy (81,155-158). During normal progression through the cell cycle, errors occur

during DNA replication. Generally, the cellular repair process is sufficient for correcting these errors. Critical to this response are checkpoints in the cell cycle that pause progression to allow time for DNA damage repair to occur prior to permanent establishment of these errors in daughter cells following mitosis. As described above, Tax can abrogate these checkpoints during the cell cycle that decrease time for DNA repair, but Tax can also directly inhibit DNA repair by interfering with the chromosome maintenance and DNA repair pathways.

DNA is repaired using several pathways including base excision repair, nucleotide excision repair, and double-strand break repair (159). There is evidence that base excision repair activity is specifically repressed by Tax (159) partly by repressing transcription of human DNA polymerase β (160). This enzyme is involved in both base excision repair and mismatch repair, and suggests that Tax may also inhibit mismatch repair (MMR), although additional studies are needed to confirm inhibition of MMR by Tax (144). Tax may impair nucleotide excision repair by *trans*-activating transcription of proliferating cell nuclear antigen (PCNA) (156). Increased PCNA has been shown to promote DNA replication by DNA polymerase δ through damaged regions of template DNA, thus inhibiting nucleotide excision repair of those regions (161,162). Damage resulting in double-strand breaks (DSB) typically requires repair via the error-prone non-homologous end joining (NHEJ) pathway. This pathway recognizes DSBs, processes the ends by deleting 1-10 bases, and joins the two broken ends (163). By microarray analysis, Tax-expressing cells were found to have decreased expression of two important members of this pathway, Ku and DNA-PKcs (164). The induction of micronuclei is a sensitive measurement of mitogen-induced DNA damage (165). Majone *et al* found that

Tax increases mitogen-induced micronuclei formation and that Tax-induced micronuclei formation is dependent on Ku80 (166,167). Our lab has shown that Tax binds to and functionally impairs DNA-PK as well as the downstream DNA-PK target checkpoint protein Chk2 and early damage response gene 53BP1 (134,168). DNA-PK is also involved in the maintenance of telomeric ends to prevent them from being recognized as DSBs (169). Tax represses expression of another enzyme involved in telomere maintenance, human telomerase (hTert) (170). Together the repression of hTert and inhibition of DNA-PKcs by Tax may result in telomeres being treated as DSBs which results in translocations, chromosome breaks, and chromosomal end-to-end fusion leading to aneuploidy. The overall repression of DNA repair by Tax is thought to contribute to an accumulation of mutations resulting in genomic instability and eventual cellular transformation.

Tax-mediated Dysregulation of Apoptosis

Cells with significant DNA damage are usually induced to undergo apoptosis. Tax-expressing cells are resistant to apoptotic signals (171). This resistance has been found to be mediated through the *trans*-repression by Tax of apoptotic genes, *trans*-activation by Tax of anti-apoptotic genes and constitutive activation by Tax of the NF-κB pathway all of which have been described previously. Another means of dysregulation of apoptosis by Tax involves interference with the function of p53. DNA damage leads to activation of p53 resulting in cell cycle arrest or apoptosis (172). Moderate damage can usually be repaired during the pausing of the cell cycle at the p53-mediated G1/M checkpoint, but extensive damage causes p53 to trigger apoptosis through upregulating pro-apoptotic genes and activating caspase cascades (172). Tax has been shown to

inactivate the function of p53, although the exact mechanism of the inactivation is poorly understood (147,173,174). Some studies indicate that Tax may compete with p53 for binding to p300/CBP (175) . Other studies suggest that inactivation of p53 by Tax involves the NF-κB/RelA pathway (174). Tax also inhibits apoptosis through activation of AKT and the subsequent expression of the anti-apoptotic gene BCL-xl (176). This tips the balance between the pro- and anti-apoptotic Bcl proteins towards survival and resistance to apoptosis. The functions of Tax which dysregulate cell cycle, DNA repair, and apoptosis result in an accumulation of mutations and chromosomal aberrations that are characteristic of genomic instability and lead to cellular transformation.

Tax Cellular Localization

All of these deleterious effects can be ascribed to protein-protein interactions between Tax and cellular proteins. In order for Tax to accomplish these interactions, it is necessary that cellular nuclear proteins be brought into close proximity of Tax. One way to accomplish this is through the targeting of Tax to some of the protein complexes that exist within discrete locations within the nucleus. These complexes of subnuclear protein structures assemble at specific subnuclear sites to perform specific functions (177). Categories of proteins believed to form these subnuclear structures are transcription factors, small nuclear ribonucleorprotein particles (snRNPs), chromatin remodeling proteins, and DNA damage recognition and repair proteins (177).

There are several known types of large protein complexes present in the nucleus including speckles, paraspeckles, Cajal bodies, gems, and Nuclear Domain 10 (ND10)/

promelocytic leukemia (PML) bodies (178,179). Nearly all of these subnuclear structures contain subpopulations of cellular splicing factors, but each is distinguished by the presence of a nuclear protein unique to each structure (180). Cajal Bodies contain snRNPs for pre-messenger RNA and ribosomal RNA processing and the autoantigen p80 coilin (180). Gems, or Gemini of Cajal bodies, contain the "survival of motor neurons" protein, SMN (181). ND10/PML bodies contain promyelocytic leukemia protein (182). Paraspeckles contain paraspeckle proteins 1 and 2 and p54/nrb (180). Nuclear Speckles are interchromatin granule clusters (IGCs) that contain the pre-messenger RNA splicing machinery including snRNPs, non-snRNP splicing factors, and spliceosome subunits such as the spliceosome component 35 protein (SC35) (180). These speckles are also referred to as SC35 domains.

Nuclear Tax localizes to discrete nuclear bodies that we previously named Tax Speckled Structures (TSS) (183). These foci are IGCs located at sites partially overlapping with transcriptional hot spots as indicated by the cellular splicing marker SC35. These nuclear bodies do not contain promyelocytic leukemia protein, do not colocalize with nucleoli, and are therefore defined as nuclear speckles (184). The Tax Speckled Structures overlap with SC35 domains at their periphery, but contain other cellular proteins within their cores making them nuclear structures unique to Tax-expressing cells. We found that expression of Tax results in the recruitment of usually diffuse nuclear proteins into the TSS. These proteins include DNA-PKcs, Chk2, and 53BP1, proteins involved in DNA damage recognition and repair (129,134,168). The formation of TSS and the colocalization of SC35, DNA-PKcs, Chk2, and 53BP1 in the TSS with Tax places Tax near the cellular machinery for transcription, splicing, and

DNA damage response and checkpoint activation. This may help explain how Tax is able to affect so many different cellular proteins and functions simultaneously (134).

Tax possesses both a nuclear localization signal (NLS) and a nuclear export signal (NES) and "shuttles" between the nuclear and cytoplasmic compartments (85,91,93,185). Tax has both nuclear and cytoplasmic functions, and the control of Tax localization to different subcellular compartments is critical to Tax function. While in the cytoplasm, Tax activates the NF-κB pathway by interacting with IKKγ/NEMO and releasing NF-κB proteins to enter the nucleus and activate transcription of NF-κB–responsive genes (124). NF-κB transcription factors are key regulators of immune, inflammatory, proliferative, and apoptotic pathways (124). Constitutive NF-κB activation is a hallmark of HTLV-1-infected and Tax-expressing cells and is believed to be necessary for transformation (124). Restriction of Tax localization to the cytoplasm would increase the activation of the NF-κB pathway and could possibly accelerate the process of transformation or exacerbate the immune response. The nuclear functions of Tax include transcriptional activation and repression, interaction with cell cycle proteins, and interactions with DNA damage recognition and repair proteins (129,132,134,168). Many of these nuclear functions are believed to occur in the TSS. Restriction of Tax to the nucleus and the TSS could result in increased genomic instability leading to accelerated transformation. Therefore the regulation of the localization of Tax to the TSS and other subcellular regions may be critical to Tax-induced transformation.

SECTION 2

SPECIFIC AIMS

Human T-cell leukemia virus type 1 (HTLV-1) is the etiological agent for both adult T-cell leukemia (ATL) and a neurodegenerative disorder known as HTLV-associated myelopathy/Tropical spastic paraperesis (HAM/TSP) as well as other subneoplastic conditions. In ATL, the immortalization and transformation of T-lymphocytes can be attributed to the expression and activity of a single HTLV-1 viral protein, namely the transactivating protein Tax. Although the exact mechanism of Tax-mediated transformation is unknown, studies indicate that Tax expression leads to genomic instability within the host cell by disruption of cellular DNA repair mechanisms, dysregulation of cell cycle, and interference with chromosome separation during mitosis.

Tax has both nuclear and cytoplasmic functions, and the control of Tax localization to the different subcellular compartments is critical to regulation of Tax function. While in the cytoplasm, Tax activates transcription via the NF-κB pathway by directly binding to IκB kinase γ/Nf-κB essential modulator (IKKγ /NEMO) leading to phosphorylation and degradation of IκB. While in the nucleus, Tax interacts with cellular transcription factors to activate or repress transcription of cellular genes via the CREB and SRF pathways, and Tax interacts with proteins involved in DNA damage recognition and repair, cell cycle regulation, and chromosomal separation during mitosis. Tax enters the nucleus by its NLS and is directed to discrete nuclear foci referred to as Tax Speckled Structures (TSS). These TSS are interchromatin granules made of multi-protein complexes that contain Tax and cellular proteins involved in diverse functions such as transcription, DNA damage recognition and DNA repair.

In order to develop more effective treatments for ATL and HAM/TSP, we must obtain a more thorough knowledge of how Tax expression contributes to genomic instability within the host cell. The studies proposed in this dissertation are significant because they will provide insight into the underlying molecular events that localize Tax to specific nuclear sites that may regulate DNA damage response, DNA repair, and cell cycle checkpoint activation and where interference with these processes by Tax could lead to genomic instability. These studies may also provide specific therapeutic targets to prevent Tax-mediated cellular transformation by preventing Tax localization to TSS.

Although the nuclear localization signal (NLS) for Tax has been previously defined, the domain in Tax that dictates TSS localization and cellular proteins that may be involved in the regulation of Tax subcellular localization remain unknown. The objective of this project is to characterize the regulation of the subcellular localization of Tax. The hypothesis is that the targeting of Tax into different subcellular and subnuclear compartments is critical to Tax function and is directed by internal domains, dimerization, and protein-protein interactions. This study will make a significant contribution to understanding how Tax localization and function affects cell functions leading to cellular transformation.

The objective of this proposal will be accomplished by pursuing the following specific aims:

Aim 1. Determine the domain(s) within Tax that dictate subnuclear localization to the Tax Speckled Structures. Using an extensive deletion mutagenesis approach, we will define the protein domain(s) that are required for proper targeting of Tax to the TSS. We will examine the functional significance of TSS targeting.

Aim 2. Determine the role of Tax dimerization in subcellular localization. Using Tax deletion mutants generated in Aim 1, we will perform dimerization assays and fine map the Tax dimerization domain. We will investigate the relationship between Tax dimerization, nuclear localization, and function.

Aim 3. Determine the role of protein-protein interactions in Tax subcellular localization. Ubiquitylated forms of Tax are localized to the cytoplasm whereas sumoylated forms are localized in the nucleus. RNF4 was recently found to be a SUMO-dependent ubiquitin ligase protein with no previously identified targets. We will determine the effect of RNF4 on Tax localization.

SECTION 3

IDENTIFICATION OF TAX TSS LOCALIZATION SIGNAL

Introduction

Human T-cell Leukemia Virus Type 1 (HTLV-1) is the causative agent of both HTLV-1 Associated Myelopathy/ Tropical Spestic Paraperesis (HAM/TSP) and Adult T-cell Leukemia (ATL). In ATL, the transformation of lymphocytes is due to the expression of a single viral protein, Tax. Tax has both nuclear and cytoplasmic functions, thus necessitating that control of Tax localization to subcellular compartments is critical to overall Tax function (85,91,183). Tax has an NLS sequence in the N-terminal region of the protein that is necessary and sufficient for nuclear localization (91,185,186). We previously showed that Tax "shuttles" between the nuclear and cytoplasmic subcellular compartments and identified a consensus NES sequence defined by amino acids 190 to 203 (85). Fine mapping mutational analysis of this region by Alefantis et al (93) clearly demonstrated a functional NES at this site. These signals presumably mediate interactions between Tax and karyopherins in the nuclear pore complex (NPC) to allow Tax to translocate through the nuclear membrane (187,188). The specific importins and exportins involved in Tax transport have yet to be identified, but recent studies indicate that Tax can be both imporedt and exported from the nucleus without the aid of carrier proteins or energy and can interact directly with the FG-nucleoporins within the core of the NPC (189). Both the NLS and the NES of Tax are atypical. The NLS is rather large, involving the first forty-eight amino acids of Tax, and it is lacking in the highly basic residues that define classical NLSs (91,185,186). It contains a zinc finger domain (two zinc fingers) at amino acids 22-53 (185,186) and a

phosphorylation site at threonine 48 (86), and it overlaps most of the CREB-binding domain (106). The NES of Tax is a leucine-rich region between amino acids 188 and 202 that is capable of mediating export of Tax via the CRM-1 pathway although with notably slower kinetics (85,93). This NES is believed to be masked in the native Tax protein and there is strong evidence that ubiquitination may "unmask" the NES in response to DNA damage (90) . In fact, "nuclear" Tax is predominately sumoylated whereas "cytoplasmic" Tax appears to be primarily ubiquitylated (89).

While in the cytoplasm, Tax activates transcription via the NF-κB pathway by directly binding to IκB kinase γ/NF-κB essential modulator (IKKγ /NEMO), leading to phosphorylation and degradation of IκB and release of NF-κB (96,123,124). In the nucleus, Tax interacts with cellular transcription factors to activate or repress transcription of cellular and viral genes via ATF/CREB, NF-κB and SRF pathways (107). Tax is capable of dimerization, and studies indicate that optimal transcriptional *trans*-activation by Tax requires that it be in a dimeric or oligomeric form (91,100,101). Nuclear Tax also physically interacts with several cellular proteins and modulates their functions (129-143). While the NLS and NES provide one level of regulation for Tax localization, it is likely that there are other mechanisms at work in regulating Tax subcellular and subnuclear localization and thus function.

In previous studies we and others have demonstrated that Tax enters the nucleus and is directed to discrete nuclear foci that we termed Tax Speckled Structures (TSS) (183,190). TSS coincide with interchromatin granules and consist of multi-protein complexes that partially overlap with subnuclear regions involved in splicing and transcription. We have also shown that Tax recruits cellular proteins involved in the

DNA damage recognition and repair response into the TSS as well (129,134,168,191). The formation of TSS and the colocalization of SC35, DNA-PKcs, Chk2, and 53BP1 in the TSS places Tax near cellular machinery for transcription, splicing, DNA damage response and checkpoint activation and may explain how Tax is able to affect multiple cellular functions simultaneously (134,144). Although the nuclear localization signal (NLS) for Tax has been previously defined, the domain in Tax that dictates TSS localization remains unknown.

Since the Tax NLS itself is so unusual, it may likely also contain the sequence responsible for directing Tax to the TSS. In order to separate the NLS function from the possible TSS targeting function, we have introduced an exogenous NLS from the large T antigen of SV40 to ensure transport of Tax into the nucleus. In this study, we transiently expressed Tax constructs containing partial deletions of the Tax NLS and evaluated the effect of each deletion on the protein's localization to TSS. We also created deletions along the length of Tax to test for possible TSS targeting function in regions outside of the NLS. We isolated a region containing the likely TSS targeting sequence and tested whether it alone could target a normally diffuse GFP protein into the TSS. In this manner we defined the minimal sequence that is both sufficient and necessary for dictating Tax targeting to TSS.

Experimental Procedures

Plasmids

The *STaxGFP* and *SGFP* expression vectors were constructed by inserting the *tax*-EGFP fusion or the *EGFP* ORF into the *SmaI* site of *pTriEx4-Neo* (Novagen, Madison, WI) in frame with the amino terminal S- and His-tags.

Site-Directed Mutagenesis

The *STaxGFP* mutants were created with PCR-based site-directed deletion mutagenesis using Quickchange XL mutagenesis kit (Stratagene, La Jolla, CA). Forward and reverse primers were designed containing the desired mutations according to the manufacturer's protocol. Primers used were 5'(GGTCCCCCGAGGATCGCCCATCT CTG GGGG) and 3'(CCCCAGAGATGGGCGATCCTCGGGGGACC) for *STax(d1-29)GFP*, 5'(CAAGGCGACTGGTGCCAGATCACCTGGGACCCC) and 3'(GGGGT CCCACGGTGAT CTGGCACCAGTCGCCTTG) for *STax(d29-52)GFP*, 5'(GGCCAC CTGTCCAGAGCATAAC ATTCCACCCTCC) and 3'(GGAGGGTGGAATGTTATG CTCTGGACAGGTGGCC) for *STax(d52-99)GFP*, 5'(CGCCAATCACTCATACAACC CCCGTTGTCTGCATGTACC) and 3'(GGTACATGCAGACAACGGGGGTTGTATG AGTGATTGGCG) for *STax(d99-150)GFP*, 5'(CCCTCTGGGGAGGCTCCGGGGCCC TAATAATTC) and 3'(GAATTATTAGGGCCCCG GAGCCTCCCCAGAGGG) for *STax(d150-202)GFP*, 5'(CTATAAAATTTCCCTCACCACACCTATGATTTCCGGG CCC) and 3'(GGGCCCGGAAATCATAGGTGTGGTGAGGGAAATTT TATAG) for *STax(d202-254)GFP*, 5'(GGACATTTACCGATGGCACGGGACATTTACCGAT GGCACG) and 3'(CGTGCCATCGGTAAATGTCCCGTGCCATCGGTAAATGTCC)

for *STax(d254-289)GFP*, 5'(GGCCTACCACCCCTCAGAAAAAGAGGCAGATGAC) and 3'(GTCATCTGCCTCTTTTTCTGAGGGGTGGTAGGCC) for *STax(d289-322)GFP*, and 5'(CCCCATTTCTCTACTTTTTAACGTGGATCCACCGGTCGCCAC C) and 3'(GGTGGC GACCGGTGGATCCACGTTAAAAAGTAGAGAAATGGGG) for *STax(d322-353)GFP*. Methylated *STaxGFP* plasmid derived from bacteria was used as the template, and mutagenic primers that would "loop out" the desired deletion were extended using *PfuTurbo* high-fidelity DNA polymerase. Following an 18 cycle PCR, the remaining methylated template was digested using the DpnI provided, and the mutated PCR product was used to transform BL10-Gold competent bacteria. Bacterial colonies growing under ampicillin selection were isolated, amplified, and plasmid DNA was purified using the Qiagen Miniprep Kit (Qiagen, Valencia, CA). The non-GFP versions of the Tax deletion mutants were created by digestion of the *STaxGFP* mutants (which have BamH1 restriction sites flanking the GFP fusion) with *BamH1* followed by re-ligation with DNA T4 ligase in the buffer provided by the manufacturer (Invitrogen, Carlsbad, CA). The *S-NLS-TaxGFP* constructs were created by inserting the SV40 T-antigen nuclear localization signal in frame between the S tag and the *tax-GFP* fusion using the PCR-based Excite mutagenesis kit (Stratagene, La Jolla, CA). Primers used were 5' (GGTCCCCCGAGGATCGGATCCAAAAAAGAA GAGAAAGGTAATG GCCCACTTCCC) and 3' (CTGGGAAGTGGGCCATTACCTTTCTCTTCTTTTTTG GATCCGATCCTCGGGGGACC). *STax1-75GFP* and *SNLSTax50-75GFP* were constructed by PCR-based mutagenesis using the Phusion site directed mutagenesis kit (Finnzymes Inc. Woburn, MA) using the primers 5' (GTGGATCCACCGGTCGCCA CCATG) and 3'(GAGTCGAGGGATAAGGAA CTGTAGAGCTGA) and

5'(GAGCATCAGAT CACCTGGGACCCC) and 3'(TACCTTTCTCTTCTTTTT TGGATCCGATCC) and using *STaxGFP* and *S-NLS-TaxGFP* as the templates. Sequences of all mutants were confirmed by DNA sequence analysis using a T7 forward primer (Davis Sequencing, Davis, CA), and expression was confirmed by transfection and immunoblot anaylsis as described below with polyclonal anti-Tax or anti-GFP antibody (Santa Cruz Biotechnology, Santa Cruz, CA).

Cell Culture and Transfection

HEK 293 cells and HeLa cells were maintained at 37°C in a humidified atmosphere of 5% CO_2 in air in Iscove's modified Delbecco's medium supplemented with 10% fetal bovine serum (Cambrex, East Rutherford, NJ) and 1% penicillin/streptomycin (Invitrogen, Carlsbad, CA). Transfections were performed by the standard calcium phosphate precipitation method. Plasmid DNA for each construct was prepared using a Qiagen Plasmid Maxiprep Kit following manufacturer's protocol following amplification of transformed DH5α competent *E. coli* bacteria grown overnight under ampicillin selection. For immunoblotting assays, cells were plated in 100-mm plates at 2 x 10^6 cells per plate. For transcriptional activation assays cells were plated into 6-well plates at 2x 10^5 cells per well. The day 10 μg plasmid DNA in 10cm plates or 3μg DNA in each single well of a 6-well plate in 2M $CaCl_2$ and 2x HEPES-buffered saline was added dropwise to the cells in fresh medium. The cells were washed 16 hours post-transfection and incubated at 37°C until harvest. Cells were harvested 48 hours post-transfection following a single wash with 1x phosphate-buffered saline in 400 μl of Mammalian Protein Extraction Reagent M-PER (Pierce, Rockford, IL) with protease inhibitor cocktail (Roche Applied Science, Palo Alto, CA) and immediately frozen.

Transcriptional Transactivation Assay

HEK 293 cells were transiently transfected with 1 ug plasmid DNA for either p*HTLV-LTR-Luciferase* or p*NFκB-Luciferase* (Clontech, Mountain View, CA) and 2 ug plasmid DNA of the appropriate Tax construct to be assayed. Total DNA per transfection was normalized to 3μg total DNA with the addition of parental vector, *pTriEx4-Neo* (Novagen, Madison, WI). Cells were harvested 48 hours post-transfection by washing once with ice cold phosphate-buffered saline (PBS) and then lysing the cells in 400 μl 1X Reporter/Lysis Buffer (Promega, Madison, WI). Lysates were immediately frozen at -80°C. Samples were allowed to thaw on ice, collected, and protein concentration was determined using the Bradford Protein Assay (Bio-Rad, Hercules, CA). A total of 1 μg protein of each sample was applied to 100 μl of luciferase substrate (Promega, Madison, WI) and luciferase activity was immediately measured in a Turner TD-20/20 luminometer (Turner Designs, Sunnyvale, CA). Transcriptional activation was analyzed and expressed as fold activation over reporter alone (fold activation=1). All assays were performed three times with triplicates of each sample.

Cell Cycle Analysis

To determine the effect of the Tax mutants on cell cycle progression, HEK293T cells were transiently transfected with STaxGFP or deletion mutant as previously described. 48 hours post transfection, cells were washed once with PBS and collected by harvesting and centrifugation at 1000rpm for 10 minutes at 4°C. Cells were fixed with the addition of 1 mL ice cold 70% ethanol and incubated at 4°C overnight. The ethanol was removed by centrifugation and cells were washed twice with 1 mL PBS. Cells were

resuspended in 1 mL propidium iodide solution (50 μg/mL propidium iodide and 100 units/mL RNase A in PBS) and incubated for 30 minutes at room temperature with gentle rotation. The cells were washed once with PBS and then resuspended in 500μL PBS. DNA flow analysis was conducted on a FACScan (BD Biosciences, San Jose, CA) with Modfit LT software (Verity Software House, Topsham, ME).

Immunofluorescence Confocal Microscopy

HEK 293 cells or HeLa cells were seeded at 1x 10^5 cells/well on ethanol-washed 22-mm diameter glass coverslips in 6-well plates. Each well was transiently transfected with the indicated expression plasmids. After 48 hours, the cells were washed three times with PBS and subsequently fixed in 4% paraformaldehyde/PBS for 12 minutes at room temperature. Coverslips were washed twice with PBS, permeablized with methanol for two minutes at room temperature, washed three times with PBS, and incubated overnight at 4°C with primary antibodies diluted 1:1000 in 3% bovine serum albumin-PBS. Cells were washed twice with PBS/0.1% Tween 20 and twice with PBS and then incubated for 1 hour at room temperature with AlexaFluor-488 (green) or -594 (red) secondary antibodies (Molecular Probes, Eugene, OR) and TO-PRO-3' iodide (Molecular Probes, Eugene, OR) diluted 1:1000 in 3% BSA-PBS. Coverslips were washed twice with BSA-PBS and twice with PBS and then mounted on glass slides using Vectashield with 4', 6-diamidino-2-phenylindole (DAPI) (Vector Laboratories, Burlingame, CA). Confocal fluorescent images were acquired on a Zeiss LSM 510 confocal microscope (Carl Zeiss, Jena, Germany) using argon (488nm), HeNe1 (543nm), and HeNe2 (633nm) lasers with 63× objective oil lens with 2× zoom and imaged with LSM Image Browser software (Carl Zeiss, Jena, Germany).

Complementation Analysis

A myc-tagged version of the NLS mutant, *mycTax(d29-52)* was coexpressed with the TSS targeting mutant, *STax(d52-99)GFP*. Localization of the coexpressed proteins was visualized with confocal immunofluorescence microscopy as previously described. Tax and mutants were detected by direct fluorescence of GFP. Myc-tagged Tax and myc-Tax mutant were detected by indirect immunofluorescence staining with rabbit polyclonal anti-myc tag primary antibody (Abcam) at a dilution of 1:1000 followed by goat anti-rabbit secondary antibody conjugated to Alexafluor 594 (Molecular Probes, Eugene, OR) at 1:1000 dilution.

Results

Deletion Scanning Mutational Analysis of Tax

We constructed a series of consecutive 25-52 amino acid deletions that covered the length of the Tax protein as depicted in Figure 1A. These constructs included an N-terminal S tag for protein purification and a C-terminal GFP tag for localization studies. Expression of each of the mutants was confirmed by imunnoblot analysis (data not shown). We then analyzed each of the mutants for transcriptional *trans*-activation, cell cycle dysregulation, and subcellular localization. Nearly all of the deletion mutants had no transcriptional *trans*-activation for either an HTLV-1 responsive or an NFKB-responsive promoter/reporter (Figure 1B). The only exception was the C-terminal deletion mutant STax(d322-353)GFP which had a *trans*-activation activity higher than that of wildtype Tax for both promoters. Tax expression leads to an accumulation of cells

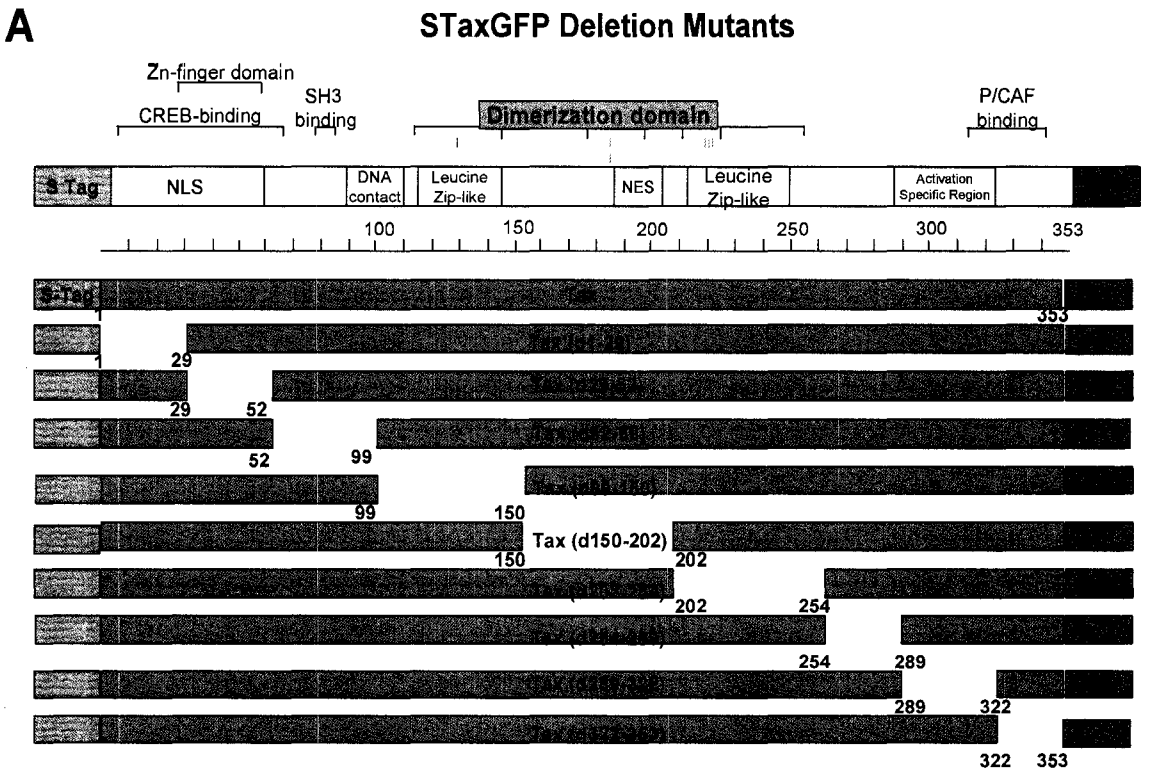

FIG.1. **Tax Mutant design and Transcriptional Activation.** A.) Diagram depicting domains in STaxGFP deleted in scanning series of Tax mutants. B.) Transcriptional transactivation of mutants on HTLV1-LTR-Luciferase and NF-κB-Luciferase promoters/reporters. 293T cells were transiently transfected with reporter and either STaxGFP (STG) or deletion mutant, and lysates were analyzed for relative activity compared to empty vector-transfected cells (relative activity=1).

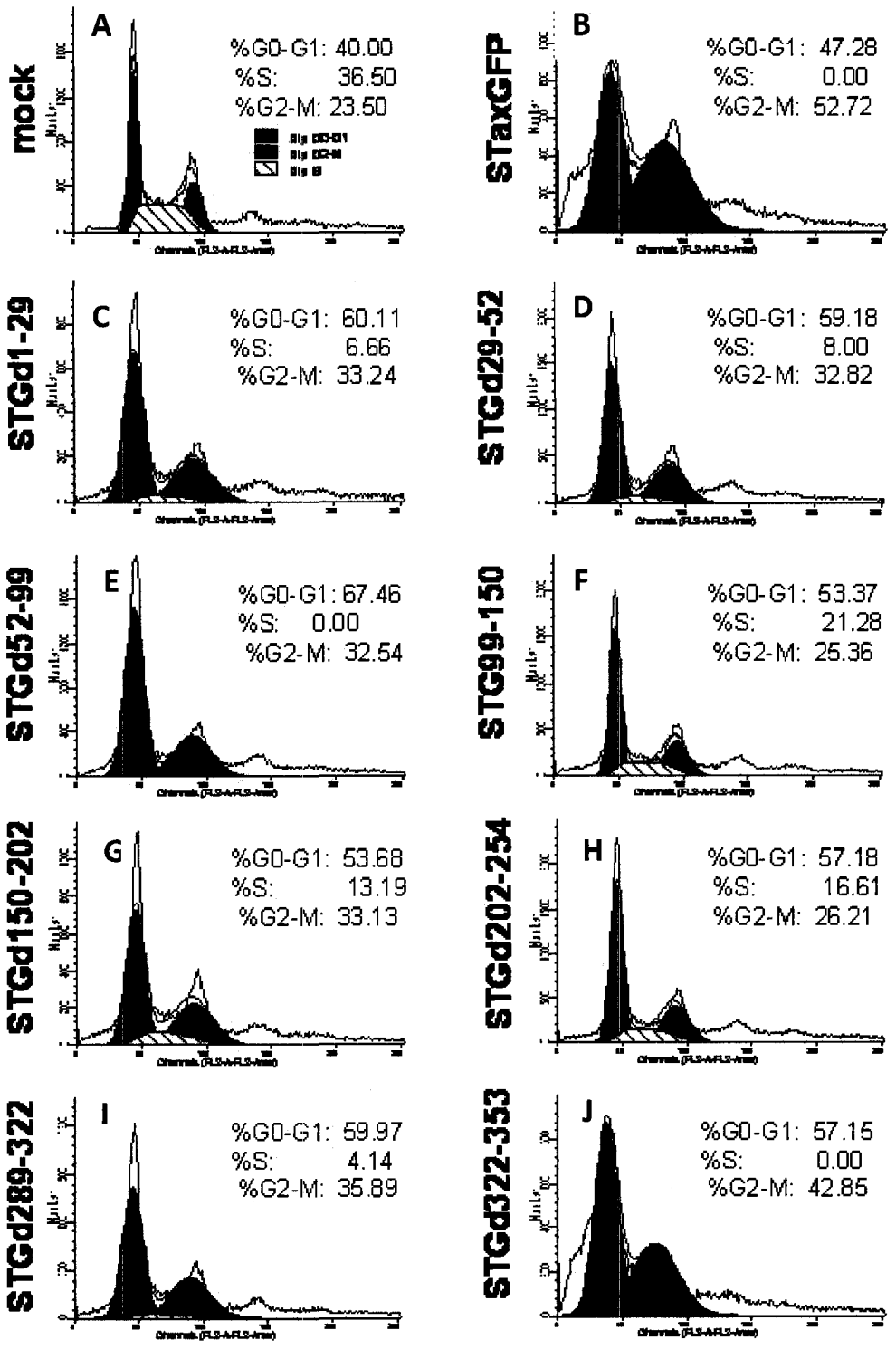

FIG. 2. **Cell Cycle Analysis of 293T cells Expressing Tax Mutants.** The histograms represent the distribution of cells throught the cell cycle measured by flow cytometry and analyzed by Modfit. Cells were transiently transfected with plasmid DNA for pTri-Ex4 Neo (mock), STaxGFP, or Tax deletion mutant as indicated. The percentage of cells in G2/M is shown.

in the G2/M phase of the cell cycle (Figure 2, B). Cell cycle analysis of the Tax mutants demonstrated that only STax(d322-353)GFP had an effect on cell cycle progression comparable to that of wildtype Tax (Figure 2, J). The other Tax mutants were unable to induce the accumulationof the cells in G2/M and the cell cycle distribution resembled that of the mock-transfected cells (Figure 2, A, C-I). These results were not surprising since earlier studies indicate that almost any mutations of Tax, including point mutations, completely ablate Tax activity (92). Confocal microscopy studies revealed that the mutants displayed one of three phenotypes: localization in discrete nuclear foci, diffuse nuclear localization, or cytoplasmic localization (Figure 3). One mutant deleted in part of the Tax NLS, STax(d1-29)GFP, was weakly able to enter the nucleus and form foci while the other NLS mutant, STax(d29-52)GFP was completely confined to the cytoplasm. Mutants deleted in the mid region of Tax including STax(d99-150)GFP, STax(d150-202)GFP, STax(d202-254)GFP, and STax(d254-289)GFP were also confined to the cytoplasm. The two C-terminal deletion mutants, STax(d289-322)GFP and STax(d322-353)GFP formed nuclear foci. One mutant, STax(d52-99)GFP displayed a diffusely nuclear localization with no apparent foci.

Tax Mutant Localization into TSS

We next confirmed whether the foci formed by the nuclear Tax mutants were true Tax Speckled Structures (TSS) as defined as having colocalization with the cellular marker of transcriptional hot spots, spliceosome component 35 (SC35). Three of the four mutants were able to form TSS (Figure 4) including STax(d1-29)GFP, and two C-terminal Tax deletions, STax(d289-322)GFP and STax(d322-353)GFP. One construct, STax(d52-99)GFP, was able to enter the nucleus, but did not form TSS, demonstrating

FIG. 3. **Localization of STaxGFP Mutants.** Confocal microscopy images of Tax mutants transiently expressed in 293T cells. Cells were fixed, and nuclei were stained with TO-PRO-3' iodide at a dilution of 1:1000. Tax expression is detected via the GFP fusion.

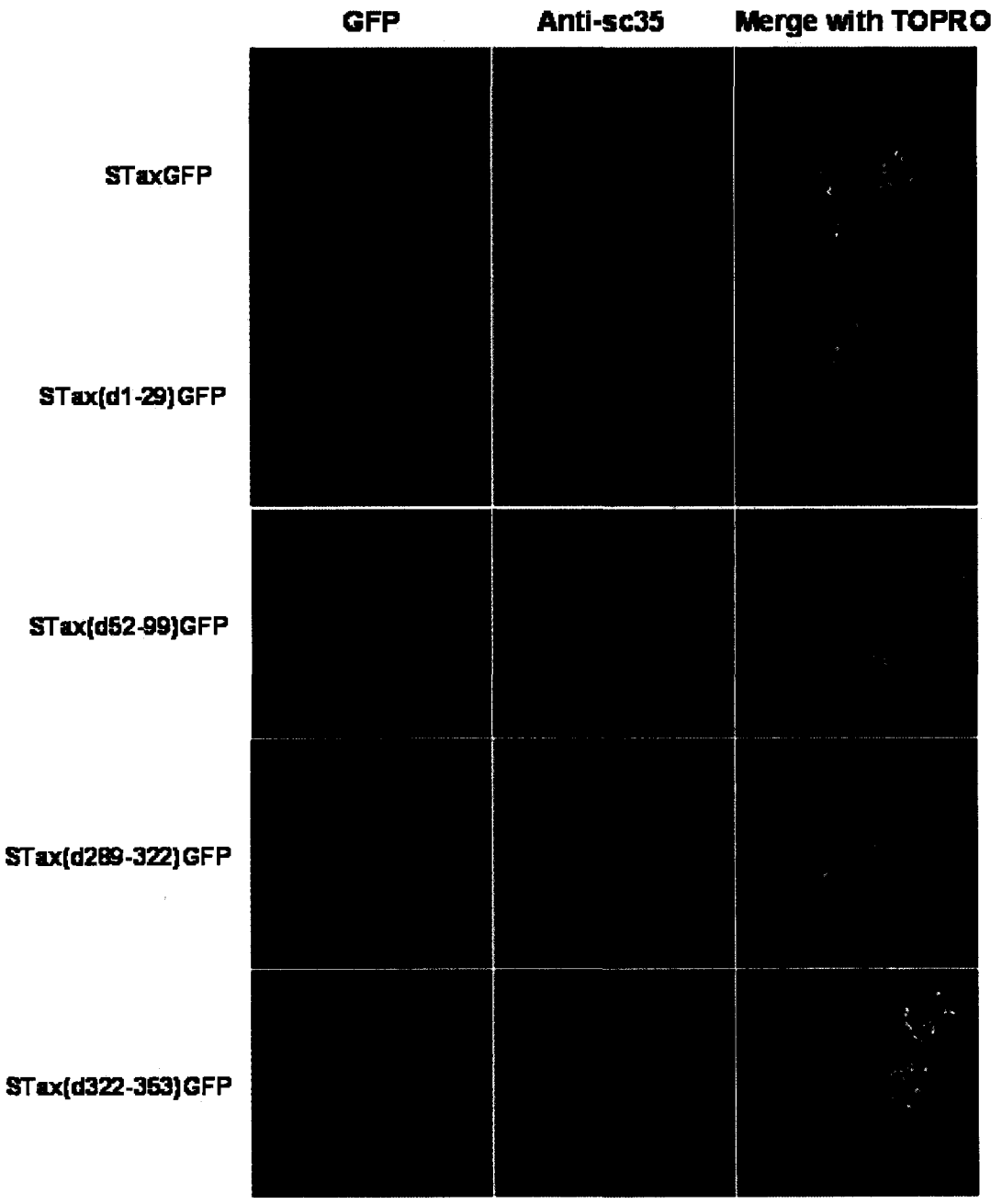

FIG. 4. **Colocalization of Tax Mutants with SC35 in TSS.** Confocal microscopy images of fixed 293T cells transiently expressing nuclear Tax mutants. SC35 was detected with mouse anti-SC35 antibody (Invitrogen) at a dilution of 1:1000 followed by goat anti-mouse Alexafluor 594-conjugated secondary antibody at a dilution of 1:1000 (Molecular Probes). Nuclei were stained with TO-PRO 3' iodide (Molecular Probes) at a dilution of 1:1000.

the retention of NLS function and implicating this deleted region as a TSS specific targeting sequence.

A Novel N-Terminal Domain Is Sufficient for Localization of Tax to TSS

In order to more precisely define the TSS targeting domain, we designed constructs containing only the first 75 amino acids of Tax inserted in frame between the N-terminal S tag and the C-terminal GFP. This construct was able to target GFP into TSS that were indistinguishable from those of wildtype Tax (Figure 5, A and C). A construct containing only the S tag and GFP was expressed diffusely throughout the cell with no targeting to nuclear foci (Figure 5B). The nuclear localization signal (NLS) for Tax is defined as amino acids 2 to 48 (91,185,186), and deletion of this region would interfere with nuclear translocation. In order to determine if the TSS targeting domain is distinct from the NLS, we inserted an exogenous NLS from the SV40 Large T Antigen (Tag) in frame between the S tag and Tax1-75GFP. This insertion did not interfere with the targeting of GFP to TSS (Figure 5D). We then deleted the first 49 amino acids of Tax to create S-NLS-Tax50-75GFP and observed that this construct was also able to target the GFP fusion into the TSS (Figure 5E). This indicates that the Tax speckle targeting signal (TSTS) is outside of the Tax NLS and within amino acids 50-75 of Tax.

Cytoplasmic Phenotype is Not Cell- or Fusion Tag-Specific

In our original scanning series of deletion mutants of Tax, there were four mutants that were confined to the cytoplasm despite having an intact nuclear localization signal. In order to determine whether this was a phenotype specific to 293T cells, we expressed the same Tax deletion constructs in HeLa cells. Confocal microscopy analysis revealed

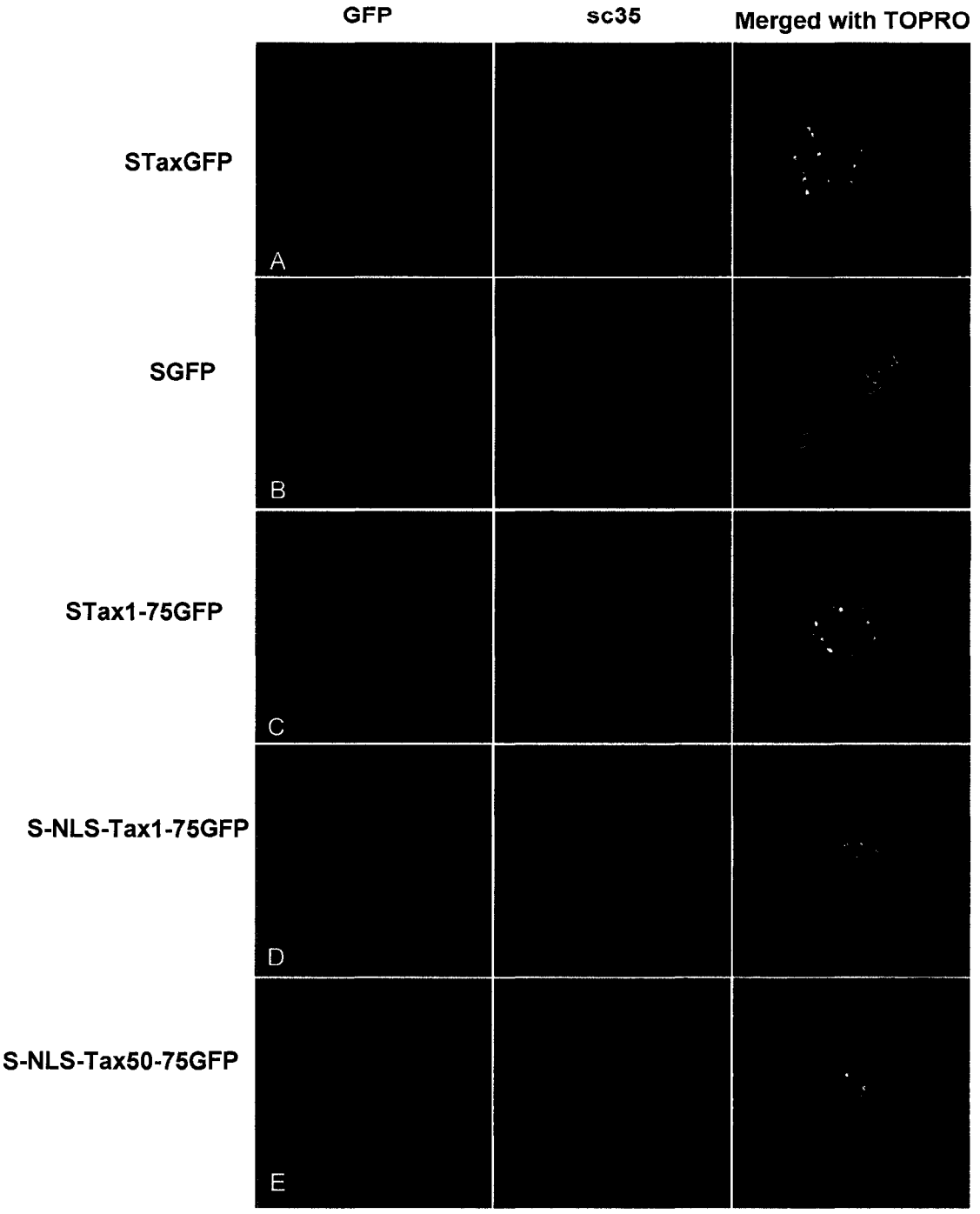

FIG. 5. **Confocal Microscopy Analysis of the Localization of Tax N-terminal Peptides Fused to GFP.** Fixed 293T cells transiently expressing STaxGFP, SGFP, or N-terminal fragments of Tax fused to GFP were assayed for TSS formation as confirmed by colocalization with SC35.

that the nuclear exclusion of the mid-region Tax deletion mutants was not unique to 293T cells as the same cytoplasmic localization of these mutants was observed in the HeLa cells (Figure 6).

We next questioned whether the localization of our mutants was altered by the addition of the large C-terminal GFP fusion. To be certain that the GFP was not the cause of the mislocalization of the mutants, we removed the GFP fusion from each of the Tax mutants using restriction digestion and re-ligation and used confocal microscopy to assay localization. As summarized in Figure 7, the removal of the GFP fusion did not restore nuclear translocation to any of our mid-region mutants.

We hypothesized that the large deletions in our mid-region Tax mutants affected the functioning of the Tax NLS, and therefore the addition of an exogenous NLS would restore nuclear translocation. We added the SV40 T-antigen NLS in frame after the S tag to each of the five cytoplasmic mutants. The exogenous NLS was able to partially restore nuclear translocation for the mutant that was deleted in part of the Tax NLS, STax(d29-52)GFP (Fig. 8A), but not for the non-NLS mutants (Fig 8B-E). This suggests that Tax nuclear translocation is dependent on more than the nuclear localization signal alone, and additional regulatory mechanisms must exist for Tax subcellular localization.

Complementation Analysis of NLS Mutant and TSS Targeting Mutant

We decided to examine the effect of cotransfection of the NLS mutant with the TSS targeting mutant. Expression of a myc-tagged version of the NLS mutant alone

FIG. 6. **Localization of Mid-region Tax Mutants in HeLa cells**. HeLa cells were transiently transfected with plasmid DNA for mid-region Tax deletion mutants that had displayed cytoplasmic localization in 293T cells. HeLa cells were fixed and stained for SC35 and nuclei as previously described.

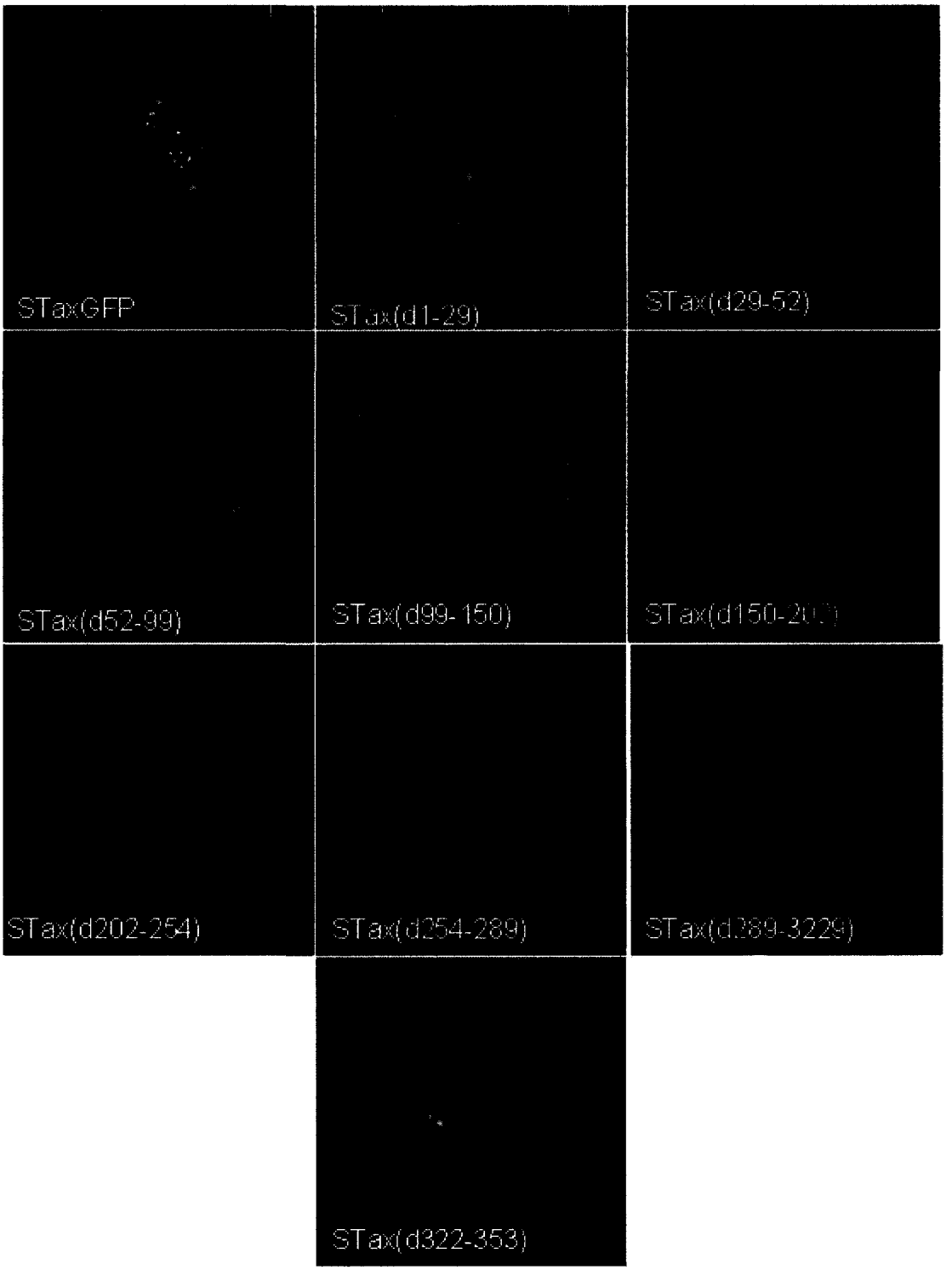

FIG. 7. **Confocal Microsopy Analysis of Tax Deletion Mutants After Removal of GFP Fusion.** 293T cells were transiently transfected with plasmid DNA for STax deletion mutants without the C-terminal GFP tag as indicated. Cells were fixed and stained for SC35 and nuclei.

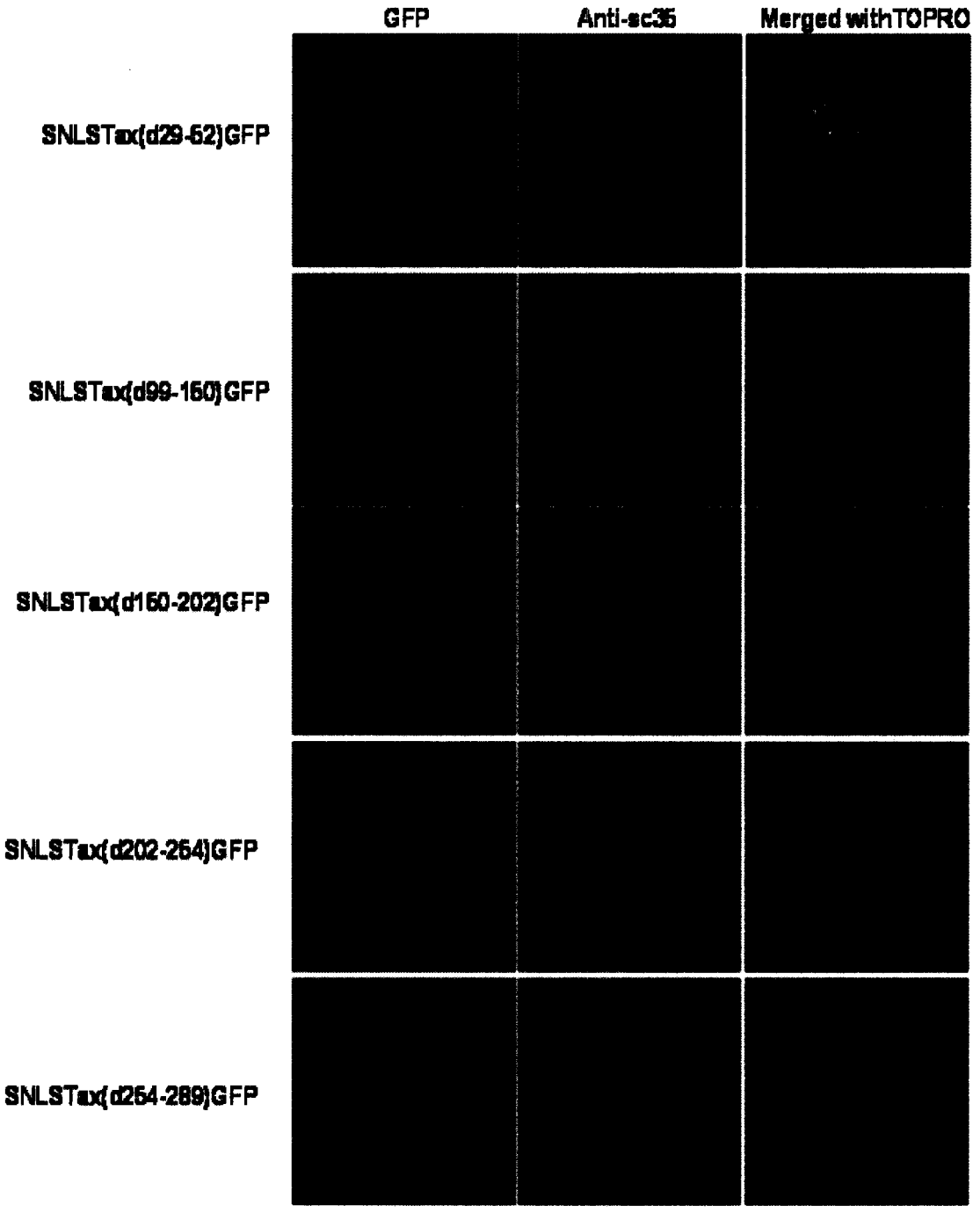

FIG. 8. **Localization of Tax Mutants with Exogenous NLS Tagging**. The NLS from SV40 T-antigen was added in frame to nuclear-excluded Tax mutants by site-directed mutagenesis, and constructs were transiently expressed in HEK 293 cells. Cells were fixed and stained for nuclei and SC35.

(*myc-Tax(d29-52)* resulted in no nuclear translocation, and expression of the TSS targeting mutant alone *STax(d52-99)GFP* resulted in no TSS formation as previously observed (Figure 9A). However, coexpression of the NLS mutant with the TSS targeting mutant resulted in normal nuclear translocation and TSS formation (Figure 9A). To confirm that the foci formed by the coexpression of the mutants were true TSS, we expressed the GFP-fusion version of each mutant either alone or in combination (Figure 9B), and observed colocalization of each with SC35. Coexpression resulted in the formation of true TSS. Complementation by these two different domain mutants confirms that the NLS and TSTS are distinct domains with the ability to independently target Tax into the nucleus and into TSS, respectively. This assay also suggests there is dimerization between the Tax mutants and supports a connection between dimerization and nuclear localization.

Discussion

In addition to the known regulation of Tax localization via the NLS, the NES, and post-translational modification by sumoylation and ubiquitylation, we have now described a novel mechanism for the regulation of Tax subcellular localization. This mechanism involves a signal that directs Tax into nuclear bodies called Tax Speckled Structures. These structures are nuclear protein complexes located at sites partially overlapping with transcriptional hot spots. There are several known types of large protein complexes present in the nucleus including speckles, paraspeckles, Cajal bodies, gems, and Nuclear Domain 10 (ND10) (179)/ promelocytic leukemia (PML) bodies (178).

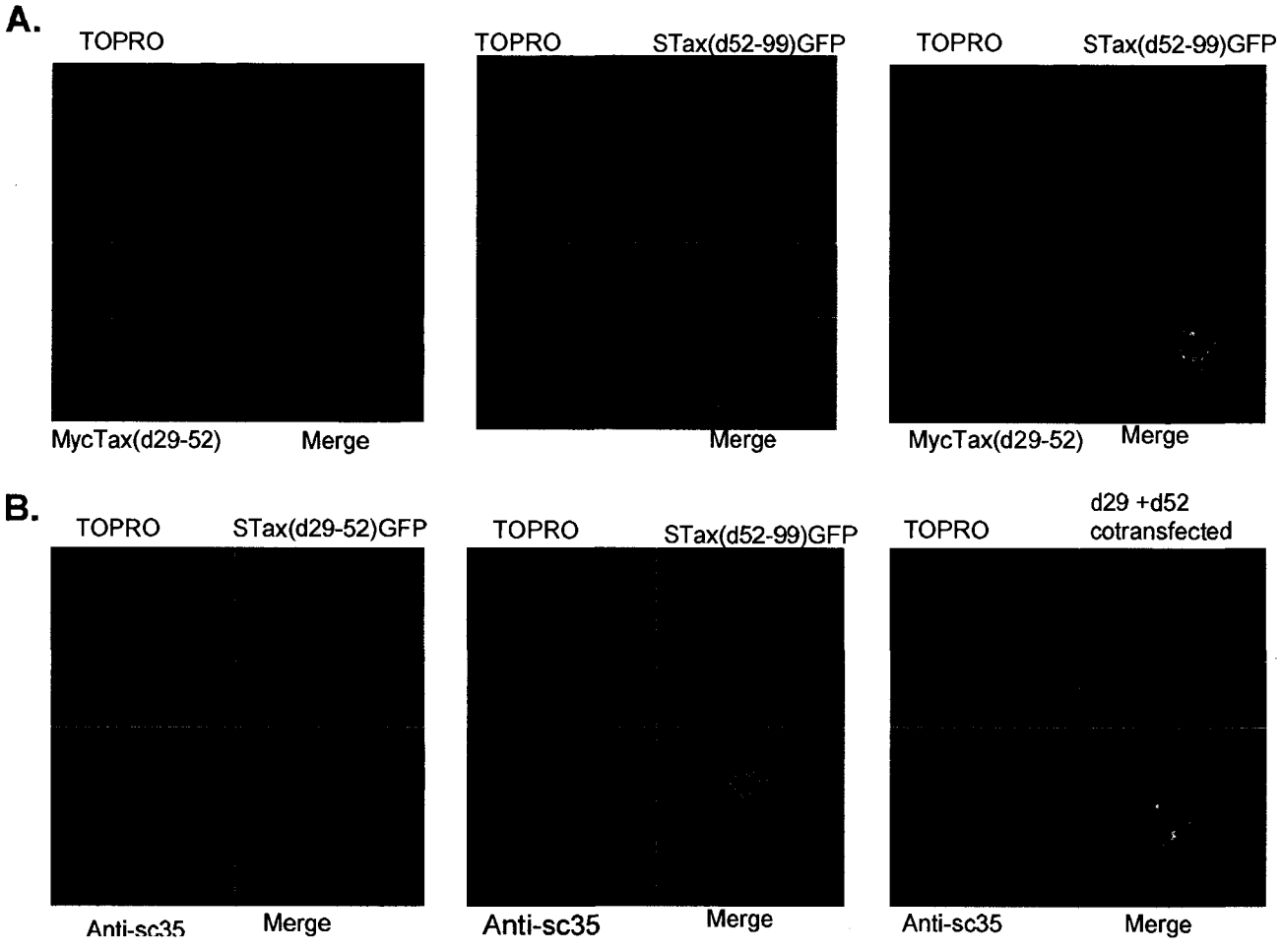

FIG. 9. **Complementation Analysis of NLS mutant and TSS targeting mutant.** (A) Confocal microscopy images of expression of MycTax(d29-52) or STax(d52-99)GFP expressed alone or in combination. Myc-tagged Tax mutant was detected with rabbit anti-myc antibody (Abcam) followed by Alexfluor 594 goat anti rabbit secondary antibody. B: Colocalization with SC35 of STax(d29-52)GFP alone, STax(d52-99)GFP alone, or STax(d29-52)GFP with STax(d52-99)GFP.

These nuclear bodies are believed to form in response to gene expression and contain characteristic sets of nuclear proteins that are continually associating and dissociating with other nuclear components while remaining in distinct subnuclear regions (192). Nearly all of these nuclear structures contain subpopulations of splicing factors, but each is distinguished by the presence of a nuclear protein unique to each structure (180). Nuclear Speckles are interchromatin granule clusters (IGCs) that contain the pre-messenger RNA splicing machinery including small nuclear ribonucleic proteins (snRNPs), non-snRNP splicing factors, and spliceosome subunits such as the spliceosome component 35 protein (SC35) (178).

The Tax Speckled Structures colocalize with SC35 domains at their periphery, do not contain promyelocytic leukemia protein, and do not colocalize with nucleoli, and are therefore defined as nuclear speckles (184). However, they are structures unique to Tax-expressing cells in that they contain various other non-splicing cellular proteins as well. These proteins include DNA-PKcs, Chk2, and 53BP1, proteins involved in DNA damage recognition and repair (129,134,168). The targeting of Tax to TSS and the colocalization of SC35, DNA-PKcs, Chk2, and 53BP1 in the TSS with Tax places Tax near cellular machinery for transcription, splicing, and DNA damage response and checkpoint activation.

Studies of intranuclear protein targeting indicate that it is a multistep process requiring at least two trafficking signals: one for nuclear import (the NLS) and one for mediating interactions with the nuclear matrix (the nuclear matrix-targeting signal) to direct the protein to a specific subnuclear domain (193-195). In our study, we found that the Tax speckle targeting signal (TSTS) was physically distinct from the NLS and could

function independently to direct Tax to its specific intranuclear site. The TSTS for Tax is enriched for proline residues, a characteristic shared by many splicing speckle proteins, but it does not contain the arginine-serine (RS domain) motif common to targeting signals of splicing speckle components (196-199). This may reflect the unique nuclear address of TSS and the ability of Tax to form complexes with diverse nuclear proteins in addition to those involved in mRNA processing.

Another feature within our identified TSTS is an SH3 binding domain. The Src Homology 3 (SH3) domain belongs to a family of modules that recognize proline-rich ligands (200-202). The SH3 domains regulate protein localization, enzymatic activity and often participate in the assembly of multicomponent signaling complexes (203,204). The minimal sequence requirement for the SH3 domain ligands is the PxxP motif (205). This sequence is contained within our identified TSTS, and interactions through this domain may help mediate interactions with the nuclear matrix proteins to direct Tax into TSS.

The targeting of Tax to TSS via the TSTS may have particular implications for the development of Adult T-cell Leukemia. Barseguian *et al* found that mutations in the transcription factor *AML-1* (core binding factor α/ polyoma enhancer binding protein 2) gene that abrogated the nuclear matrix targeting signal resulted in concomitant loss of transcriptional activity (195,206). The *AML-1* gene is one of the most frequently mutated genes in human leukemias, and the authors suggested that the fidelity of transcriptional control may be dependent on the proper localization of transcriptional regulatory proteins like AML-1 to specific subnuclear regions. In promyelocytic leukemia, the normal subnuclear localization of the PML protein is altered from discrete foci to diffusely distributed throughout the nucleus, providing another example of dysregulation of

intranuclear targeting leading to a leukemic phenotype (207,208). In the case of HTLV-1 infection, the ability of Tax to perturb the subnuclear organization of the cell by redirecting nuclear proteins into TSS and away from their normal intranuclear sites may be yet another mechanism by which Tax is able to affect gene expression leading to transformation.

SECTION 4

INFLUENCE OF DIMERIZATION ON TAX LOCALIZATION

Introduction

HTLV-1 is the causative agent of ATL and HAM/TSP. In ATL, the transformation of $CD4^+$ lymphocytes is the result of the expression of the viral protein Tax. This protein is a transcriptional transactivator that influences cellular and viral gene expression and can physically interact with cellular proteins and modulate their functions. Previous studies have established that Tax forms dimers and that optimal transcriptional transactivation by Tax requires Tax dimerization (100,101). However, how and where in the cell this dimerization occurs remains unknown. Tax has pleiotropic activity requiring that it shuttle between the nuclear and cytoplasmic compartments, and the regulation of the subcellular localization of Tax is therefore critical to Tax function (85). Tax localization is partially regulated by previously defined nuclear localization and nuclear export signals in Tax (91,185). Lamsoul *et al* have demonstrated that Tax localization is also influenced by post-translational modifications including sumoylation and ubiquitylation, adding another layer of complexity to the regulation of Tax localization (89).

In our previous studies, we observed Tax deletion mutants that were unable to accumulate in the nucleus despite having intact nuclear localization signals, indicating that nuclear accumulation requires more than a localization signal alone. The four non-NLS mutants of Tax that were nuclear excluded contained deletions within a region that has been previously defined as the Tax dimerization domain (100,101). This

dimerization domain is usually large, taking up nearly half of the Tax protein itself. Within the large dimerization domain are three subdomains that have been shown to be critical for Tax dimerization (101). Although these subdomains have been identified, their interdependence for Tax dimerization has not been established. Each of our first three Tax mid-region mutants is missing one of the dimerization subdomains. The remaining mutant is missing only a few amino acids of the larger dimerization domain. We hypothesized that dimerization of Tax may be prerequisite to Tax nuclear localization and may explain why our mid-region Tax mutants failed to accumulate in the nucleus.

In this study, we examined the link between Tax dimerization and its nuclear localization. We confirmed that the mid-region Tax mutants missing one or two subdomains of the dimerization domain were partially or completely deficient for dimerization. We demonstrate that the mutants missing a single subdomain for dimerization retained the ability to weakly dimerize with wildtype Tax, and this dimerization was associated with rescue of nuclear localization. However, the single subdomain mutants were not able to homodimerize or to heterodimerize with another single subdomain mutant, and were therefore unable to rescue nuclear localization. We demonstrate that the mutant missing two dimerization subdomains is unable to dimerize with wildtype Tax and is not rescued for nuclear localization. We created a Tax mutant that was inducible for dimerization and correlated an increase in nuclear accumulation with an increase in the concentration of the chemical dimerizer. In addition, we show that dimerization between mutants missing either the NLS or the TSS targeting domain allows for complementation between the mutants and restoration of nuclear localization and TSS targeting for the dimer.

Experimental Procedures

Plasmids

The myc-tagged Tax construct *mycTax* was a kind gift from Ralph Grassmann. The *mycTax(D29-52)* construct was created by site-directed mutagenesis of *mycTax* using the QuickchangeXL mutagenesis kit (Stratagene, La Jolla, CA) and the primers 5'(CAAGGCGACTGGTGCCAGATCACCTGGGACCCC) and 3'(GGGGTCCCACG GTGAT CTGGCACCAGTCGCCTTG). Construction of the Tax deletion mutant *STax(d99-150)GFP* was described previously. The Tax deletion mutant *STax(d99-150/202-254)GFP* was constructed using the Excite Mutagenesis kit (Stratagene, La Jolla, CA) using the primers 5'(CCCTCTGGGGAGGCTCCGGGGCCC TAATAATTC) and 3'(GAATTATTAGGGCCCCG GAGCCTCCCCAGAGGG) and using *STax(d99-150)GFP* as the template. The inducible dimerization construct *S-Tax(d99-150)-Fv-GFP* was created by amplifying the Fv domain of *pC4-Fv1E* (ARIAD Pharmaceutical) adding *ClaI* restriction sites with the primers 5'(ACCATCGATGGAGT GCAGGTGGAG ACTT) and 3'(ACCATCGATTTCGAGTTTTAGAAGCTCCAC), digesting the PCR product with *ClaI* and then inserting in frame into the *ClaI* site located at Tax amino acid 58 within *STax(d99-150)GFP*.

Cell Culture and Transfection

HEK 293 cells were maintained at 37°C in a humidified atmosphere of 5% CO_2 in air in Iscove's modified Delbecco's medium supplemented with 10% fetal bovine serum and 1% penicillin/streptomycin (Invitrogen). Transfections were performed by the standard calcium phosphate precipitation method. For S-bead purification and Western

blotting assays, cells were plated in 100-mm plates at 2 x 10^6 cells per plate. For transcriptional activation assays cells were plated into 6-well plates at 2x 10^5 cells per well. The following day 10 μg plasmid DNA in 2M $CaCl_2$ and 2x HEPES-buffered saline was added dropwise to the cells in fresh medium. The cells were washed 16 hours post tranfection and incubated at 37°C until harvest. Cells were harvested 48 hours post transfection following a single wash with 1x phosphate-buffered saline in 400 μl of mammalian protein extraction reagent M-PER (Pierce) with protease inhibitor cocktail (Roche Applied Science) and immediately frozen at -80°C.

Immunofluorescence Confocal Microscopy

HEK 293 cells were seeded at 1x 10^5 cells/well on ethanol-washed 22-mm diameter coverslips in 6-well plates. Each well was transiently transfected with the indicated expression plasmids. After 48 hours the cells were washed three times with PBS and subsequently fixed in 4% paraformaldehyde/PBS for 12 minutes at room temperature. Coverslips were washed twice with PBS, permeablized with methanol for two minutes at room temperature, washed three times with PBS, and incubated overnight at 4°C with primary antibodies diluted 1:1000 in 3% bovine serum albumin-PBS. Cells were washed twice with PBS/0.1% Tween 20 and twice with PBS and then incubated for 1 hour at room temperature with AlexaFluor secondary antibodies (Molecular Probes, Eugene, OR) and TO-PRO-3 iodide (Molecular Probes, Eugene, OR) diluted 1:1000 in 3% BSA-PBS. Coverslips were washed twice with BSA-PBS and twice with PBS and then mounted on glass slides using Vectashield with 4',6-diamidino-2-phenylindole (Vector Laboratories, Burlingame, CA). Confocal fluorescent images were acquired on a Zeiss LSM 510 confocal microscope (Carl Zeiss, Jena, Germany) using argon (488nm),

HeNe1 (543nm), and HeNe2 (633nm) lasers at 63× objective with 2× zoom and imaged with LSM Image Browser software (Carl Zeiss, Jena, Germany).

S-TaxGFP Purification

Lysates from transiently transfected HEK 293 cells were assayed for total protein concentration using the Bradford Protein Assay (Bio-Rad, Hercules, CA) and normalized using a BSA standard curve. For each sample, 500 μg protein was brought to a total volume of 500 μl with M-PER (Pierce, Rockford, IL), and 150 μl of S-protein agarose beads (Novagen, Madison, WI) were applied to the sample. Lysates and beads were incubated at 4°C overnight with rotation and then centrifuged at 500×g for 5 minutes at 4°C. Supernatants were removed and the beads were washed three times with 1ml S-bead Bind/Wash buffer (20 mM Tris-HCL pH 7.5, 150mM NaCl, 0.1% TritonX-100). Purified S-tagged proteins and bound proteins were eluted from the beads by addition of 100 μl 2× Laemmli Sample Buffer (Bio-Rad, Hercules, CA) with 5% β-mercaptoethanol and incubation of beads at 100°C for 10 minutes. Supernatants containing purified proteins were loaded on an 8-12% gradient SDS-PAGE gel (Bio-Rad, Hercules, CA) and separated by electrophoresis, transferred to Immobilon-P membrane (Millipore, Billerica, MA) by semidry transfer method and subjected to immunoblot analysis.

Immunoblot Analysis

Proteins separated by electrophoresis were transferred to Immobilon-P membrane (Millipore, Billerica, MA) using a Trans-blot SD semi-dry transfer cell (Bio-Rad, Hercules, CA) with 400 milliamps applied for 50 minutes in transfer buffer (25mM Tris, 200mM glycine, 20% methanol, 0.1% SDS). Membranes were then blocked for one hour

at room temperature in 1x Odyssey Blocking Buffer (LI-COR Biosciences, Lincoln, NE). Primary antibodies against the myc-tag (Invitrogen, Carlsbad, CA) were diluted 1:1000 in 1X Odyssey Blocking Buffer were applied to the membranes and allowed to interact with the membranes at 4°C overnight on an orbital shaker. Membranes were washed four times for five minutes with 1%PBS-Tween. LI-COR Odyssey secondary antibodies diluted in 1X Odyssey Blocking Buffer with 0.5% SDS and 0.5% Tween were applied at a concentration of 1:20000, and were incubated with the membranes for one hour at room temperature on an orbital shaker while protected from light. Membranes were washed four times for five minutes with PBS-1% Tween20 and then stored in PBS and protected from light until analyzed. Blots were scanned and analyzed with a LI-COR Odyssey scanner and software.

Dimerization Assay

Full length myc-tagged Tax was coexpressed with STaxGFP or mutant missing one or two dimerization subdomains, STax(d99-150)GFP and STax(d99-150/202-254)GFP, respectively, in HEK 293 cells. Lysates were subjected to S-bead purification followed by electrophoresis and immunoblot analysis. STaxGFP and mutants were detected with mouse monoclonal anti-GFP antibody (Santa Cruz Biotechnology, Santa Cruz, CA) at 1:1000 dilution followed by Odyssey goat anti-mouse IR Dye680 (LI-COR Biosciences, Lincoln, NE) at 1:20000 dilution. Copurified myctax was detected by polyclonal anti-myc-tag (Abcam,) at a dilution of 1:1000 followed by Odyssey goat anti-rabbit IR Dye800 (LI-COR) at a dilution of 1:20000. Membranes were scanned and analyzed with LI-COR Odyssey scanner and software.

Complementation Analysis

Full length myc-tagged Tax was coexpressed with all mutants deficient for nuclear translocation or TSS formation. Mid-region Tax mutants were coexpressed in pairs: *STax(d99-150GFP)* with *STax(d150-202)GFP*, *STax(d202-254)GFP* with *STax(d254-289)GFP, STax(d99-150)GFP* with *STax(d202-254)GFP*, and *STax(d150-202)GFP* with *STax(d254-289)GFP*. Localization of the coexpressed proteins was visualized with confocal immunofluorescence microscopy as previously described. Tax and mutants were detected by direct fluorescence of GFP. Myc-tagged Tax and myc-Tax mutant were detected by indirect immunofluorescence staining with rabbit polyclonal anti-myc tag primary antibody (Abcam) at a dilution of 1:1000 followed by goat anti-rabbit secondary antibody conjugated to Alexafluor 594 (Molecular Probes, Eugene, OR) at 1:1000 dilution.

Induced Dimerization Assay

STax(d99-150)-Fv-GFP was transiently transfected in HEK 293 cells seeded onto glass coverslips at 2 x 10^5 cells per well in 6-well plates. 48 hours after transfection, the cells were treated with AP20187 from the Argent Homodimerization kit (ARIAD Pharmaceutical,) at a concentration of 0 nM, 0.01 nM, 0.1 nM, 1.0 nM, 10 nM, 50 nM, or 100 nM for 24 hours. Cells were washed, fixed with 4% paraformaldehyde/PBS, permeablized with methanol, and processed as previously described for confocal microscopy analysis. Images were analyzed for nuclear accumulation using Metamorph Image Analysis software (Molecular Devices, Sunnyvale, CA). Briefly, 100 cells of each condition were analyzed for green nuclear fluorescence expressed as a percentage of total

green cell fluorescence for each individual cell. For each cell analyzed, a region of interest (ROI) was traced around the nuclear membrane, and the area contained within the ROI was analyzed for total fluorescence intensity for the GFP emission wavelength. Then a second ROI was drawn around the plasma membrane of the same cell, and that region was analyzed for total fluorescence intensity for the same wavelength to give the total cell fluorescence intensity. The percentage of nuclear fluorescence intensity was determined by dividing the nuclear intensity by the total cell intensity for each individual cell.

Results

Tax Mid-region Mutants are Deficient for Dimerization

To test if our mid-region mutants were deficient for dimerization, we coexpressed a myc-tagged full length Tax construct with *STaxGFP* or mutant missing either one subdomain or two subdomains of the dimerization domain, *STax(d99-150)GFP* or *STax(d99-150/202-254)GFP*, respectively. We then examined dimerization by S-bead purification of the S-tagged Tax lysates followed by immunoblot analysis for the myc-tagged Tax (Figure 10A). Full length STaxGFP was able to bind to myc-tagged Tax demonstrating strong dimerization between the two full length proteins (Fig. 10A, lane 7). A reduced signal for myctax in lane 6 indicates that STax(d99-150)GFP could at least weakly dimerize with full length Tax while STax(d99-150/202-254)GFP displayed no dimerization with full length Tax (lane 5). Myctax did not bind nonspecifically to the

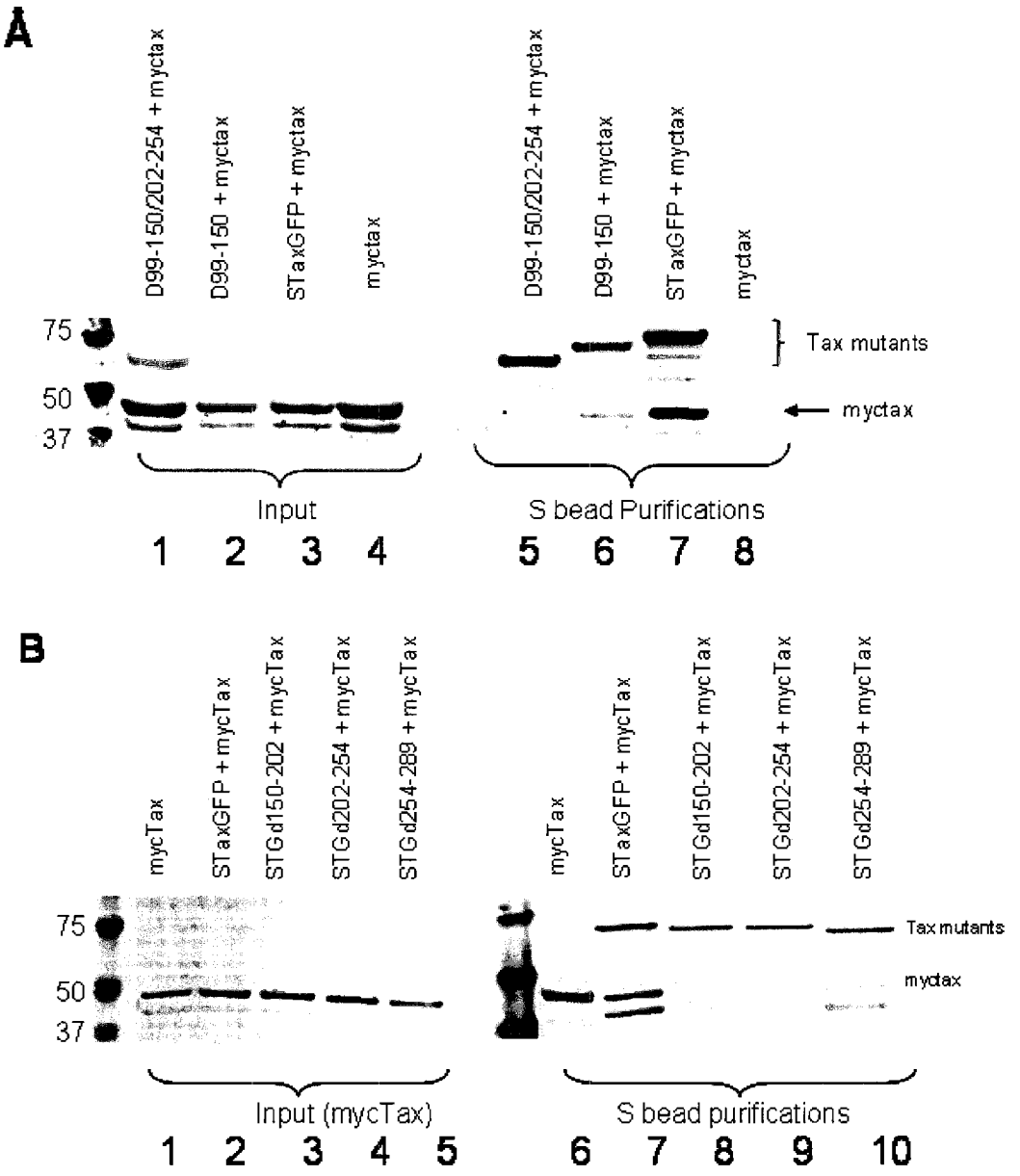

FIG. 10. **Dimerization Assay of Tax Mid-region Mutants.** A) Full length myc-tagged Tax was coexpressed with STaxGFP or mutant missing 1 or 2 dimerization subdomains, STax(d99-150)GFP and STax(d99-150/202-254)GFP, respectively. Ability of STaxGFP and mutants to dimerize with mycTax was assayed by S-bead purification of mutants followed by immunoblot analysis for mycTax using polyclonal anti-myc-tag and for the Tax mutants using monoclonal anti-GFP . B) Dimerization assay of remaining single dimerization subdomain mutants STGd150-202, STGd202-254, & STGd254-289.

S-beads alone (lane 8). Lanes 1-4 show that the abundance of mycTax was not limiting in the reactions in any of the samples. Similar results of weak dimerization were observed with mycTax and the other mid-region Tax mutants (Fig. 10B, lanes 8-10).

Rescue of Nuclear Translocation and TSS formation by Full Length Tax

Since the mutants missing only one subdomain of the mid-region dimerization domain were still able to weakly dimerize with full length Tax, we assayed the effect of coexpression of full length Tax on the subcellular localization of the mutants. Immunofluorescence confocal microscopy studies revealed that coexpression of full length Tax with the mutants was able to partially restore nuclear localization to those mutants missing only one subdomain of the dimerization domain (Figure 11, C-F) but not for the mutant missing two subdomains of the dimerization domain (Figure 11, G). In addition, the coexpression of full length Tax with the NLS mutant or the TSS targeting domain mutant was able to restore nuclear localization or TSS formation to these as well (Figure 11, A-B). Complementation analysis of the mutants indicated that coexpression of mutants deleted in different subdomains of the dimerization domain was not able to rescue nuclear localization as no green fluorescence is observed in the nuclei (Figure 12).

Complementation Analysis of NLS Mutant and TSS Targeting Mutant

Earlier we had coexpressed the Tax NLS mutant and TSS targeting mutant and observed that the mutants could rescue each other. This was similar to our previously observed rescue with wildtype Tax. Expression of a myc-tagged version of the NLS mutant alone (*myc-Tax(d29-52)*) resulted in no nuclear translocation, and expression of

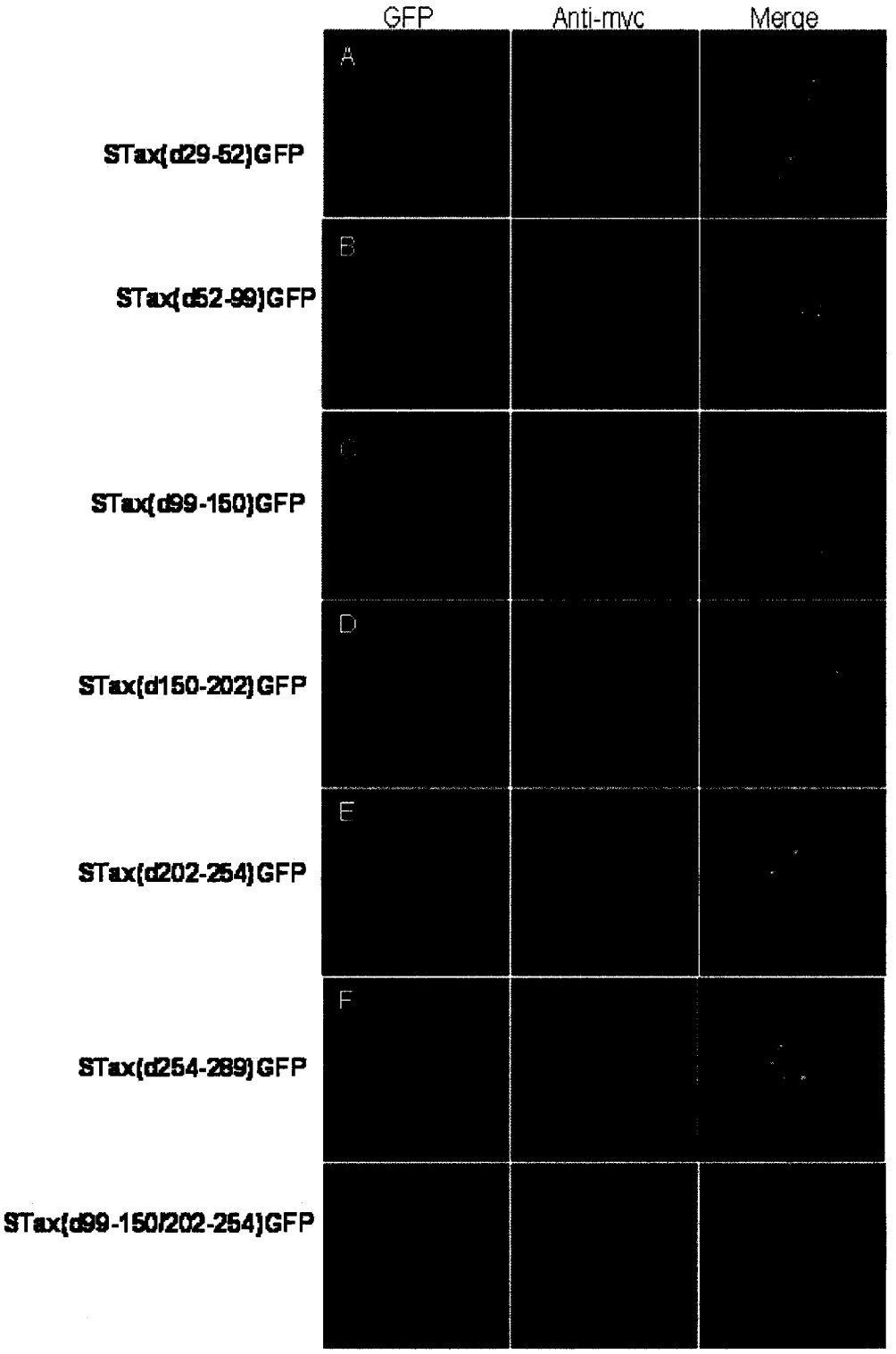

FIG. 11. **Rescue By Full Length Tax of the Nuclear Localization of Tax Deletion Mutants.** Full length mycTax and Tax deletion mutants were transiently cotransfected into 293T cells. Tax mutants were detected by GFP. MycTax was detected by indirect immunofluorescence with rabbit anti-myc primary antibody f(Abcam) followed by Alexafluor594 goat anti-rabbit secondary antibody. (Molecular Probes)

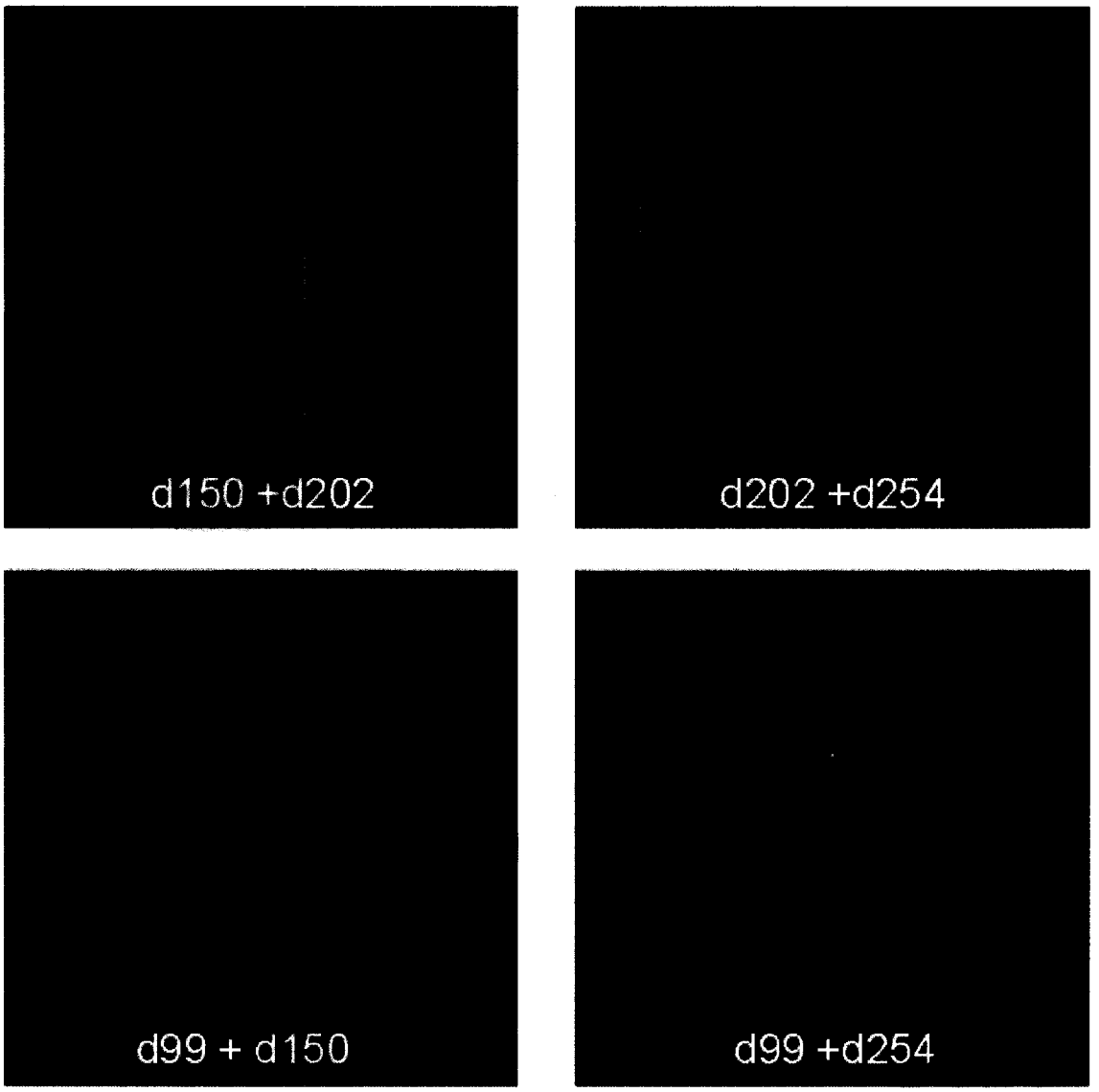

FIG. 12. **Confocal Microscopy Analysis of Coexpression of Dimerization Subdomain Mutants.** 293T cells were transiently cotransfected with plasmids deleted for different dimerization subdomains. Cells were fixed and stained for nuclei and SC35.

the TSS targeting mutant alone *(STax(d52-99)GFP)* resulted in no TSS formation as previously observed (Figure 9A). However, coexpression of the NLS mutant with the TSS targeting mutant resulted in normal nuclear translocation and TSS formation (Figure 9A). Coexpression resulted in the formation of true TSS. Complementation by these two different domain mutants suggests there is dimerization between the Tax mutants and supports a connection between dimerization and nuclear localization.

To definitively link Tax dimerization and nuclear localization, we designed a Tax construct that contains an inducible dimerization domain, *STax(d99-150)-Fv-GFP*. This assay is based on the binding domain of the human protein FK506 Binding Protein (FKBP) and its ability to bind to the immunosuppressive drugs FK506 and rapamycin. Fv is a modified version of the FKBP binding domain containing a phenylanaline to valine substitution that increases the affinity of a rapamycin derivative, AP20187, for the Fv-fusion protein by 1000-fold over the wildtype protein. AP20187 is a small molecule able to crosslink any two proteins containing the FKBP binding domain thus inducing dimerization (ARIAD Pharmaceutical). The expression of *STax(d99-150)-Fv-GFP* in the absence of the chemical dimerizer AP20187 resulted in a completely cytoplasmic localization of the protein. Upon the addition of increasing concentrations of the dimerizer, the Tax protein began to accumulate in the nucleus in a dose-dependent manner from less than 1% to more than 40% nuclear accumulation (Figure 13). This demonstrates that Tax must be in a dimeric or oligomeric form in order to localize in the nucleus. The site of insertion of the dimerizer domain was within the TSS targeting sequence, which disrupted the speckle localization signal and prevented the induced dimers from localizing into TSS.

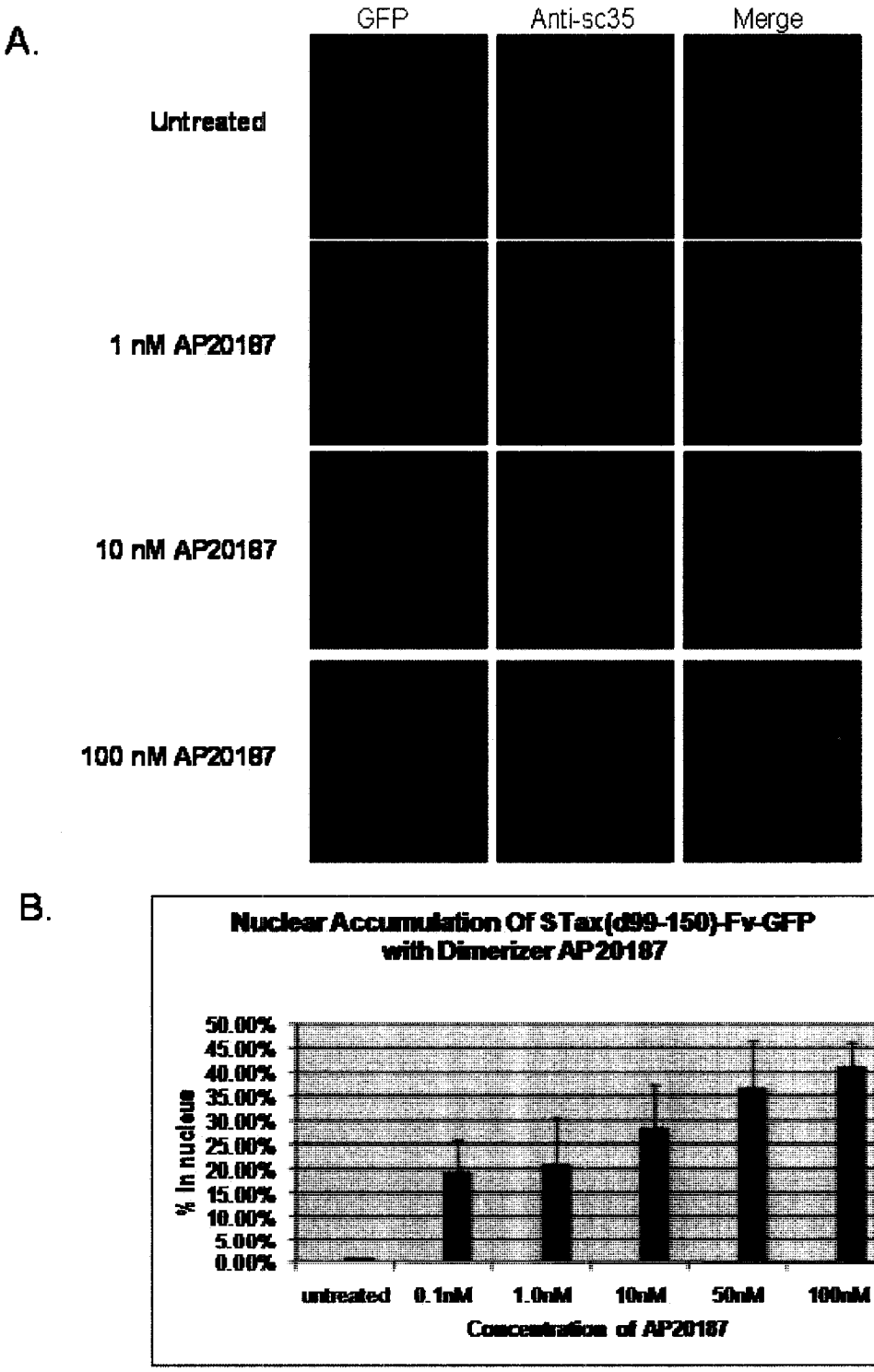

FIG. 13. **Effect of Induced Dimerization on Nuclear Accumulation of Tax Mutant**. (A) Confocal microscopy images of cells expressing STax(d99-150)-Fv-GFP treated with 0nM, 1nM, 10nM, or 100nM of the chemical dimerizer AP20187. Cells were fixed and stained for SC35 and nuclei as previously described. (B) Quantitation of the nuclear accumulation of STax(d99-150)-Fv-GFP with increasing concentration of dimerizer.

Discussion

The second novel mechanism described in this study for regulation of Tax subcellular localization is Tax dimerization as a requirement for nuclear accumulation. There are numerous examples of proteins that must dimerize or oligomerize prior to nuclear translocation including the Human Cytomegalovirus protein ppUL44 and the cellular protein p53 (209,210). Other proteins such as the AP-1 family including c-Jun, JunD, JunB and c-Fos enter the nucleus as monomers but require heterodimerization in order to remain in the nucleus (211). In our studies, we were able to link the inability of Tax mutants to accumulate in the nucleus with a deficiency in dimerization. Those Tax mutants that retained the ability to weakly dimerize with wildtype Tax were also able to weakly accumulate in the nucleus with wildtype Tax. Induced dimerization of a previously cytoplasmic Tax dimerization mutant resulted in restored nuclear translocation. A mutant lacking an NLS and therefore unable to enter the nucleus on its own was able to dimerize to either wildtype Tax or the TSTS mutant and thentranslocate into the nucleus. Our studies definitively link dimerization and nuclear accumulation and that this dimerization occurs in the cytoplasm as a prerequisite to nuclear entry.

Previous studies on the dimerization of Tax have suggested that the N-terminal zinc finger domain is important for Tax self-association (100,101). These findings were based on yeast two-hybrid assays where an N-terminal mutant of Tax failed to interact with wildtype Tax. Our functional complementation assay between the NLS mutant, STax(d29-52)GFP, which is also missing the zinc-finger domain, and the TSTS mutant demonstrates that the zinc finger domain is not required for dimerization within the cell (Fig. 9). Also, the addition of an exogenous NLS to the same zinc finger NLS Tax

mutant was able to restore nuclear localization and subsequent accumulation, providing more evidence that the zinc finger domain is dispensable for Tax self-association (Fig.8).

Additional questions also remain as to the stoichiometry of Tax self-association. Our complementation assays between the NLS mutant and TSTS mutant suggest that the Tax self-interaction exists in a one-to-one relationship. In addition, for the processes of nuclear localization and subnuclear targeting, our studies suggest that a single copy of each signal is sufficient for targeting the multimer into its proper location. The inability of the dimerization subdomain mutants to complement each other to restore nuclear accumulation, however, suggests that a higher order oligomer, such as a tetramer, may be required to overcome the absence of a part of the dimerization domain. This is supported by our findings in the induced dimerization assay. The design of the heterologous "dimerizer" domain is such that only dimers, and not higher order oligomers, are formed upon the addition of the chemical dimerizer. Although induced dimerization was able to increase the nuclear accumulation of the mutant protein, it did not result in a total restoration of nuclear accumulation to wildtype level (Figure 13). This suggests that under certain conditions, Tax may oligomerize. Tax oligomerization could provide even more complex regulation of Tax functions. Oligomerization could generate new intermolecular interfaces to improve stability, control the accessibility and specificity of active sites, and increase the number of cellular binding partners for Tax, and may help explain how this single protein has such a wide range of pleiotropic activities.

SECTION 5

INFLUENCE OF CELLULAR PROTEINS ON TAX LOCALIZATION

Introduction

Human T-cell Leukemia Virus Type-1 (HTLV-1) infection can lead to Adult T-cell Leukemia (ATL), HTLV-1 Associated Myelopathy/ Tropical Spastic Paraparesis (HAM/TSP), and several other subneoplastic conditions. The viral transactivating protein, Tax, encoded by the pX region, has been recognized by its pleiotropic actions to play a critical role in transformation. Although many studies have demonstrated changes in cellular proteins through protein-protein interactions with Tax (126,131,134,168,175,212), fewer studies have investigated the effect of these cellular protein interactions on the localization and function of Tax.

Tax is a predominantly nuclear phosphoprotein with the ability to shuttle between the nuclear and cytoplasmic compartments (85,86). Recent evidence indicates that Tax is post-translationally modified by ubiquitylation and sumoylation, and these modifications direct the subcellular localization of Tax (89,90,213).

Ubiquitin is a small 76-amino acid polypeptide that is present in all eukaryotic cells (214). Modification of a cellular protein by the addition of ubiquitin involves the covalent attachment of ubiquitin to lysine residues within the target protein. Ubiquitylation is a multistep, ATP-dependent process involving three individual enzymes (215) . The first enzyme (E1) activates the ubiquitin, the second enzyme (E2) ligates the ubiquitin to the target protein specified by the third enzyme (E3) (214). The ubiquitylation of a protein can result in its activation, affect its localization, or direct it to

the proteosome for degradation (215). Often the number of ubiquitins added can partially determine the fate of the target protein. Monoubiquitylation often has a regulatory function while conjugation of a polyubiquitin chain of four or more ubiquitins onto a target protein can target it for degradation by the proteosome (216).

The Small Ubiquitin-like Modifier (SUMO) is similar to ubiquitin in that it is a small polypeptide that is conjugated to a target protein on lysine residues by a series of three enzymes (217). Sumoylation results in similar changes in the activation and location of the modified protein as ubiquitylation. Lamsoul *et al* have previously demonstrated that ubiquitylation of Tax is associated with its accumulation in the cytoplasm while sumoylation of Tax results in nuclear entry and TSS formation (89,90). In particular, the lysine residues located at amino acids 280 and 284 of Tax have been implicated as the critical sites for both sumoylation and ubiquitylation of Tax leading to the nuclear or cytoplasmic accumulation of Tax respectively (89,90). Although it is clear that both ubiquitylation and sumoylation of Tax play a role in Tax regulation, the cellular proteins involved in the ubiquitylation and sumoylation of Tax have yet to be identified.

In this study, we have identified a novel physical interaction between Tax and the ring finger protein 4, RNF4, a cellular ubiquitin E3 ligase with no known cellular target (215). RNF4, also known as small nuclear ring finger protein (SNURF), preferentially targets sumoylated proteins for ubquitination, and as such is referred to as a SUMO-targeted ubiquitin ligase (STUbL) (215). We show, through the work of our collaborator Oliver Kerscher, that RNF4 is able to ubiquitylate previously sumoylated Tax *in vitro.* We show that the overexpression of RNF4 causes an egress of Tax from the Tax Speckled Structures and the nucleus to form a perinuclear ring in the cytoplasm. We

mapped the domain in Tax responsible for its interaction with RNF4 to be between Tax amino acids 202 and 254. Further, we demonstrate that increasing expression of RNF4 results in decreasing Tax *trans*-activation of the HTLV-1-LTR responsive promoter (a nuclear function of Tax) and increasing Tax *trans*-activation of the NF-κB responsive promoter (a cytoplasmic function of Tax) in a dose-dependent manner. In this way we demonstrate that RNF4 is able to affect both the localization and function of Tax.

Experimental Procedures

Plasmids

The *STaxGFP* and *SGFP* expression vectors were constructed by inserting the *tax*-EGFP fusion or the *EGFP* ORF from *HisTaxGFP* and *C-EGFP* vectors respectively into the *SmaI* site of *pTriEx4-Neo* (Novagen, Madison, WI) in frame with the amino terminal S- and His-tags. The Tax double point mutant *STaxK280/284R-GFP* was created using *STaxGFP* as the template and the Quickchange Site-directed Mutagenesis Kit (Strategene, La Jolla, CA) with the primers 5'(TCCTCCTTTATATTTCACAGATTTC AA) and 3' (GGGGTGGTAGGCCCTGGT TTGAAA). *pRNF4-GFP and pGFP-RNF4* were kind gifts from Oliver Kerscher.

Cell Culture and Transfection

HEK 293 cells were maintained at 37°C in a humidified atmosphere of 5% CO_2 in air in Iscove's modified Delbecco's medium supplemented with 10% fetal bovine serum and 1% penicillin/streptomycin (Invitrogen, Carlsbad, CA). Transfections were

performed by the standard calcium phosphate precipitation method. For S-bead purification and Western blotting assays, cells were plated in 100-mm plates at 2 x 10^6 cells per plate. For transcriptional activation assays cells were plated into 6-well plates at 2x 10^5 cells per well. The following day 10 μg plasmid DNA for 10cm plates or 1-6μg in a single well of a 6-well plate in 2M $CaCl_2$ and 2x HEPES-buffered saline was added dropwise to the cells in fresh medium. The cells were washed 16 hours post-transfection and incubated at 37°C until harvest. Cells were harvested 48 hours post-transfection following a single wash with 1× phosphate-buffered saline in 400 μl of mammalian protein extraction reagent M-PER (Pierce, Rockford, IL) with protease inhibitor cocktail (Roche Applied Science, Palo Alto, CA) and immediately frozen at -80°C.

Immunofluorescence Confocal Microscopy

HEK 293 cells were seeded at 1x 10^5 cells/well on ethanol-washed 22-mm diameter coverslips in 6-well plates. Each well was transiently transfected with the indicated expression plasmids. After 48 hours the cells were washed three times with ice cold phosphate buffered saline (PBS) and subsequently fixed in 4% paraformaldehyde/PBS for 12 minutes at room temperature. Coverslips were washed twice with PBS, permeablized with methanol for two minutes at room temperature, washed three times with PBS, and incubated overnight in a humidifying chamber at 4°C with primary antibodies diluted in 3% bovine serum albumin-PBS. Rabbit polyclonal anti-Tax antibody and mouse anti-SC35 antibody (Invitrogen, Carlsbad, CA) were used at a dilution of 1:1000. Cells were washed twice with PBS/0.1% Tween 20 and twice with PBS and then incubated for 1 hour at room temperature with AlexaFluor594 anti-rabbit and anti-mouse secondary antibodies and TO-PRO-3' iodide (Molecular Probes,

Eugene, OR) diluted 1:1000 in 3% BSA-PBS. Coverslips were washed twice with BSA-PBS and twice with PBS and then mounted on glass slides using Vectashield with 4',6-diamidino-2-phenylindole (DAPI) (Vector Laboratories, Burlingame, CA). Confocal fluorescent images were acquired on a Zeiss LSM 510 confocal microscope (Carl Zeiss, Jena, Germany) using argon (488nm), HeNe1 (543nm), and HeNe2 (633nm) lasers with 63× objective oil lens with 2× zoom and imaged with LSM Image Browser software (Carl Zeiss, Jena, Germany).

S-TaxGFP and RNF4 Binding Assay

Lysates from HEK 293 cells transiently transfected with *STaxGFP, SGFP*, or *STaxGFP* deletion mutants and *GFP-RNF4* were assayed for total protein concentration using the Bradford Protein Assay (Bio-Rad, Hercules, CA) and normalized using a BSA standard curve. 500 μg protein was brought to a total volume of 500 μl with M-PER (Pierce, Rockford, IL) with protease inhibitors (Roche,) for each sample, and 150 μl of S-protein agarose beads (Novagen, Madison, WI) were applied to the sample. Lysates and beads were rotated for 30 minutes at room temperature and then centrifuged at 500×g for 5 minutes at 4°C. Supernatants were removed and the beads were washed three times with 1ml S-bead Bind/Wash buffer (20 mM Tris-HCL pH 7.5, 150mM NaCl, 0.1% TritonX-100). Purified S-tagged proteins and bound proteins were eluted from the beads by addition of 100 μl 2× Laemmli Sample Buffer (Bio-Rad, Hercules, CA) with β-mercaptoethanol and incubation of beads at 100°C for 10 minutes. Supernatants containing purified proteins and bound proteins were loaded on an 8-12% gradient SDS-PAGE gel (BioRad, Hercules, CA) and separated by electrophoresis, transferred to

Immobilon-P membrane (Millipore, Billerica, MA) by semidry transfer, and subjected to immunoblot analysis.

Immunoblot Analysis

Proteins separated by electrophoresis were transferred to Immobilon-P membrane (Millipore, Billerica, MA) using a Trans-blot SD semi-dry transfer cell (Bio-Rad, Hercules, CA) with 400 milliamps applied for 50 minutes in transfer buffer (25mM Tris, 200mM glycine, 20% methanol, 0.1% SDS). Membranes were then blocked for one hour at room temperature in 1× Odyssey Blocking Buffer (LI-COR Biosciences, Lincoln, NE). Primary antibodies diluted in 1× Odyssey Blocking Buffer were applied to the membranes and allowed to interact with the membranes at 4°C overnight on an orbital shaker. Membranes were washed four times for five minutes with PBS-1%Tween20. LI-COR Odyssey secondary antibodies diluted in 1× Odyssey Blocking Buffer with 0.5% SDS and 0.5% Tween20 were applied at a concentration of 1:20000, and were incubated with the membranes for one hour at room temperature on an orbital shaker while protected from light. Membranes were washed four times for five minutes with PBS-1% Tween20 and then stored in PBS and protected from light until analyzed. Blots were scanned and analyzed with a LI-COR Odyssey scanner and software (LI-COR Biosciences, Lincoln, NE).

Transcriptional Transactivation Assay

HEK 293 cells were transiently transfected with 1 μg plasmid DNA for either p*HTLV-LTR-Luciferase* or p*NFκB-Luciferase* (Clontech, Mountain View, CA) with 0-5 ug *pGFP-RNF4* and 1μg *STaxGFP* plasmid DNA. Total DNA per transfection was

normalized to 6μg total DNA per well with the addition of parental vector, *pTriEx4-Neo* (Novagen, Madison, WI). Cells were harvested 48 hours post-transfection by washing once with ice cold PBS and then lysing in 400 μl 1× Reporter/Lysis Buffer (Promega, Madison, WI). Lysates were immediately frozen at -80°C. Samples were allowed to thaw on ice, collected, and protein concentration was determined using the Bradford Protein Assay (Bio-Rad, Hercules, CA). A total of 1 μg protein of each sample was applied to 100 μl of luciferase assay substrate (Promega, Madison, WI), and luciferase activity was immediately measured in a Turner TD 20/20 luminometer. Transcriptional activation was analyzed and expressed as fold activation over reporter alone (fold activation=1). All assays were performed three times with triplicates of each sample.

Results

Tax interacts with RNF4

Previous studies in our laboratory provide evidence that Tax binds to member of the ring finger (RNF) family (unpublished observation). We were interested in whether Tax could bind to a specific RNF family protein, RNF4, which is a SUMO-targeted ubiquitin ligase with no known target. In our previous studies we designed expression constructs for Tax with an affinity S-tag (STax, STaxGFP) that allows for purification of Tax and Tax-binding complexes from transfected cell lysates. In order to determine if RNF4 is able to interact with Tax, we transfected GFP-RNF4 either alone or with SGFP, STaxGFP, or a mutant of Tax with point mutations at lysines 280 and 284, STaxK280/284R-GFP. This construct is not able to be ubiquitylated or sumoylated on the

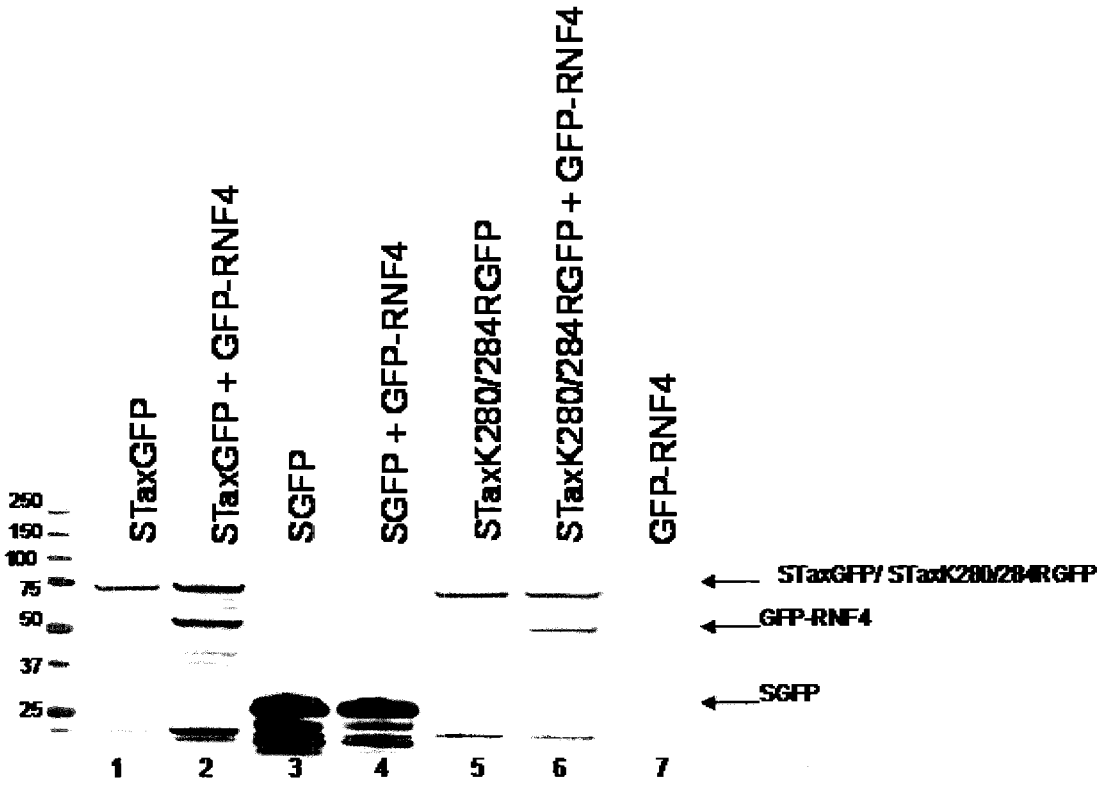

FIG. 14. **Copurification of GFP-RNF4 and Tax.** 293T cells were transiently transfected with SGFP, STaxGFP, or STaxK280/284R in the presence or absence of GFP-RNF4. Lysates were subjected to S-bead purification.Purified S-taggged proteins and bound proteins were separated by SDS-PAGE and subjected to immunoblot analysis with detection by polyclonal anti-GFP antibody.

two lysine residues that were previously shown to be critical to Tax localization. We then purified the S-tagged proteins with S-protein agarose beads, separated them by electrophoresis, and then subjected them to immunoblot analysis using an anti-GFP antibody that would detect the SGFP , the STaxGFP, the Tax mutant and the RNF4-GFP. Purified STaxGFP also precipitated GFP-RNF4 indicating that they interact in the same complex (Fig. 14, lane 2). The S-beads did not bind to GFP-RNF4 alone demonstrating the specificity of the S-beads for the S-tagged proteins, and purified SGFP did not coprecipitate GFP-RNF4 (Fig. 14, lanes 4 and 7) demonstrating that the interaction was specific to Tax and RNF4. Surprisingly, the Tax double point mutant that could not be ubiquitylated or sumoylated, STaxK280/284R-GFP, retained the ability to interact with RNF4 (lane 6), indicating that the RNF4-Tax interaction does not require the ubiquitylating activity of RNF4.

RNF4 Overexpression Leads to Cytoplasmic Accumulation of Tax

We next wanted to determine if the interaction between Tax and RNF4 causes them to colocalize in TSS. Confocal microscopy studies indicated that overexpression of RNF4 resulted in an egress of Tax from the nucleus (Figure 15). The Tax Speckled Structures were lost as Tax exited the nucleus to form a perinuclear ring within the cytoplasm of the cotransfected cells.

RNF4 Ubiquitylates Tax In Vitro

RNF4 is an ubiquitin ligase that preferentially targets sumoylated proteins. Earlier studies by Lamsoul *et al* demonstrated that Tax can be both sumoylated and ubiquitylated and that ubiquitylation on Tax lysine residues 280 and 284 resulted in cytoplasmic

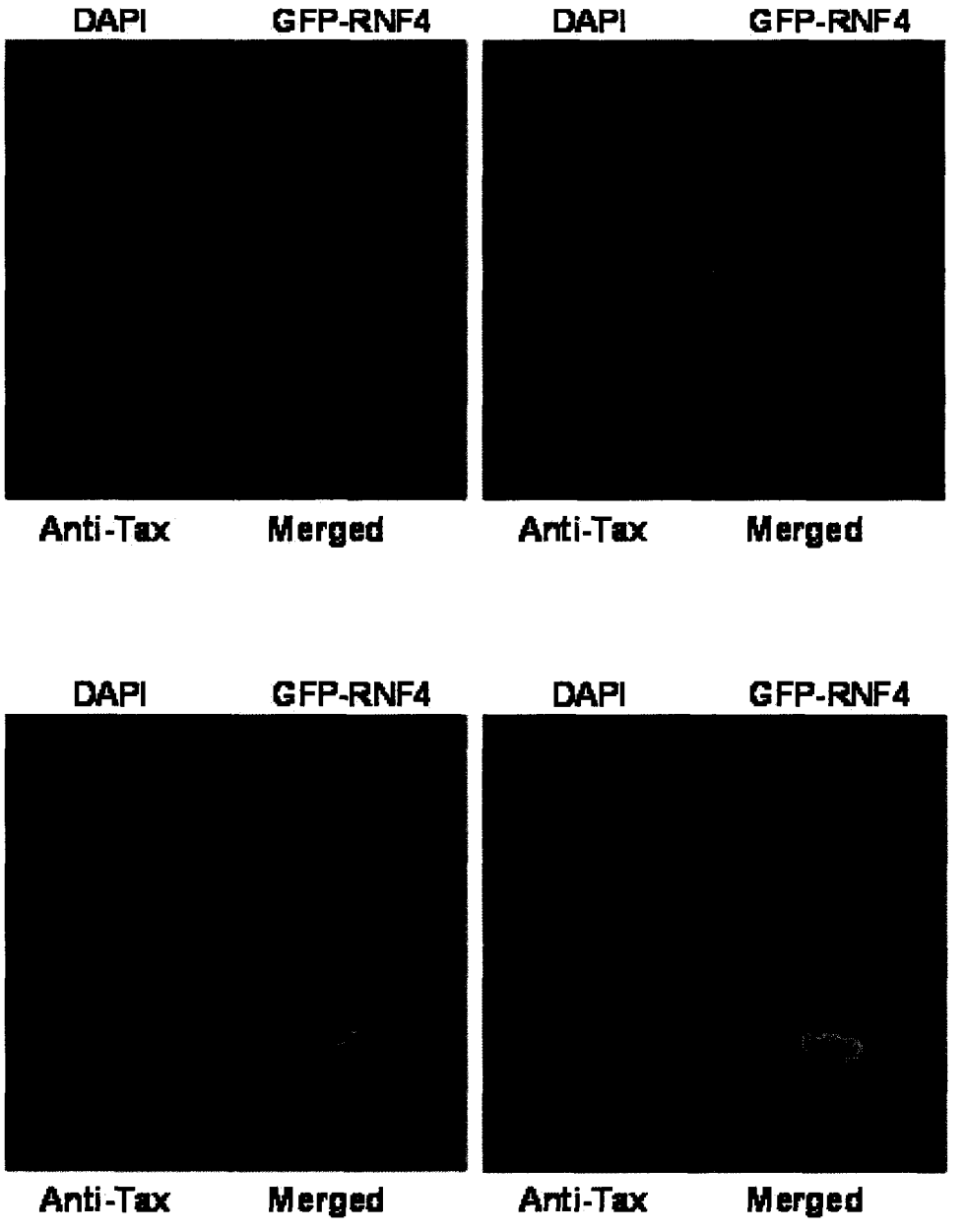

FIG. 15. **Confocal Microscopy Analysis of GFP-RNF4 and STax Coexpression.** 293T cells were transiently transfected with GFP-RNF4 and STax. Cells were fixed and subjected to indirect immunofluorescence staining with polyclonal anti Tax antibody followed by Alexafluor 594-conjugated goat anti rabbit antibody. GFP was used to detect RNF4. Nuclei were stained with TO-PRO- 3'-iodide and DAPI.

localization of Tax while sumoylation on the same lysine residues resulted in nuclear localization (89). Our findings that overexpression of RNF4 led to an egress of Tax from the nucleus led us to question whether RNF4 could ubiquitylate Tax. Through an *in vitro* ubquitination assay, our collaborator, Dr. Oliver Kerscher at the College of William and Mary, demonstrated that RNF4 is able to ubiquitylate Tax (Figure 16). Following preincubation with RNF4, Tax was able to form high molecular weight adducts corresponding to ubiquitylated Tax (Fig. 16 lanes 4 and 5). This ubiquitination of Tax required the presence of ATP and was mediated through ubc13, an E2 ubiquitin ligase. When free SUMO was added to the reaction, the free SUMO outcompeted Tax in binding RNF4 and prevented the ubiquitination of Tax (Fig. 16 lanes 6 and 7). A complete description of the experimental procedure for this assay is in Appendix A of this dissertation.

RNF4 Overexpression Affects Tax Trans-Activation

We have demonstrated that Tax and RNF4 interact with each other in a complex, and that this interaction can result in the ubiquitylation of Tax *in vitro*. We also observed that overexpression of RNF4 results in a relocalization of Tax from the nucleus to the cytoplasm. Next we wanted to see if this relocalization of Tax could affect its *trans*-activation activity on both the HTLV-1 LTR, a nuclear function of Tax, and on the NF-κB pathway, a cytoplasmic function of Tax. We performed promoter/reporter transcriptional activation assays for STaxGFP in the presence of increasing RNF4 expression. We found that RNF4 expression resulted in a decrease in the activation of HTLV-LTR-Luc by STaxGFP (Figure 17A). The activation of HTLV-LTR-Luc was reduced from a 60-fold increase over activity of reporter alone to 2-fold in the presence

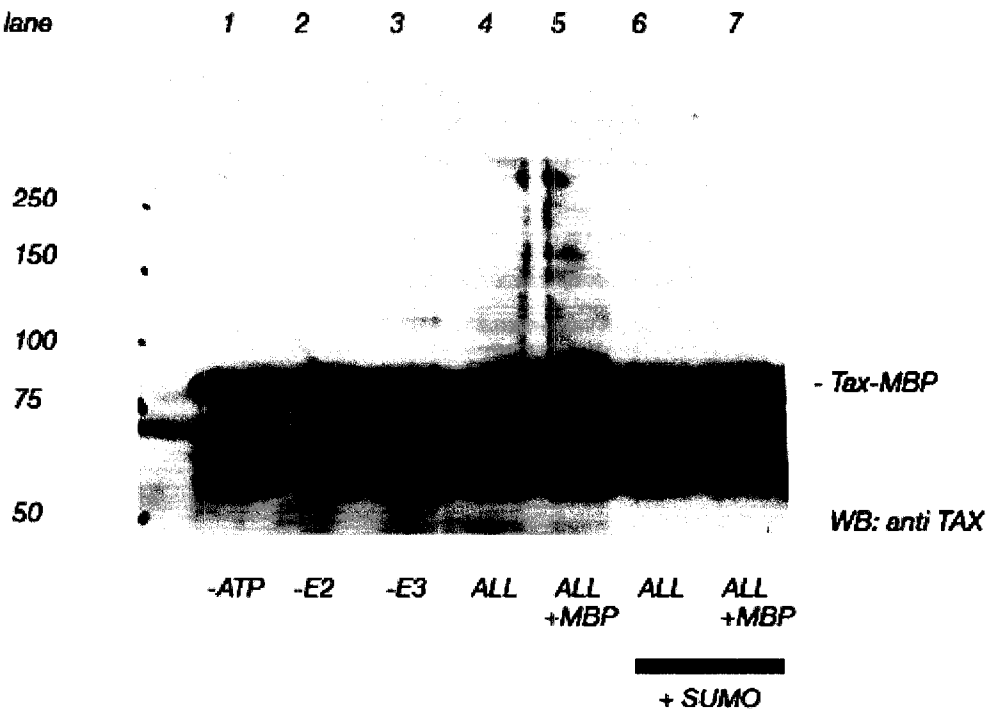

FIG. 16. **Ubiquitylation of Tax-MBP After Preincubation with RNF4.** Tax fused to maltose binding protein (MBP) was allowed to incubate with RNF4 (lanes 1-2, 5-7) and then was subjected to *in vitro* ubiquitylation assay in the absence of ATP (lane 1), without the E2 ligase ubc13/mms2 (lane 2), without the E3 ligase RNF4 (lane 3), or with all of these +/- MBP (lanes 4-5). In lanes 6 and 7 free SUMO was added. The reaction products were separated by SDS-PAGE and subjected to immunoblot analysis with anti-Tax antibody.

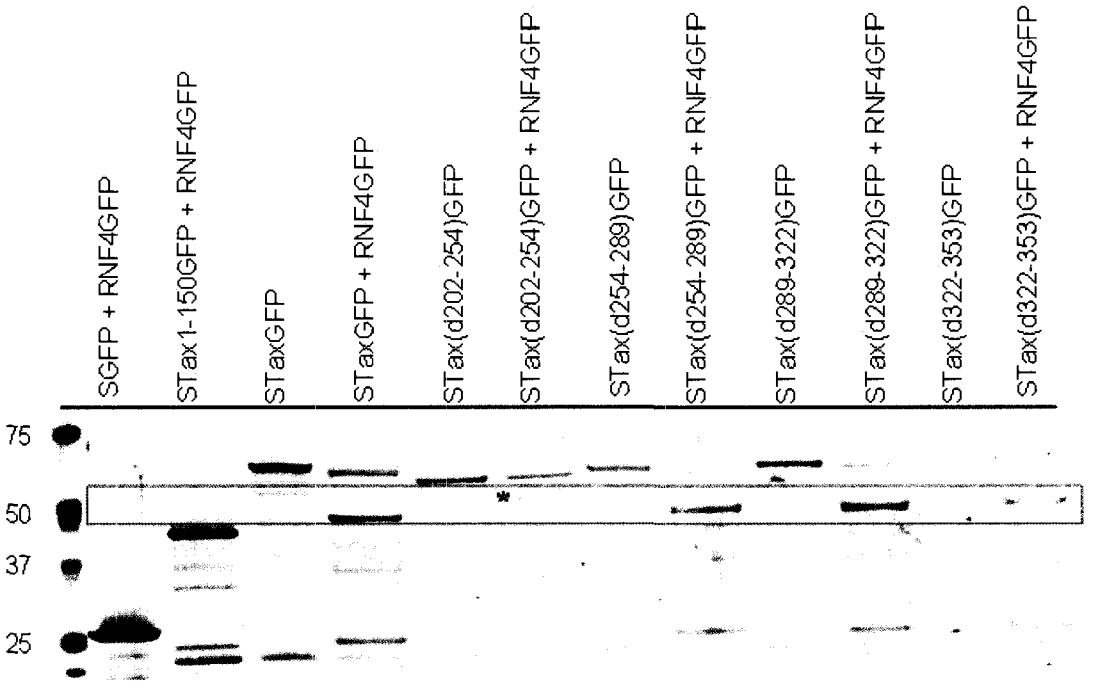

FIG. 17. **Mapping the Tax-RNF4 Interacting Domain.** 293FT cells were transiently transfected with SGFP, STax1-150GFP, STaxGFP, or deletion mutants of Tax in the presence or absence of RNF4-GFP. Lysates were subjected to S-bead purification, and bound proteins were eluted, separated by SDS-PAGE, and subjected to immunoblot analysis with polyclonal anti-GFP antibody (Invitrogen).

of RNF4. We found that increasing RNF4 expression resulted in an increase in the *trans*-activation of NF-κB-Luciferase activity from 30-fold to nearly 60-fold (Figure 17B).

Mapping the Tax-RNF4 Interaction Domain

We next wanted to determine the region in Tax responsible for its interaction with RNF4. We expressed each of our Tax deletion mutants either alone or with RNF4-GFP in 293FT cells. We then purified the Tax mutants using the S-bead purification followed by SDS-PAGE and immunoblot analysis as described previously. There was no interaction between RNF4-GFP and SGFP (Figure 18, lane 1) or between RNF4-GFP and a Tax mutant containing only the N-terminal 150 amino acids of Tax, STax1-150GFP (lane 2). We were able to copurify RNF4-GFP with STaxGFP (lane 4), STax(d254-289)GFP (lane 8), STax(d289-322)GFP (lane 10), and with STax(d322-353)GFP (lane 12). Only the deletion mutant STax(d202-254)GFP failed to interact with RNF4-GFP (lane 6) suggesting that this region is required for the interaction of Tax with RNF4.

Discussion

Many of the functions of Tax are accomplished through direct protein-protein interactions with cellular partners. Although there have been many studies to examine the effect of Tax expression on the functions of cellular proteins, there have been fewer studies of how these interactions may affect the activities of Tax. In this study we have identified a novel cellular binding partner for Tax, the ubiquitin ligase RNF4. This member of the SUMO-targeted ubiquitin ligase (STUbL) family has no previously

A

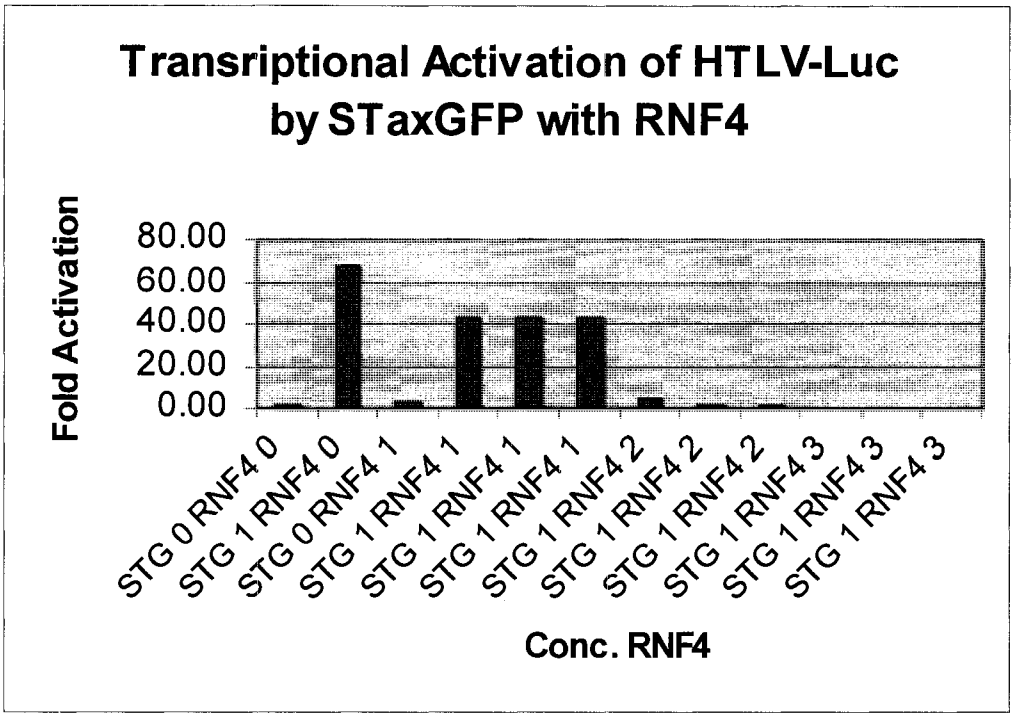

B

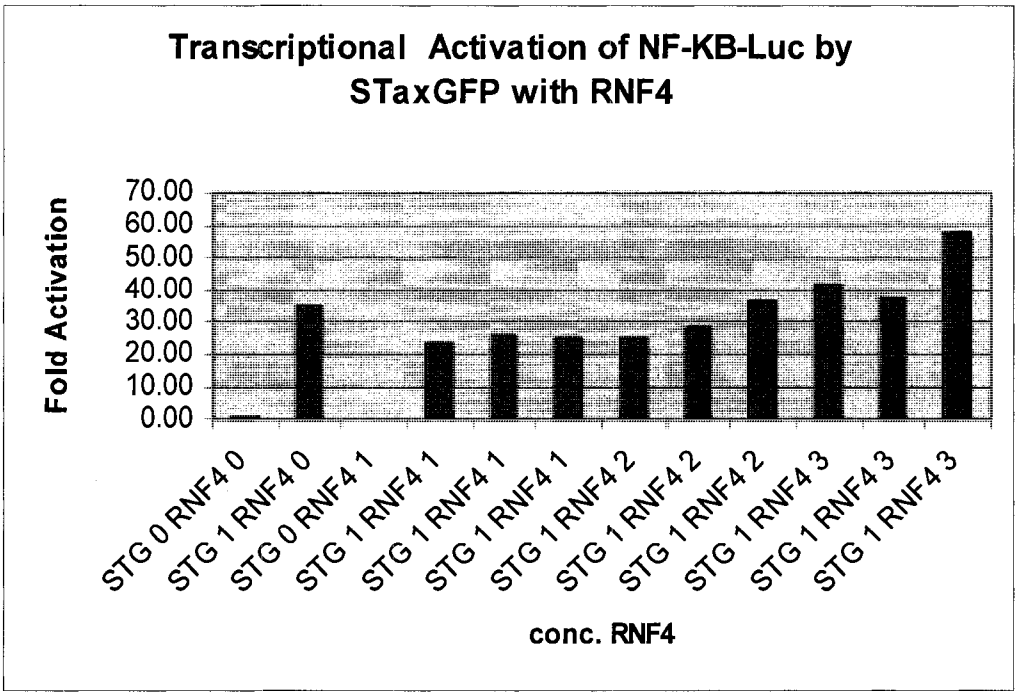

Fig. 18. **Effect of RNF4 Expression on the Transcriptional Activation Activity of Tax.** 293T cells were transiently transfected with promter/reporter constructs, STaxGFP, and increasing concentrations of RNF4-GFP. Lysates were subjected to luciferase assays and fold activation over reporter alone (fold acitivation=1) is indicated for each sample.

identified specific cellular target for ubiquitylation (215). STUbLs possess a SUMO-interacting motif (SIM) that allows them to interact with sumoylated proteins and proteins containing SUMO-like domains (SLDs) (218). RNF4 contains four putative SIMs, and targets proteins that have been modified by the addition of multiple SUMO peptides (216). Unlike ubiquitylation which can mark a protein for degradation via the proteosome, sumoylation may prevent degradation and result in accumulation of sumoylated proteins (219). Therefore, the interaction between STUbLs and sumoylated proteins may serve to target the previously sumoylated proteins for ubiquitin-mediated proteosomal degradation (218).

Our studies demonstrate that RNF4 is able to ubiquitylate previously sumoylated Tax *in vitro.* These findings provide the first specific protein target for RNF4. This interaction was found to be sumoylated-Tax-specific since it could be outcompeted by the addition of free SUMO. Tax is sumoylated on multiple lysines including those at residues 280 and 284 making it an attractive target for the poly-SUMO-specific activity of RNF4 (89,90,213,216). We show that this ubiquitylation results in a relocalization of Tax from its normal nuclear location in Tax Speckled Structures to the cytoplasm where it forms a perinuclear ring. One possible explanation for the relocalization of Tax to the cytoplasm following ubiquitylation may be to promote proteosomal degradation of Tax. Earlier studies of Tax ubiquitylation , however, indicated that the addition of ubiquitin resulted in an increase in Tax binding to proteosomes without proteosomal degradation of Tax (213,220). This same study indicated that ubiquitylation of Tax resulted in a loss of transcriptional activation of the viral LTR (213). We were able to link the ubiquitin-induced cytoplasmic relocalization of Tax to a decrease in the transcriptional *trans-*

activation of the HTLV-LTR, which is a nuclear function of Tax, and an increase in the *trans*-activation of NF-κB by Tax, which is a cytoplasmic function of Tax. The loss of transcriptional activation, therefore, is more likely a result of the relocalization of Tax rather than an inactivation of Tax by ubiquitylation.

Our studies suggest that the domain within Tax that mediates its interaction with RNF4 lies between amino acids 202 and 254. This region lies just N-terminal to the two lysine residues shown to be involved in linking ubiquitylation and relocalization of Tax. Interestingly, the mutation of these two residues from lysines to arginines which would prevent ubiquitylation did not prevent the interaction between Tax and RNF4.

The purpose for Tax ubiquitylation may be to regulate the nucleocytoplasmic shuttling of Tax. Our laboratory has previously shown that Tax is able to shuttle between the nucleus and cytoplasm via an NLS and an NES (85). Lamsoul *et al* have shown that sumoylation of Tax results in nuclear localization while ubiquitylation results in cytoplasmic localization (89). Alefantis *et al* have suggested that the NES of Tax may often be "masked" by protein folding or other means (93). We have shown in this study that Tax must enter the nucleus as a dimer and that it is directed into TSS by a specific TSS targeting signal. Putting all of these findings together, we suggest a possible model for Tax shuttling. Since the Tax NES is within the dimerzation domain, Tax dimerization in the cytoplasm may mask the NES while having no effect on the functions of the N-terminal NLS and TSTS. The Tax dimer is then sumoylated by an as yet unidentified SUMO ligase and translocates into the nucleus where it is directed into TSS. The sumoylated Tax is targeted by RNF4 for ubiquitylation, and this modification may either

cause disruption of the Tax dimer or another conformational change that exposes the Tax NES and results in the nuclear export of Tax.

SECTION 6

CONCLUSIONS

Summary

We have identified two novel mechanisms for the regulation of Tax subcellular localization. The first is the Tax Speckle Targeting Sequence that mediates interactions between Tax and the nuclear matrix to direct Tax into its discrete nuclear foci. We found that this sequence is physically and functionally separate from the previously identified nuclear localization signal of Tax. This region from Tax amino acids 50 to 75 was found to be sufficient for targeting the normally diffuse green fluorescent protein (GFP) into Tax-like nuclear speckles. Deletion of the region in Tax from amino acids 52 to 99 resulted in loss of TSS targeting and demonstrates that this region is also necessary for TSS targeting. Tax Speckled Structures are nuclear structures unique to Tax in that they contain proteins from both the transcription/splicing machinery and from the DNA damage recognition and repair machinery (134,168,183). The targeting sequence for TSS, therefore, may have some similarity to targeting signals for other nuclear speckle proteins without the requirement for complete homology. Our identified TSTS is enriched in proline residues, is relatively short in length, and is predominantly unstructured based on predicted motif searches. These are all features shared by other nuclear speckle-associated targeting signals (196,199,206). Our signal differs from previously identified speckle-targeting sequences in that it does not possess an arginine/serine motif common to many speckle proteins (195,197,198).

The second novel means of regulating Tax subcellular localization is through Tax dimerization. Although it was previously demonstrated that Tax could self-associate to form dimers, the significance of dimerization in localization had not been demonstrated (100). Tax deletion mutants that were deficient for dimerization were unable to localize into the nucleus. Coexpression with wildtype Tax was able to partially restore nuclear accumulation and correlated with weak dimerization between the single dimerization subdomain mutants and wildtype Tax. Complete loss of dimerization capability resulted in inability to be rescued by wildtype and failure to localize to the nucleus. We found that deletion mutants missing one of the two critical targeting signals, the NLS or the TSTS, were able to heterodimerize with each other and rescue the deficient localization by functional complementation. Finally, restoration of self-association through induced dimer formation resulted in restoration of nuclear accumulation.

We also identified a novel functional and physical relationship between Tax and the ubiquitin ligase RNF, providing the first known target for RNF4. Previous studies have shown that Tax can be ubiquitynylated and that this modification is associated with cytoplasmic localization of Tax (89,213). The ubiquitin ligase involved in this modification, however, has not been identified. We have shown that Tax can be ubiquitylated by RNF4 *in vitro* and that increased expression of RNF4 leads to a relocalization of Tax from the nucleus to the cytoplasm. We demonstrated that Tax and RNF4 can interact physically in a complex, and we have mapped the domain in Tax responsible for this interaction with RNF4 to be the region between amino acids 202 and 254. This region is upstream from the two lysine residues in Tax (280 and 284) that are believed to be modified by ubiqitinylation and associated with Tax relocalization (89).

We also showed that this relocalization resulted in changes in the *trans*-activation function of Tax. Increased RNF4 expression resulted in a decrease in the transcriptional activation of the viral LTR, a nuclear function of Tax, while increasing activation of NF-κB, a cytoplasmic function of Tax. These findings have broadened our knowledge of the regulation of Tax subcellular localization and have identified new physical and functional relationships for Tax.

Significance of Findings

It is estimated that there are currently 20-30 million people infected with HTLV-1 (12). Out of those people about 1.5 million will develop one of the two debilitating and invariably fatal diseases ATL or HAM/TSP (31). In certain distinct geographical areas such as the Caribbean, as many as 3-4% of the population is seropositive for HTLV-1(31). In Japan, it is estimated that there are 1.2 million people infected with HTLV-1, and there are 800 new cases of ATL diagnosed each year (9,32). Current therapies are ineffective in treating these two conditions and provide little relief and hope for patients and their families (64).

The mechanisms by which Tax is able to induce cellular transformation are still unknown. Any new information that we gain regarding the functioning of Tax is a step toward developing possible new therapies. There is significant evidence that the transformation potential of Tax is related to its ability to dysregulate cell cycle, DNA repair, and apoptosis through its direct protein-protein interactions and *trans*-activation functions. In order to achieve such diverse cellular effects, Tax must interact with cellular

binding partners in several subcellular compartments. The regulation of the subcellular localization of Tax is therefore critical to the functions of Tax.

In this study we have gained significant knowledge in the regulation of the subcellular localization of Tax. Our identification of a Tax Speckle Targeting Signal that shares characteristics with other nuclear matrix targeting sequences suggest that Tax is able to interact with the nuclear matrix proteins and opens up an entire new category for Tax cellular binding partners. Also, mutations that remove or alter intranuclear-targeting signals are prevalent in leukemias and have been linked to altered localization of transcription factors within the nucleus (193-195). In some leukemias, these mutations in the intranuclear targeting of transcription factors reduce fidelity of gene expression by influencing the organization or assembly of machineries involved in transcription and mRNA processing (193). The expression of Tax and its ability to relocalize cellular proteins to TSS may have a similar effect as mutation of the intranuclear targeting signal for these transcription factors. By binding to Tax, the transcription factor may be removed from its normal subcellular address to a new site within TSS, leading to similar dysregulation of transcription and mRNA processing as would result from mutation of its intranuclear targeting signal. This would provide yet another means for Tax to influence transcription and effect changes leading to transformation.

We have also supplied additional insight into regulation of the nuclear localization of Tax through dimerization. There are many examples of proteins that must be in dimeric or oligomeric form to enter or to remain in the nucleus such as the HCMV processivity factor ppUL44, the Ku proteins, the AP-1 family members c-Fos, c-Jun, JunB and JunD, and the cellular protein p53 (209-211,221). Previous studies of Tax

indicated that Tax is capable of forming dimers and that optimal *trans*-activation by Tax requires Tax dimerization (100-102). We are the first to show that nuclear localization of Tax requires Tax self-association. Since Tax is a predominantly nuclear protein, this finding is quite significant and suggests that Tax spends a majority of its time in a dimeric state. The formation of Tax dimers may also serve to "mask" the nuclear export signal of Tax resulting in nuclear retention. The nuclear export signal for Tax is located between amino acids 190 and 203 (85,93), and this area partially overlaps one of the previously identified dimerization subdomains (101). Although this signal was found to be CRM-1 dependent for Tax export, normal Tax export is CRM-1 independent (93). Alefantis *et al* suggest that this NES is usually "masked" in Tax (93). Disruption of dimerization, then, could be one means for uncovering the NES and relocalizing Tax from the nucleus into the cytoplasm.

Finally, we have identified a novel interaction between Tax and RNF4. This is a significant finding because there has been no previously identified specific target for the ubiquitnylating activity of RNF4. We have shown that RNF4 can ubiquitylate Tax *in vitro* and suggest that RNF4 may be the ubiquitin ligase responsible for Tax ubiquitylation *in vivo.* This is also significant because we were able to link this posttranslational modification with a change in both the localization and *trans*-activation function of Tax. Recent studies by Gatza *et al* have indicated that Tax is ubiquitylated following DNA damage due to genotoxic stress or UV irradiation and that this ubiquitylation results in the nuclear export of Tax via a CRM-1 dependent pathway (90,222). Our findings suggest that this ubiquitylation of Tax may be accomplished though RNF4, but additional studies will be required to confirm this role for RNF4.

Future Directions

During these studies we identified a new localization sequence, the TSS targeting signal (TSTS), that directs Tax into TSS. We determined that Tax must dimerize as a prerequisite for nuclear translocation, and we identified a novel binding partner for Tax, RNF4. In the process we have developed several tools that will be invaluable in future studies of Tax. These tools can be used to further develop the Tax interactome, to establish Tax functions which occur in the TSS, to link oligomerization of Tax with Tax function, and to investigate other possible targets for RNF4.

These tools will be useful in defining the Tax interactome. We began these studies with a scanning series of Tax mutants with deletions of 29 to 54 amino acids in length. Although these constructs were originally designed to map the TSTS domain of Tax, they may be used in future studies to begin fine mapping the domains in Tax required for interactions with previously identified Tax-binding proteins such as DNA-PKcs, Chk2, and 53BP1. As our continued studies of the Tax interactome identify new Tax binding partners, we can employ these constructs to define the Tax domains required for each interaction. In addition, our earlier studies using these mutants revealed one mutant, STax(d322-353)GFP, that displayed transcriptional *trans*-activation activity higher than that of wildtype Tax (Fig. 1B). This same mutant was the only one that induced a G2/M arrest comparable to that of wildtype in the cell cycle analysis (Fig. 2), and it expressed extremely high levels of protein that seemed to localize to the nucleus more efficiently than wildtype Tax. Studies by Tsuji *et al* suggested that the C-terminus of Tax may contain a cytoplasmic retention signal (189). STax(d322-353)GFP may be a more potent

transcriptional activator due to the absence of the C-terminal region, and future studies with this construct may be able to confirm the role of this region of Tax.

We can use the Tax NLS mutant, STax(d29-52)GFP, and the TSTS mutant, STax(d52-99)GFP, for studies to link Tax subcellular localization and function. Since each of these mutations results in specifically altered Tax localization to the cytoplasm or to the nucleus but outside of the TSS, we can analyze these mutants for known Tax functions and assign each function to a particular subcellular compartment. Specifically, we can analyze the ability of the TSTS mutant to perform known Tax functions and determine which Tax functions are associated with Tax Speckled Structures and which require only nuclear entry. Possible Tax functions to be assayed could include the activation of DNA-PKcs, induction of micronuclei, and the modulation of Chk2 kinase activity. We were also able to demonstrate functional complementation between these two mutants resulting in rescue of nuclear localization and TSS formation. It would be of interest to determine if this rescue of proper localization also resulted in a rescue of the transcriptional *trans*-activation activity of these Tax constructs.

We can use these tools to examine the link between Tax oligomerization and function. A useful tool for these studies is the inducible dimerization construct. In our studies we chose the Tax deletion mutant STax(d99-150)GFP for addition of the inducible dimerizer domain. We were able to show that induced dimerization of this construct resulted in an increase in its nuclear accumulation. Just as for the NLS and TSTS mutants, future studies with this construct will analyze the effect of induced dimerization of this mutant on its *trans*-activation capabilities. Also, we have constructed three other Tax dimerization domain mutants that are excluded from the nucleus. Each of

these constructs will have the dimerizer domain added to see if induced dimerization of these mutants results in a similar rescue of nuclear accumulation as for STax(d99-150)-Fv-GFP. ARIAD Pharmaceutical, who created the inducible homodimerization system employed in these studies, has also developed a system to induce heterodimerization. We could introduce different dimerizing domains into the dimerization deficient mutants. We could then determine whether induced heterodimerization between constructs missing different dimerization subdomains is also able to restore nuclear localization.

A particularly interesting finding in our study was the cytoplasmic localization of STax(d254-289)GFP. This construct is deleted in a region that only overlaps the previously identified Tax dimerization domain by two residues (101), and yet this deletion mutant displays a similar cytoplasmic localization and ability to be rescued by wildtype Tax as the dimerization subdomain mutants. This mutant did display a slightly stronger ability to dimerize with wildtype Tax than the dimerization mutants as indicated in Figure 9. This construct is also deleted in the region containing the two lysine residues sumoylated and ubiquitylated affecting the localization of Tax. Additional studies will focus on determining whether this construct represents an additional region required for Tax dimerization or if the cytoplasmic localization is due to the loss of another Tax function such as the ability to be ubiquitylated or sumoylated.

The most exciting area for future studies is the relationship between Tax and RNF4. We have shown that RNF4 is capable of ubiquitinylating Tax *in vitro,* and overexpression of RNF4 results in a relocalization of Tax to the cytoplasm. Since Tax is a predominantly nuclear protein, we would expect that Tax-expressing cells might repress the expression of RNF4. There are several cell lines that are HTLV-1 infected and

immortalized or transformed and express varying amounts of Tax. It would be of interest to examine the levels of RNF4 transcription by quantitative real time polymerase chain reaction (RT-PCR) in these cells and compare RNF4 mRNA levels to non-Tax-expressing parental lines. Recent studies by Gatza *et al* demonstrated that UV irradiation of Tax-expressing cells resulted in the ubiquitination and nuclear egress of Tax (90). We will use RT-PCR and immunoblot analysis to look at transcription and expression of RNF4 in response to UV irradiation to see if the ubiquitination of Tax following DNA damage may be mediated through RNF4. Also, by identifiying Tax as the target for RNF4 and characterizing this interaction, we may be able to begin to define other cellular proteins that are ubiquitylated by RNF4 and affect cellular functions.

The interaction of Tax with RNF4 is only half of the Tax ubiquitylation/ sumoylation story. Although in this study we have identified an ubiquitin ligase that may modify Tax by ubiquitylation, no cellular protein has been shown to be responsible for the sumoylation of Tax to date. Previously, our lab has performed liquid chromotography -tandem mass spectrometry (LC-MS/MS) analysis of Tax-binding proteins in which we identified a cellular SUMO ligase, RanBP2. This is a nucleoporin with SUMO ligase activity that is localized to the cytoplasmic filaments of the nuclear pore complex (223). The interaction between Tax and RanBP2 may provide the missing piece to the sumoylation/ubiquitylation story for Tax. We propose a model for the regulation of Tax nucleocytoplasmic shuttling in which RanBP2 sumoylates Tax dimers (with NES masked) in the cytoplasm, leading to nuclear localization via its NLS and TSS targeting via the TSTS. RNF4 then targets sumoylated Tax for ubiquitylation, exposing the Tax NES and resulting in the nuclear export of Tax. Future studies will focus on efforts to

examine the nature of the interaction between RanBP2, RNF4 and Tax and on finding assays to test the validity of our model.

REFERENCES

1. Poiesz, B. J., Ruscetti, F. W., Gazdar, A. F., Bunn, P. A., Minna, J. D., and Gallo, R. C. (1980) *Proc Natl Acad Sci U S A* **77**, 7415-7419

2. Yoshida, M., Seiki, M., Yamaguchi, K., and Takatsuki, K. (1984) *Proc Natl Acad Sci U S A* **81**, 2534-2537

3. Gessain, A., Barin, F., Vernant, J. C., Gout, O., Maurs, L., Calender, A., and de The, G. (1985) *Lancet* **2**, 407-410

4. Osame, M. (2002) *J Neurovirol* **8**, 359-364

5. Jeang, K. T., Giam, C. Z., Majone, F., and Aboud, M. (2004) *J Biol Chem* **279**, 31991-31994

6. Coffin, J. M., Hughes, S.H., and Varmus, H. . (1997) *Retroviruses*, Cold Spring Harbor Laboratory Press, Plainview

7. Manel, N., Kim, F. J., Kinet, S., Taylor, N., Sitbon, M., and Battini, J. L. (2003) *Cell* **115**, 449-459

8. Azran, I., Schavinsky-Khrapunsky, Y., and Aboud, M. (2004) *Retrovirology* **1**, 20

9. Matsuoka, M. (2005) *Retrovirology* **2**, 27

10. Seiki, M., Hattori, S., Hirayama, Y., and Yoshida, M. (1983) *Proc Natl Acad Sci U S A* **80**, 3618-3622

11. Yoshida, M. (2005) *Oncogene* **24**, 5931-5937

12. Nicot, C., Harrod, R. L., Ciminale, V., and Franchini, G. (2005) *Oncogene* **24**, 6026-6034

13. Hidaka, M., Inoue, J., Yoshida, M., and Seiki, M. (1988) *EMBO J* **7**, 519-523

14. Derse, D., Hill, S. A., Lloyd, P. A., Chung, H., and Morse, B. A. (2001) *J Virol* **75**, 8461-8468

15. Ohshima, K., Ohgami, A., Matsuoka, M., Etoh, K., Utsunomiya, A., Makino, T., Ishiguro, M., Suzumiya, J., and Kikuchi, M. (1998) *Cancer Lett* **132**, 203-212

16. Shuh, M. a. B., Mark. (2005) *Microscopy Research and Technique*, 176-196

17. Semmes, O. J. (2006) *J Clin Invest* **116**, 858-860

18. Wattel, E., Vartanian, J. P., Pannetier, C., and Wain-Hobson, S. (1995) *J Virol* **69**, 2863-2868

19. Manel, N., Battini, J. L., and Sitbon, M. (2005) *J Biol Chem* **280**, 29025-29029

20. Manel, N., Battini, J. L., Taylor, N., and Sitbon, M. (2005) *Oncogene* **24**, 6016-6025

21. Igakura, T., Stinchcombe, J. C., Goon, P. K., Taylor, G. P., Weber, J. N., Griffiths, G. M., Tanaka, Y., Osame, M., and Bangham, C. R. (2003) *Science* **299**, 1713-1716

22. Proietti, F. A., Carneiro-Proietti, A. B., Catalan-Soares, B. C., and Murphy, E. L. (2005) *Oncogene* **24**, 6058-6068

23. de The, G., and Bomford, R. (1993) *AIDS Res Hum Retroviruses* **9**, 381-386

24. Nicot, C. (2005) *Am J Hematol* **78**, 232-239

25. Yamaguchi, K. (1994) *Lancet* **343**, 213-216

26. Mueller, N., Okayama, A., Stuver, S., and Tachibana, N. (1996) *J Acquir Immune Defic Syndr Hum Retrovirol* **13 Suppl 1**, S2-7

27. Mueller, N. (1991) *Cancer Causes Control* **2**, 37-52

28. Manns, A., Hisada, M., and La Grenade, L. (1999) *Lancet* **353**, 1951-1958

29. Gessain, A., and de The, G. (1996) *Adv Virus Res* **47**, 377-426

30. Kazanji, M., and Gessain, A. (2003) *Cad Saude Publica* **19**, 1227-1240

31. Edlich, R. F., Arnette, J. A., and Williams, F. M. (2000) *J Emerg Med* **18**, 109-119

32. Matsuoka, M. (2003) *Oncogene* **22**, 5131-5140

33. Slattery, J. P., Franchini, G., and Gessain, A. (1999) *Genome Res* **9**, 525-540

34. Seiki, M., Hattori, S., and Yoshida, M. (1982) *Proc Natl Acad Sci U S A* **79**, 6899-6902

35. Gessain, A., Louie, A., Gout, O., Gallo, R. C., and Franchini, G. (1991) *J Virol* **65**, 1628-1633

36. Gessain, A., Gallo, R. C., and Franchini, G. (1992) *J Virol* **66**, 2288-2295

37. Ehrlich, G. D., Andrews, J., Sherman, M. P., Greenberg, S. J., and Poiesz, B. J. (1992) *Virology* **186**, 619-627

38. Fujino, T., and Nagata, Y. (2000) *J Reprod Immunol* **47**, 197-206

39. Moriuchi, M., and Moriuchi, H. (2002) *J Med Virol* **67**, 427-430

40. Goncalves, D. U., Guedes, A. C., Carneiro-Proietti, A. B., Pinheiro, S. R., Catalan-Soares, B., Proietti, F. A., and Lambertucci, J. R. (1999) *Int J STD AIDS* **10**, 336-337

41. Freitas, V., Gomes, I., Bittencourt, A., Fernandes, D., and Melo, A. (1997) *Arq Neuropsiquiatr* **55**, 325-328

42. Kawai, H., Nishida, Y., Takagi, M., Nakamura, K., Masuda, K., Saito, S., and Shirakami, A. (1989) *Neurology* **39**, 1129-1131

43. Yoshida, M., Osame, M., Kawai, H., Toita, M., Kuwasaki, N., Nishida, Y., Hiraki, Y., Takahashi, K., Nomura, K., Sonoda, S., and et al. (1989) *Ann Neurol* **26**, 331-335

44. Bartholomew, C., Jack, N., Edwards, J., Charles, W., Corbin, D., Cleghorn, F. R., and Blattner, W. A. (1998) *J Hum Virol* **1**, 302-305

45. Maloney, E. M., Cleghorn, F. R., Morgan, O. S., Rodgers-Johnson, P., Cranston, B., Jack, N., Blattner, W. A., Bartholomew, C., and Manns, A. (1998) *J Acquir Immune Defic Syndr Hum Retrovirol* **17**, 167-170

46. Pawson, R., Schulz, T., Matutes, E., and Catovsky, D. (1998) *Br J Haematol* **102**, 872-873

47. Hino, S., Yamaguchi, K., Katamine, S., Sugiyama, H., Amagasaki, T., Kinoshita, K., Yoshida, Y., Doi, H., Tsuji, Y., and Miyamoto, T. (1985) *Jpn J Cancer Res* **76**, 474-480

48. Uchiyama, T., Yodoi, J., Sagawa, K., Takatsuki, K., and Uchino, H. (1977) *Blood* **50**, 481-492

49. Hinuma, Y., Komoda, H., Chosa, T., Kondo, T., Kohakura, M., Takenaka, T., Kikuchi, M., Ichimaru, M., Yunoki, K., Sato, I., Matsuo, R., Takiuchi, Y., Uchino, H., and Hanaoka, M. (1982) *Int J Cancer* **29**, 631-635

50. Yoshida, M., Miyoshi, I., and Hinuma, Y. (1982) *Proc Natl Acad Sci U S A* **79**, 2031-2035

51. Watanabe, T., Seiki, M., and Yoshida, M. (1984) *Virology* **133**, 238-241

52. Kondo, T., Kono, H., Nonaka, H., Miyamoto, N., Yoshida, R., Bando, F., Inoue, H., Miyoshi, I., Hinuma, Y., and Hanaoka, M. (1987) *Lancet* **2**, 159

53. Takatsuki, K., Yamaguchi, K., Kawano, F., Hattori, T., Nishimura, H., Tsuda, H., and Sanada, I. (1984) *Princess Takamatsu Symp* **15**, 51-57

54. Kinoshita, K., Amagasaki, T., Ikeda, S., Suzuyama, J., Toriya, K., Nishino, K., Tagawa, M., Ichimaru, M., Kamihira, S., Yamada, Y., and et al. (1985) *Blood* **66**, 120-127

55. Gallart, T., Anegon, I., Woessner, S., de la Fuente, R., Florensa, L., Sans-Sabafren, C., and Vives, J. (1983) *Lancet* **1**, 769-770

56. Shimoyama, M., Minato, K., Tobinai, K., Nagai, M., Setoya, T., Takenaka, T., Ishihara, K., Watanabe, S., Hoshino, H., Miwa, M., Kinoshita, M., Okabe, S., Fukushima, N., and Inada, N. (1983) *Jpn J Clin Oncol* **13 Suppl 2**, 165-187

57. Yamaguchi, K., Nishimura, H., Kawano, F., Kohrogi, H., Jono, M., Miyamoto, Y., and Takatsuki, K. (1983) *Jpn J Clin Oncol* **13 Suppl 2**, 189-199

58. Hattori, T., Uchiyama, T., Toibana, T., Takatsuki, K., and Uchino, H. (1981) *Blood* **58**, 645-647

59. Hanaoka, M. (1982) *Acta Pathol Jpn* **32 Suppl 1**, 171-185

60. Hisada, M., Okayama, A., Tachibana, N., Stuver, S. O., Spiegelman, D. L., Tsubouchi, H., and Mueller, N. E. (1998) *Int J Cancer* **77**, 188-192

61. Morimoto, C., Matsuyama, T., Oshige, C., Tanaka, H., Hercend, T., Reinherz, E. L., and Schlossman, S. F. (1985) *J Clin Invest* **75**, 836-843

62. Gallo, R. C., Kalyanaraman, V. S., Sarngadharan, M. G., Sliski, A., Vonderheid, E. C., Maeda, M., Nakao, Y., Yamada, K., Ito, Y., Gutensohn, N., Murphy, S., Bunn, P. A., Jr., Catovsky, D., Greaves, M. F., Blayney, D. W., Blattner, W., Jarrett, W. F., zur Hausen, H., Seligmann, M., Brouet, J. C., Haynes, B. F., Jegasothy, B. V., Jaffe, E., Cossman, J., Broder, S., Fisher, R. I., Golde, D. W., and Robert-Guroff, M. (1983) *Cancer Res* **43**, 3892-3899

63. Blayney, D. W., Jaffe, E. S., Blattner, W. A., Cossman, J., Robert-Guroff, M., Longo, D. L., Bunn, P. A., Jr., and Gallo, R. C. (1983) *Blood* **62**, 401-405

64. Taylor, G. P., and Matsuoka, M. (2005) *Oncogene* **24**, 6047-6057

65. Shimoyama, M. (1991) *Br J Haematol* **79**, 428-437

66. Yamaguchi, K., Nishimura, Y., Fukuyoshi, Y., Machida, J., Ueda, S., Kusumoto, Y., Shimada, H., Asamoah-Adu, A., and Takatsuki, K. (1990) *Lancet* **336**, 1070

67. Jaffe, E. S., Blattner, W. A., Blayney, D. W., Bunn, P. A., Jr., Cossman, J., Robert-Guroff, M., and Gallo, R. C. (1984) *Am J Surg Pathol* **8**, 263-275

68. Takatsuki, K., Yamaguchi, K., Kawano, F., Hattori, T., Nishimura, H., Tsuda, H., Sanada, I., Nakada, K., and Itai, Y. (1985) *Cancer Res* **45**, 4644s-4645s

69. Iwasaki, Y. (1990) *J Neurol Sci* **96**, 103-123

70. Orland, J. R., Engstrom, J., Fridey, J., Sacher, R. A., Smith, J. W., Nass, C., Garratty, G., Newman, B., Smith, D., Wang, B., Loughlin, K., and Murphy, E. L. (2003) *Neurology* **61**, 1588-1594

71. Osame, M., Usuku, K., Izumo, S., Ijichi, N., Amitani, H., Igata, A., Matsumoto, M., and Tara, M. (1986) *Lancet* **1**, 1031-1032

72. Gout, O., Baulac, M., Gessain, A., Semah, F., Saal, F., Peries, J., Cabrol, C., Foucault-Fretz, C., Laplane, D., Sigaux, F., and et al. (1990) *N Engl J Med* **322**, 383-388

73. Ono, A., Ikeda, E., Mochizuki, M., Matsuoka, M., Yamaguchi, K., Sawada, T., Yamane, S., Tokudome, S., and Watanabe, T. (1998) *Jpn J Cancer Res* **89**, 608-614

74. Murphy, E. L., Wang, B., Sacher, R. A., Fridey, J., Smith, J. W., Nass, C. C., Newman, B., Ownby, H. E., Garratty, G., Hutching, S. T., and Schreiber, G. B. (2004) *Emerg Infect Dis* **10**, 109-116

75. Yakova, M., Lezin, A., Dantin, F., Lagathu, G., Olindo, S., Jean-Baptiste, G., Arfi, S., and Cesaire, R. (2005) *Retrovirology* **2**, 4

76. Shida, H., Tochikura, T., Sato, T., Konno, T., Hirayoshi, K., Seki, M., Ito, Y., Hatanaka, M., Hinuma, Y., Sugimoto, M., and et al. (1987) *EMBO J* **6**, 3379-3384

77. Kataoka, R., Takehara, N., Iwahara, Y., Sawada, T., Ohtsuki, Y., Dawei, Y., Hoshino, H., and Miyoshi, I. (1990) *Blood* **76**, 1657-1661

78. Sundaram, R., Sun, Y., Walker, C. M., Lemonnier, F. A., Jacobson, S., and Kaumaya, P. T. (2003) *Vaccine* **21**, 2767-2781

79. Sundaram, R., Lynch, M. P., Rawale, S., Dakappagari, N., Young, D., Walker, C. M., Lemonnier, F., Jacobson, S., and Kaumaya, P. T. (2004) *J Acquir Immune Defic Syndr* **37**, 1329-1339

80. Sundaram, R., Beebe, M., and Kaumaya, P. T. (2004) *J Pept Res* **63**, 132-140

81. Tanaka, A., Takahashi, C., Yamaoka, S., Nosaka, T., Maki, M., and Hatanaka, M. (1990) *Proc Natl Acad Sci U S A* **87**, 1071-1075

82. Jin, D. Y., Giordano, V., Kibler, K. V., Nakano, H., and Jeang, K. T. (1999) *J Biol Chem* **274**, 17402-17405

83. Ross, T. M., Pettiford, S. M., and Green, P. L. (1996) *J Virol* **70**, 5194-5202

84. Grassmann, R., Dengler, C., Muller-Fleckenstein, I., Fleckenstein, B., McGuire, K., Dokhelar, M. C., Sodroski, J. G., and Haseltine, W. A. (1989) *Proc Natl Acad Sci U S A* **86**, 3351-3355

85. Burton, M., Upadhyaya, C. D., Maier, B., Hope, T. J., and Semmes, O. J. (2000) *J Virol* **74**, 2351-2364

86. Durkin, S. S., Ward, M. D., Fryrear, K. A., and Semmes, O. J. (2006) *J Biol Chem* **281**, 31705-31712

87. Bex, F., Murphy, K., Wattiez, R., Burny, A., and Gaynor, R. B. (1999) *J Virol* **73**, 738-745

88. Krause Boehm, A., Stawhecker, J. A., Semmes, O. J., Jankowski, P. E., Lewis, R., and Hinrichs, S. H. (1999) *J Biomed Sci* **6**, 206-212

89. Lamsoul, I., Lodewick, J., Lebrun, S., Brasseur, R., Burny, A., Gaynor, R. B., and Bex, F. (2005) *Mol Cell Biol* **25**, 10391-10406

90. Gatza, M. L., Dayaram, T., and Marriott, S. J. (2007) *Retrovirology* **4**, 95

91. Gitlin, S. D., Lindholm, P. F., Marriott, S. J., and Brady, J. N. (1991) *J Virol* **65**, 2612-2621

92. Smith, M. R., and Greene, W. C. (1990) *Genes Dev* **4**, 1875-1885

93. Alefantis, T., Barmak, K., Harhaj, E. W., Grant, C., and Wigdahl, B. (2003) *J Biol Chem* **278**, 21814-21822

94. Gachon, F., Thebault, S., Peleraux, A., Devaux, C., and Mesnard, J. M. (2000) *Mol Cell Biol* **20**, 3470-3481

95. Harrod, R., Tang, Y., Nicot, C., Lu, H. S., Vassilev, A., Nakatani, Y., and Giam, C. Z. (1998) *Mol Cell Biol* **18**, 5052-5061

96. Nicot, C., Tie, F., and Giam, C. Z. (1998) *J Virol* **72**, 6777-6784

97. Xiao, G., and Sun, S. C. (2000) *Oncogene* **19**, 5198-5203

98. Jeang, K. T. (2001) *Cytokine Growth Factor Rev* **12**, 207-217

99. Semmes, O. J., and Jeang, K. T. (1992) *Virology* **188**, 754-764

100. Jin, D. Y., and Jeang, K. T. (1997) *Nucleic Acids Res* **25**, 379-387

101. Basbous, J., Bazarbachi, A., Granier, C., Devaux, C., and Mesnard, J. M. (2003) *J Virol* **77**, 13028-13035

102. Tie, F., Adya, N., Greene, W. C., and Giam, C. Z. (1996) *J Virol* **70**, 8368-8374

103. Xie, L., Yamamoto, B., Haoudi, A., Semmes, O. J., and Green, P. L. (2005) *Blood*

104. Rousset, R., Fabre, S., Desbois, C., Bantignies, F., and Jalinot, P. (1998) *Oncogene* **16**, 643-654

105. Vendel, A. C., McBryant, S. J., and Lumb, K. J. (2003) *Biochemistry* **42**, 12481-12487

106. Semmes, O. J., and Jeang, K. T. (1995) *J Virol* **69**, 1827-1833

107. Kashanchi, F., and Brady, J. N. (2005) *Oncogene* **24**, 5938-5951

108. Jeang, K. T., Boros, I., Brady, J., Radonovich, M., and Khoury, G. (1988) *J Virol* **62**, 4499-4509

109. Kimzey, A. L., and Dynan, W. S. (1998) *J Biol Chem* **273**, 13768-13775

110. Gitlin, S. D., Dittmer, J., Shin, R. C., and Brady, J. N. (1993) *J Virol* **67**, 7307-7316

111. Giebler, H. A., Loring, J. E., van Orden, K., Colgin, M. A., Garrus, J. E., Escudero, K. W., Brauweiler, A., and Nyborg, J. K. (1997) *Mol Cell Biol* **17**, 5156-5164

112. Goren, I., Semmes, O. J., Jeang, K. T., and Moelling, K. (1995) *J Virol* **69**, 5806-5811

113. Kwok, R. P., Laurance, M. E., Lundblad, J. R., Goldman, P. S., Shih, H., Connor, L. M., Marriott, S. J., and Goodman, R. H. (1996) *Nature* **380**, 642-646

114. Lenzmeier, B. A., Giebler, H. A., and Nyborg, J. K. (1998) *Mol Cell Biol* **18**, 721-731

115. Jiang, H., Lu, H., Schiltz, R. L., Pise-Masison, C. A., Ogryzko, V. V., Nakatani, Y., and Brady, J. N. (1999) *Mol Cell Biol* **19**, 8136-8145

116. Harrod, R., Kuo, Y. L., Tang, Y., Yao, Y., Vassilev, A., Nakatani, Y., and Giam, C. Z. (2000) *J Biol Chem* **275**, 11852-11857

117. Uchiumi, F., Maruta, H., Inoue, J., Yamamoto, T., and Tanuma, S. (1996) *Biochem Biophys Res Commun* **220**, 411-417

118. Laurance, M. E., Kwok, R. P., Huang, M. S., Richards, J. P., Lundblad, J. R., and Goodman, R. H. (1997) *J Biol Chem* **272**, 2646-2651

119. Hall, W. W., and Fujii, M. (2005) *Oncogene* **24**, 5965-5975

120. Matsumoto, J., Ohshima, T., Isono, O., and Shimotohno, K. (2005) *Oncogene* **24**, 1001-1010

121. Petropoulos, L., and Hiscott, J. (1998) *Virology* **252**, 189-199

122. Wang, C. Y., Mayo, M. W., and Baldwin, A. S., Jr. (1996) *Science* **274**, 784-787

123. Li, X. H., Murphy, K. M., Palka, K. T., Surabhi, R. M., and Gaynor, R. B. (1999) *J Biol Chem* **274**, 34417-34424

124. Sun, S. C., and Yamaoka, S. (2005) *Oncogene* **24**, 5952-5964

125. Harhaj, N. S., Sun, S. C., and Harhaj, E. W. (2007) *J Biol Chem* **282**, 4185-4192

126. Fujii, M., Tsuchiya, H., Chuhjo, T., Akizawa, T., and Seiki, M. (1992) *Genes Dev* **6**, 2066-2076

127. Shuh, M., and Derse, D. (2000) *J Virol* **74**, 11394-11397

128. Harhaj, E. W., Good, L., Xiao, G., and Sun, S. C. (1999) *Oncogene* **18**, 1341-1349

129. Gupta, S. K., Guo, X., Durkin, S. S., Fryrear, K. F., Ward, M. D., and Semmes, O. J. (2007) *J Biol Chem* **282**, 29431-29440

130. Ball, K. L. (1997) *Prog Cell Cycle Res* **3**, 125-134

131. Chowdhury, I. H., Farhadi, A., Wang, X. F., Robb, M. L., Birx, D. L., and Kim, J. H. (2003) *Int J Cancer* **107**, 603-611

132. Akagi, T., Ono, H., and Shimotohno, K. (1996) *Oncogene* **12**, 1645-1652

133. Haller, K., Wu, Y., Derow, E., Schmitt, I., Jeang, K. T., and Grassmann, R. (2002) *Mol Cell Biol* **22**, 3327-3338

134. Haoudi, A., Daniels, R. C., Wong, E., Kupfer, G., and Semmes, O. J. (2003) *J Biol Chem* **278**, 37736-37744

135. Iwanaga, R., Ohtani, K., Hayashi, T., and Nakamura, M. (2001) *Oncogene* **20**, 2055-2067

136. Jin, D. Y., Spencer, F., and Jeang, K. T. (1998) *Cell* **93**, 81-91

137. Kehn, K., Fuente Cde, L., Strouss, K., Berro, R., Jiang, H., Brady, J., Mahieux, R., Pumfery, A., Bottazzi, M. E., and Kashanchi, F. (2005) *Oncogene* **24**, 525-540

138. Liu, B., Hong, S., Tang, Z., Yu, H., and Giam, C. Z. (2005) *Proc Natl Acad Sci U S A* **102**, 63-68

139. Liu, B., Liang, M. H., Kuo, Y. L., Liao, W., Boros, I., Kleinberger, T., Blancato, J., and Giam, C. Z. (2003) *Mol Cell Biol* **23**, 5269-5281

140. Mesnard, J. M., and Devaux, C. (1999) *Virology* **257**, 277-284

141. Neuveut, C., and Jeang, K. T. (2002) *Front Biosci* **7**, d157-163

142. Park, H. U., Jeong, J. H., Chung, J. H., and Brady, J. N. (2004) *Oncogene* **23**, 4966-4974

143. Ramirez, J. A., and Nyborg, J. K. (2007) *J Mol Biol* **372**, 958-969

144. Marriott, S. J., and Semmes, O. J. (2005) *Oncogene* **24**, 5986-5995

145. Low, K. G., Dorner, L. F., Fernando, D. B., Grossman, J., Jeang, K. T., and Comb, M. J. (1997) *J Virol* **71**, 1956-1962

146. Santiago, F., Clark, E., Chong, S., Molina, C., Mozafari, F., Mahieux, R., Fujii, M., Azimi, N., and Kashanchi, F. (1999) *J Virol* **73**, 9917-9927

147. Cereseto, A., Diella, F., Mulloy, J. C., Cara, A., Michieli, P., Grassmann, R., Franchini, G., and Klotman, M. E. (1996) *Blood* **88**, 1551-1560

148. de La Fuente, C., Santiago, F., Chong, S. Y., Deng, L., Mayhood, T., Fu, P., Stein, D., Denny, T., Coffman, F., Azimi, N., Mahieux, R., and Kashanchi, F. (2000) *J Virol* **74**, 7270-7283

149. LaBaer, J., Garrett, M. D., Stevenson, L. F., Slingerland, J. M., Sandhu, C., Chou, H. S., Fattaey, A., and Harlow, E. (1997) *Genes Dev* **11**, 847-862

150. Sherr, C. J., and Roberts, J. M. (1999) *Genes Dev* **13**, 1501-1512

151. Kibler, K. V., and Jeang, K. T. (2001) *J Virol* **75**, 2161-2173

152. Kehn, K., Deng, L., De La Fuente, C., Strouss, K., Wu, K., Maddukuri, A., Baylor, S., Rufner, R., Pumfery, A., Bottazzi, M. E., and Kashanchi, F. (2004) *Retrovirology* **1**, 6

153. Walker, D. H., and Maller, J. L. (1991) *Nature* **354**, 314-317

154. Kasai, T., Iwanaga, R., Iha, H., and Jeang, K. T. (2002) *J Biol Chem* **277**, 5187-5193

155. Maruyama, K., Fukushima, T., Kawamura, K., and Mochizuki, S. (1990) *Cancer Res* **50**, 5697S-5702S

156. Kao, S. Y., and Marriott, S. J. (1999) *J Virol* **73**, 4299-4304

157. Itoyama, T., Sadamori, N., Tokunaga, S., Sasagawa, I., Nakamura, H., Yao, E., Jubashi, T., Yamada, Y., Ikeda, S., and Ichimaru, M. (1990) *Cancer Genet Cytogenet* **49**, 157-163

158. Fujimoto, T., Hata, T., Itoyama, T., Nakamura, H., Tsukasaki, K., Yamada, Y., Ikeda, S., Sadamori, N., and Tomonaga, M. (1999) *Cancer Genet Cytogenet* **109**, 1-13

159. Philpott, S. M., and Buehring, G. C. (1999) *J Natl Cancer Inst* **91**, 933-942

160. Jeang, K. T., Widen, S. G., Semmes, O. J. t., and Wilson, S. H. (1990) *Science* **247**, 1082-1084

161. Mozzherin, D. J., and Fisher, P. A. (1996) *Biochemistry* **35**, 3572-3577

162. Mozzherin, D. J., Shibutani, S., Tan, C. K., Downey, K. M., and Fisher, P. A. (1997) *Proc Natl Acad Sci U S A* **94**, 6126-6131

163. Chu, G. (1997) *J Biol Chem* **272**, 24097-24100

164. Ng, P. W., Iha, H., Iwanaga, Y., Bittner, M., Chen, Y., Jiang, Y., Gooden, G., Trent, J. M., Meltzer, P., Jeang, K. T., and Zeichner, S. L. (2001) *Oncogene* **20**, 4484-4496

165. Semmes, O. J., Majone, F., Cantemir, C., Turchetto, L., Hjelle, B., and Jeang, K. T. (1996) *Virology* **217**, 373-379

166. Majone, F., Luisetto, R., Zamboni, D., Iwanaga, Y., and Jeang, K. T. (2005) *Retrovirology* **2**, 45

167. Majone, F., Semmes, O. J., and Jeang, K. T. (1993) *Virology* **193**, 456-459

168. Durkin, S. S., Guo, X., Fryrear, K. A., Mihaylova, V. T., Gupta, S. K., Belgnaoui, S. M., Haoudi, A., Kupfer, G., and Semmes, O. J. (2008) *J Biol Chem* **in press**

169. Goytisolo, F. A., Samper, E., Edmonson, S., Taccioli, G. E., and Blasco, M. A. (2001) *Mol Cell Biol* **21**, 3642-3651

170. Gabet, A. S., Mortreux, F., Charneau, P., Riou, P., Duc-Dodon, M., Wu, Y., Jeang, K. T., and Wattel, E. (2003) *Oncogene* **22**, 3734-3741

171. Copeland, K. F., Haaksma, A. G., Goudsmit, J., Krammer, P. H., and Heeney, J. L. (1994) *AIDS Res Hum Retroviruses* **10**, 1259-1268

172. Neuveut, C., and Jeang, K. T. (2000) *Prog Cell Cycle Res* **4**, 157-162

173. Mulloy, J. C., Kislyakova, T., Cereseto, A., Casareto, L., LoMonico, A., Fullen, J., Lorenzi, M. V., Cara, A., Nicot, C., Giam, C., and Franchini, G. (1998) *J Virol* **72**, 8852-8860

174. Pise-Masison, C. A., and Brady, J. N. (2005) *Front Biosci* **10**, 919-930

175. Ariumi, Y., Kaida, A., Lin, J. Y., Hirota, M., Masui, O., Yamaoka, S., Taya, Y., and Shimotohno, K. (2000) *Oncogene* **19**, 1491-1499

176. Jeong, S. J., Pise-Masison, C. A., Radonovich, M. F., Park, H. U., and Brady, J. N. (2005) *Oncogene* **24**, 6719-6728

177. Negorev, D., and Maul, G. G. (2001) *Oncogene* **20**, 7234-7242

178. Spector, D. L. (2001) *J Cell Sci* **114**, 2891-2893

179. Ascoli, C. A., and Maul, G. G. (1991) *J Cell Biol* **112**, 785-795

180. Lamond, A. I., and Spector, D. L. (2003) *Nat Rev Mol Cell Biol* **4**, 605-612

181. Gall, J. G. (2000) *Annu Rev Cell Dev Biol* **16**, 273-300

182. Terris, B., Baldin, V., Dubois, S., Degott, C., Flejou, J. F., Henin, D., and Dejean, A. (1995) *Cancer Res* **55**, 1590-1597

183. Semmes, O. J., and Jeang, K. T. (1996) *J Virol* **70**, 6347-6357

184. Ariumi, Y., Ego, T., Kaida, A., Matsumoto, M., Pandolfi, P. P., and Shimotohno, K. (2003) *Oncogene* **22**, 1611-1619

185. Smith, M. R., and Greene, W. C. (1992) *Virology* **187**, 316-320

186. Semmes, O. J., and Jeang, K. T. (1992) *J Virol* **66**, 7183-7192

187. Terry, L. J., Shows, E. B., and Wente, S. R. (2007) *Science* **318**, 1412-1416

188. Sorokin, A. V., Kim, E. R., and Ovchinnikov, L. P. (2007) *Biochemistry (Mosc)* **72**, 1439-1457

189. Tsuji, T., Sheehy, N., Gautier, V. W., Hayakawa, H., Sawa, H., and Hall, W. W. (2007) *J Biol Chem* **282**, 13875-13883

190. Bex, F., McDowall, A., Burny, A., and Gaynor, R. (1997) *J Virol* **71**, 3484-3497

191. Durkin, S. S., Guo, X., Fryrear, K. F., Mihaylova, V. T., Gupta, S. K., Belgnaoui, S. M., Haoudi, A., Kupfer, G., and Semmes, O. J. (2008) *J Biol Chem* **in press**

192. Phair, R. D., and Misteli, T. (2000) *Nature* **404**, 604-609

193. Stein, G. S., van Wijnen, A. J., Stein, J. L., Lian, J. B., Montecino, M., Choi, J., Zaidi, K., and Javed, A. (2000) *J Cell Sci* **113 (Pt 14)**, 2527-2533

194. Zeng, C., McNeil, S., Pockwinse, S., Nickerson, J., Shopland, L., Lawrence, J. B., Penman, S., Hiebert, S., Lian, J. B., van Wijnen, A. J., Stein, J. L., and Stein, G. S. (1998) *Proc Natl Acad Sci U S A* **95**, 1585-1589

195. Zeng, C., van Wijnen, A. J., Stein, J. L., Meyers, S., Sun, W., Shopland, L., Lawrence, J. B., Penman, S., Lian, J. B., Stein, G. S., and Hiebert, S. W. (1997) *Proc Natl Acad Sci U S A* **94**, 6746-6751

196. Bickmore, W. A., and Sutherland, H. G. (2002) *EMBO J* **21**, 1248-1254

197. Birney, E., Kumar, S., and Krainer, A. R. (1993) *Nucleic Acids Res* **21**, 5803-5816

198. Fu, X. D. (1995) *RNA* **1**, 663-680

199. Eilbracht, J., and Schmidt-Zachmann, M. S. (2001) *Proc Natl Acad Sci U S A* **98**, 3849-3854

200. Stahl, M. L., Ferenz, C. R., Kelleher, K. L., Kriz, R. W., and Knopf, J. L. (1988) *Nature* **332**, 269-272

201. Sudol, M. (1996) *Trends Biochem Sci* **21**, 161-163

202. Mayer, B. J., Hamaguchi, M., and Hanafusa, H. (1988) *Nature* **332**, 272-275

203. Mayer, B. J., and Eck, M. J. (1995) *Curr Biol* **5**, 364-367

204. Terasawa, H., Kohda, D., Hatanaka, H., Tsuchiya, S., Ogura, K., Nagata, K., Ishii, S., Mandiyan, V., Ullrich, A., Schlessinger, J., and et al. (1994) *Nat Struct Biol* **1**, 891-897

205. Ren, R., Mayer, B. J., Cicchetti, P., and Baltimore, D. (1993) *Science* **259**, 1157-1161

206. Barseguian, K., Lutterbach, B., Hiebert, S. W., Nickerson, J., Lian, J. B., Stein, J. L., van Wijnen, A. J., and Stein, G. S. (2002) *Proc Natl Acad Sci U S A* **99**, 15434-15439

207. Dyck, J. A., Maul, G. G., Miller, W. H., Jr., Chen, J. D., Kakizuka, A., and Evans, R. M. (1994) *Cell* **76**, 333-343

208. Weis, K., Rambaud, S., Lavau, C., Jansen, J., Carvalho, T., Carmo-Fonseca, M., Lamond, A., and Dejean, A. (1994) *Cell* **76**, 345-356

209. Alvisi, G., Jans, D. A., and Ripalti, A. (2006) *Biochemistry* **45**, 6866-6872

210. Trostel, S. Y., Sackett, D. L., and Fojo, T. (2006) *Cell Cycle* **5**, 2253-2259

211. Malnou, C. E., Salem, T., Brockly, F., Wodrich, H., Piechaczyk, M., and Jariel-Encontre, I. (2007) *J Biol Chem* **282**, 31046-31059

212. Forgacs, E., Gupta, S. K., Kerry, J. A., and Semmes, O. J. (2005) *J Virol* **79**, 6932-6939

213. Peloponese, J. M., Jr., Iha, H., Yedavalli, V. R., Miyazato, A., Li, Y., Haller, K., Benkirane, M., and Jeang, K. T. (2004) *J Virol* **78**, 11686-11695

214. Kerscher, O., Felberbaum, R., and Hochstrasser, M. (2006) *Annu Rev Cell Dev Biol* **22**, 159-180

215. Sun, H., Leverson, J. D., and Hunter, T. (2007) *EMBO J* **26**, 4102-4112

216. Tatham, M. H., Geoffroy, M. C., Shen, L., Plechanovova, A., Hattersley, N., Jaffray, E. G., Palvimo, J. J., and Hay, R. T. (2008) *Nat Cell Biol* **10**, 538-546

217. Kerscher, O. (2007) *EMBO Rep* **8**, 550-555

218. Prudden, J., Pebernard, S., Raffa, G., Slavin, D. A., Perry, J. J., Tainer, J. A., McGowan, C. H., and Boddy, M. N. (2007) *EMBO J* **26**, 4089-4101

219. Ulrich, H. D. (2005) *Trends Cell Biol* **15**, 525-532

220. Chiari, E., Lamsoul, I., Lodewick, J., Chopin, C., Bex, F., and Pique, C. (2004) *J Virol* **78**, 11823-11832

221. Koike, M., Shiomi, T., and Koike, A. (2001) *J Biol Chem* **276**, 11167-11173

222. Gatza, M. L., and Marriott, S. J. (2006) *J Virol* **80**, 6657-6668

223. Forler, D., Rabut, G., Ciccarelli, F. D., Herold, A., Kocher, T., Niggeweg, R., Bork, P., Ellenberg, J., and Izaurralde, E. (2004) *Mol Cell Biol* **24**, 1155-1167

APPENDIX A

Experimental Procedure for *in vitro* Ubiquitylation Assay

RNF4 and TAX were expressed as MBP fusions in BL21 StarTM (DE3) cells containing plasmid pRIL, which expresses several rare-codon tRNAs (a gift from Sean Prigge, JHSOM, MD). Proteins were affinity purified on an amylose resin (New England Biolabs). Ubiquitylation Assays were performed using reagents purchased from BIOMOL using manufacturer's instructions (Biomol #UW9920). Briefly, 2μM purified RNF4 and 10μM TAX fusion proteins were pre-incubated at RT for 15 minutes and then added into a ubiquitylation reaction containing E1, E2 (Mms2/Ubc13), ATP, reaction buffer, and Biotin-ubiquitin. Controls were set up as indicated omitting ATP (lane 1), E2 (Mms2/Ubc13 – lane 2)), E3 (RNF4-MBP – lane 3) from the reactions or adding 1mM MBP (lane 5 and 7). Additionally, complete reactions (ALL) containing purified SUMO was included (lane 6 and 7). Ubiquitylation reactions were allowed to proceed for 60min at 37°C and terminated using reducing SDS-PAGE sample buffer. Proteins were separated on 8-12% SDS-PAGE gels, transferred to PVDF membranes, and visualized using anti TAX antibodies and ECL (Pierce 34080). Ubiquitylated Tax-MBP proteins are visible as high-molecular weight adducts extending from ~80-250kDa (lane 4 and 5).

VITA

KIMBERLY ANNE FRYREAR

Department of Study
Eastern Virginia Medical School
Department of Microbiology and Molecular Cell Biology
700 West Olney Road
Norfolk, Virginia 23507

Education
Eastern Virginia Medical School and Old Dominion University
Norfolk, Virginia
Doctor of Philosophy, Biomedical Sciences (August 2001- December 2008)

Eastern Virginia Medical School
Norfolk, Virginia
Master of Science, Biomedical Sciences (August 2001- May 2008)

Old Dominion University
Norfolk, Virginia
Bachelor of Science, Biology (August 1989- December 1997)

Professional Experience
Graduate Research Associate (August 2001- December 2008)
Eastern Virginia Medical School
Norfolk, Virginia